INFORMATION TO USERS

This manuscript has been reproduced from the microfilm master. UMI films the text directly from the original or copy submitted. Thus, some thesis and dissertation copies are in typewriter face, while others may be from any type of computer printer.

The quality of this reproduction is dependent upon the quality of the copy submitted. Broken or indistinct print, colored or poor quality illustrations and photographs, print bleedthrough, substandard margins, and improper alignment can adversely affect reproduction.

In the unlikely event that the author did not send UMI a complete manuscript and there are missing pages, these will be noted. Also, if unauthorized copyright material had to be removed, a note will indicate the deletion.

Oversize materials (e.g., maps, drawings, charts) are reproduced by sectioning the original, beginning at the upper left-hand corner and continuing from left to right in equal sections with small overlaps.

ProQuest Information and Learning
300 North Zeeb Road, Ann Arbor, MI 48106-1346 USA
800-521-0600

DYNAMIC INTERACTIONS BETWEEN OLFACTORY RECEPTOR AXONS AND GLIAL CELLS FROM THE OLFACTORY SYSTEM OF THE MOTH *MANDUCA SEXTA*

by

Eric Shane Tucker

A Dissertation Submitted to the Faculty of the

DEPARTMENT OF CELL BIOLOGY AND ANATOMY

In Partial Fulfillment of the Requirements
For the Degree of

Doctor of Philosophy

In the Graduate College

THE UNIVERSITY OF ARIZONA

2002

THE UNIVERSITY OF ARIZONA ®
GRADUATE COLLEGE

As members of the Final Examination Committee, we certify that we have read the dissertation prepared by Eric Shane Tucker entitled Dynamic Interactions Between Olfactory Receptor Axons and Glial Cells From the Olfactory System of the Moth Manduca sexta and recommend that it be accepted as fulfilling the dissertation requirement for the Degree of Doctor of Philosophy

Leslie P. Tolbert	Date 11/21/02
Paul A. St. John	Date 11/21/02
John G. Hildebrand	Date 11/21/02
Richard B. Levine	Date 11/21/02
Ray Runyan	Date 11/21/02

Final approval and acceptance of this dissertation is contingent upon the candidate's submission of the final copy of the dissertation to the Graduate College.

I hereby certify that I have read this dissertation prepared under my direction and recommend that it be accepted as fulfilling the dissertation requirement.

Leslie P. Tolbert — Dissertation Director — Date 11/21/02

STATEMENT BY AUTHOR

This dissertation has been submitted in partial fulfillment of requirements for an advanced degree at The University of Arizona and is deposited in the University Library to be made available to borrowers under rules of the Library.

Brief quotations from this dissertation are allowable without special permission, provided that accurate acknowledgment of source is made. Requests for permission for extended quotation from or reproduction of this manuscript in whole or in part may be granted by the head of the major department or the Dean of the Graduate College when in his or her judgment the proposed use of the material is in the interests of scholarship. In all other instances, however, permission must be obtained from the author.

SIGNED: 

AKNOWLEDGEMENTS

Quite simply, this dissertation would not exist without the kind, generous support that was lent so freely by my many friends and co-workers in both the ARL Division of Neurobiology and in the Department of Cell Biology and Anatomy. I will be forever grateful to Leslie Tolbert, my thesis advisor, who leads by setting a stellar example. Leslie's thoughtful guidance has truly had an immeasurable impact on the scientist that I have become. I also am indebted to Lynne Oland, who has been like a second advisor throughout my training. I sincerely thank all of the members of the Tolbert laboratory, who were more than a joy to work with during my stay in Tucson.

I kindly thank Paul St. John, Ray Runyan, John Hildebrand, and Rick Levine for their service on my dissertation committee. I was very fortunate to have their helpful suggestions and advice throughout my graduate career.

The successful completion of my dissertation requirements could not have been accomplished without the extensive network of family and friends that I am exceedingly fortunate to call my own. Last and most, I owe enormous gratitude to my wife, whose patience, understanding, love, and support, made everything possible.

DEDICATION

This dissertation is dedicated to my parents, who believed in me when I barely believed in myself.

TABLE OF CONTENTS

FIGURES AND TABLES

ABSTRACT

Across species, glial cells in both peripheral and central nervous systems cooperate extensively with neurons to shape multiple aspects of neural development. In vertebrate and invertebrate olfactory systems, neuron-glia interactions are thought to underlie critical developmental events, including glomerulus formation, and the growth, sorting, and targeting of olfactory receptor neuron (ORN) axons. The olfactory system of the moth *Manduca sexta* has many similarities to vertebrate olfactory systems, and has been used extensively to explore intercellular interactions involved in the formation of the olfactory pathway. In particular, glial reduction experiments have implicated two types of central olfactory glia, the sorting zone and neuropil-associated glia, in axon sorting and glomerulus stabilization. The developmental roles of a third glial cell type, the antennal nerve glia, remain elusive, yet their peripheral origin and association with ORN axons are similar to mammalian olfactory ensheathing cells. The present body of work uses a defined co-culture system to characterize interactions between ORN axons growing from explants of olfactory receptor epithelium and glial cells from the primary olfactory system of *Manduca*. We have monitored how particular types of glia, known to influence the behavior of ORN axons *in vivo*, directly affect the behavior and morphology of individual ORN growth cones *in vitro*. Time-lapse imaging of neuron-glia cultures revealed that olfactory receptor growth cones elaborate extensively and cease advancement following contact with sorting zone and neuropil-associated glial cells. In contrast, growth cones advance along the surfaces of antennal nerve glial cells without prolonged changes in morphology. Cytoskeletal staining of fixed preparations reinforced live-cell findings, as contact with sorting zone and neuropil-associated glial cells caused statistically

significant changes in growth cone morphology. Finally, ORN axons induce antennal nerve glia, but not sorting zone or neuropil glia, to form multicellular arrays through proliferation and process extension. These findings have led to the formation of hypotheses concerning the nature of neuron-glia interactions *in vivo*.

CHAPTER 1: INTRODUCTION

Astronomical numbers of neural interconnections are formed with amazing precision during the development of the nervous system. The correct formation of neural circuitry is essential for proper nervous system function and, inevitably, for survival of the organism. This formidable task of neural wiring is achieved during development, when neuronal growth cones integrate positional and directional guidance cues sampled from their environments to correctly navigate toward, and ultimately select, their appropriate synaptic targets. Efforts from many laboratories over the last decade have led to the discovery and characterization of a wide variety of molecular cues that guide axons, cell-surface receptors that respond to guidance cues, and intracellular molecules that transduce extracellular signals and affect changes in growth cone motility (Mueller, 1999). Despite this progress, much remains unknown about how growing axons integrate guidance signals and make appropriate decisions at precise points along their pathways.

Developing olfactory systems, in both vertebrates and invertebrates, provide models for studying growth cone guidance during axon ingrowth, in which, unlike the better characterized visual and somatosensory systems, the synaptic targeting of growing axons is independent of spatial topography in the sense organ from which they arise. Glial cells in vertebrate and invertebrate olfactory systems are thought to influence the behavior of ingrowing olfactory receptor axons, and to participate with neurons during key phases of olfactory system development. To understand how interactions between olfactory receptor axons and glial cells might influence olfactory development, I will consider three main topics of interest: 1) the biology of growth cones, 2) neuron-glia interactions during development, and 3) the development of olfactory systems.

Growth cone biology

Growing axons are tipped with specialized amoeba-like appendages, called growth cones, which sense and respond to environmental cues. Guidance cues exert both attractive and repulsive influences on growth cones, and operate over a long range, via diffusion of soluble factors, or over a short range, often bound to the substrate (Goodman, 1996; Tessier-Lavigne and Goodman, 1996; Mueller, 1999). Mechanistically, growth cone guidance is regulated by interactions between complementary sets of receptor-ligand signaling systems that are well conserved evolutionarily. Examples include cell adhesion molecules of the immunoglobulin superfamily, integrins and extracellular matrix molecules, semaphorins and neuropilins, netrins and netrin receptors, and ephrins and Eph receptors (McKerracher et al., 1996; Walsh and Doherty, 1997; Nakamura et al., 2000; Wilkinson, 2001). Internal growth cone machinery, such as the Rho family of small GTPases, acts downstream of receptor-ligand systems to regulate cytoskeletal dynamics and growth cone motility (Suter and Forscher, 2000; Kuhn et al., 2000; Korey and Van Vactor, 2000).

Growth cones receive essential supplies via fast axonal transport from their cell bodies, yet remarkably, they retain the ability to recognize and respond to guidance cues even when connections with their cell bodies have been severed. This autonomy was clearly demonstrated in the embryonic retinotectal system of *Xenopus*, where growth cones from axotomized retinal neurons continued to grow toward and innervate their correct tectal targets (Harris et al., 1987). Growth cone behavior during axon guidance should be viewed as an integrated response to concomitant and sometimes conflicting signaling pathways. An illustrative demonstration of this principle comes from recent

work by Mu-ming Poo and colleagues. They suggest that guidance cues are not explicitly attractive or repulsive, but rather that the internal state of the neuron regulates the response of growth cones to particular guidance cues (Ming et al., 1997; Song et al., 1997, 1998). Turning responses of cultured spinal growth cones to gradients of diffusible factors (netrin-1, neurotrophins, or neurotransmitters) can be converted from attraction to repulsion, or from repulsion to attraction, by manipulation of intracellular cyclic nucleotide levels (reviewed by Song and Poo, 1999).

Growth cone structure and motility

Growth cones are sensory-motor appendages located at the tips of growing neurites. More than one hundred years ago, the renowned neuroanatomist Ramon y Cajal identified neuronal growth cones in fixed embryonic tissue (Ramon y Cajal, 1890, 1937). Cajal inferred from their elaborate ameboid shapes that growth cones were soft battering rams that propelled growing axons through complex cellular environments. The subsequent realization that living growth cones could be observed *in vitro* by culturing embryonic neural tissue (Harrison, 1910) led to a detailed description of growth cone structure and locomotion.

Figure 1.1 illustrates the principal components of the neuronal growth cone. Ultrastructural studies performed both *in vivo* (Bodian, 1966; Kawana et al., 1971) and *in vitro* (Yamada et al., 1970; Bunge, 1973) have characterized the subcellular distributions of cytoskeletal filaments and organelles within growth cones. The axon shaft leading to the distal growth cone contains bundles of parallel microtubules with their fast-growing ends directed towards the body of the growth cone. The central region of the growth cone body contains unbundled microtubules that fan out from the axon shaft (Bunge,

1973). The lamellipodium is located distal to the central region of the growth cone body, and is comprised of a meshwork of filamentous actin (F-actin) (Yamada et al., 1970, 1971; Bunge, 1973; Letourneau, 1983) and membranous vesicles (Yamada et al., 1971; Bunge, 1973). Microtubules often invade the proximal portion of the lamellipodium, a region referred to as the transition zone, during axon extension (Tanaka and Kirschner, 1991). Long microspikes, called filopodia, contain bundles of F-actin that extend from the peripheral edge of the lamellipodium (Tennyson, 1970; Kawana et al., 1971; Yamada et al., 1971; Bunge, 1973). Similar to microtubule bundles in the axon shaft, F-actin bundles in filopodia have their fastest growing ends directed distally. Organelles, including mitochondria and smooth endoplasmic reticulum, are concentrated proximally, at the base of the growth cone (Bunge, 1973). Lamellipodial veils, continuous with the F-actin meshwork of the lamellipodium, often extend between filopodia in the direction of growth cone advancement (Tosney and Wessells, 1983; Goldberg and Burmeister, 1986). Cargo contained within vesicles and in vesicular membranes is transported to and from the growth cone body along microtubules via microtubule-associated molecular motors (see Hirokawa, 1998). The plasma membrane of growth cones contains adhesion molecules and receptors necessary for axon extension and guidance (Mueller, 1999; Yu and Bargmann, 2001).

Growth cone locomotion is thought to involve the coordinated activity of multiple cellular processes, including regional membrane insertion, cytoskeletal dynamics, and adhesive interactions with the extracellular substrate. When foreign particles such as glass or carmine are deposited on neurons in culture, the particles remain stationary on neurite surfaces, even as the neurites continue to advance (Bray, 1970). These observations led Bray (1970) to suggest that new membrane was added distally, at the

growth cone, during neurite elongation. The application of antibody-conjugated fluorescent beads to cultured neurons has more recently been used to indirectly visualize the movement of membrane associated proteins and/or lipids along axons (Dai and Sheetz, 1995). Unlike Bray's particles, which were suspended from the substrate but relatively immobile on cell surfaces, fluorescent beads bound to integral membrane constituents readily diffuse within the lipid bilayer and travel with bulk membrane flow. Dai and Sheetz (1995) demonstrated that beads travel towards the cell body at a rate of approximately 7 μm/min, five times faster than the rate of axon extension, and with the combined use of beads and laser tweezers, showed that different amounts of membrane tension exist at the growth cone and along the axon. These observations led Dai and Sheetz to conclude that new membrane was added at the growth cone surface, and that membrane then flowed along the axon to the cell body, where it was internalized by endocytosis. In contrast, rapidly growing *Xenopus* neurites appear to add membrane at the cell body and along the axon, since focally labeled membrane segments travel forward in these cells (Popov et al., 1993). Fluorescent vesicles generated in the cell body, however, were rapidly transported down the axon and preferentially inserted near the growth cone, suggesting that newly synthesized material could be delivered to *Xenopus* growth cones by fast axonal transport (Zakharenko and Popov, 1998). Although the biomechanics and topology of membrane insertion in growing neurons remains debatable, the necessity of neurons to supply new membrane to meet the demand of growing axons is beyond contention (Futerman and Banker, 1996).

Experiments testing fluorescence recovery after photobleaching indicate that microtubule assembly occurs more rapidly at the growth cone than along proximal portions of the axon shaft (Lim et al., 1989, 1990). Thus axon elongation proceeds as

new tubulin is added distally to the growing axon. Vinblastin and nocodazole, drugs that disrupt tubulin polymerization, prevent neurite extension without limiting growth cone motility (Tanaka et al., 1995; Rochlin et al., 1996). Growth cone motility is instead controlled by actin dynamics, which allows for the extension and retraction of lamellipodia and filopodia. Growth cones treated with drugs that block actin polymerization, like cytochalasin B, lose actin based motility at their leading edge, but continue to advance (Forscher and Smith, 1988). Actin-based filopodia can exert tension (Bray, 1979) and generate forces that propel growth cones forward (Lamoureux et al., 1989). When contacting an intermediate target or substrate of higher affinity, filopodia often dilate and "engorge" as they are selectively filled by microtubules (Sabry et al., 1991). Selective microtubule invasion at the leading edge of growth cones occurs during steering events, and is directed by localized actin polymerization (Lin and Forscher, 1993). Actin-myosin based motility has also been implicated in growth cone advancement. In the clutch hypothesis (Mitchison and Kirschner, 1988), filopodial protrusion occurs when actin filaments within filopodia are stationary relative to the substrate and F-actin is polymerized distally (clutch engaged). When adhesion to the substrate is lessened (clutch disengaged), retrograde movement of actin bundles occurs through treadmilling and the activation of myosin. As predicted by the clutch hypothesis, the loss of myosin function attenuates retrograde actin flow and filopodial growth (Lin et al., 1996). Myosin, in addition to powering the retrograde flow of F-actin, may enable the movement of vesicles and other material to the filopodial tip and link the cortical actin cytoskeleton to the membrane (reviewed by Jay, 2000). Furthermore, by coupling the extracellular substrate to the growth cone cytoskeleton, cell adhesion molecules act as molecular clutches and directly regulate growth cone motility (reviewed by Suter and

Forscher, 2000). In now classic experiments, Letourneau (1975a,b) demonstrated that growth cone adhesion to the underlying substrate determined the extent of axon elongation, growth cone morphology, and the preferred substrate for neurite growth.

Growth cone morphology as a reflection of growth cone behavior

The question of how the form of growth cones relates to their function during axon growth and guidance has intrigued developmental neurobiologists ever since their discovery by Ramon y Cajal. Since then, investigators have studied growth cone morphology and behavior, both *in vitro* and *in vivo*, in considerable detail.

David Bentley and colleagues, using the embryonic grasshopper limb bud as a model to study the behavior of identified neurons, provided some of the first detailed descriptions of growth cone morphology during periods of outgrowth by the axons that "pioneer" the nerve pathway. Pioneer axons travel a distinctive route from the distal limb bud to the CNS (Bentley and Keshishian, 1982; Ho and Goodman, 1982). Growth cones of pioneer axons are branched, contain many filopodia, and display characteristic morphological changes as they orient along different segments of their pathway (Caudy and Bentley, 1986). Pioneer growth cones enwrap and form dye-coupled connections with a sequential set of "guidepost cells" (Bentley and Keshishian, 1982; Taghert et al., 1982), whose ablation causes severe defects in pioneer axon pathfinding (Bentley and Caudy, 1983). Filopodial contact with a higher affinity substrate, such as a guidepost cell, is sufficient to reorient growth cones. This leads to retraction of processes in non-selected directions (Caudy and Bentley, 1986), dilation of the contacting filopodium (O'Connor et al., 1990), and selective microtubule invasion of the dilated filopodium, as it becomes the nascent axon (Sabry et al., 1991). Others have shown that microtubule

dynamics must be coordinated with actin dynamics within growth cones to regulate axon extension and growth cone steering in response to guidance cues (Tanaka and Kirschner, 1995; Tanaka et al., 1995).

Growth cone morphology and behavior often change at specific "choice points," where growing axons must make appropriate decisions about pathway selection. The plexuses of the vertebrate spinal cord, where spatially intermixed neurites sort into muscle fiber specific bundles prior to entering particular nerve trunks, serve as an example of this principle. Motoneuron growth cones are highly complex, large and lamellipodial, upon entering decision regions such as the lumbar plexus, and remain simple, small and blunt, while traversing non-decision regions such as the spinal nerve (Tosney and Landmesser, 1985). Behavior of axons, measured by frequency of turning, turn angle, and fiber divergence is also considerably different between decision and non-decision regions: axons greatly alter their trajectory in the plexus, while remaining on straight courses in spinal nerves.

Likewise, growth cones of retinal axons display markedly different morphologies and behaviors along different segments of the vertebrate retinofugal pathway. Mason and colleagues, using the mouse visual system as a model, have elegantly described differences between growth cones of "crossed" and "uncrossed" retinal axons at the optic chiasm. Both crossed and uncrossed retinal axons are tipped with relatively simple growth cones in non-decision regions of the retinofugal pathway, such as the optic nerve, and are tipped with complex growth cones that are broad and contain many filopodia, at the chiasmatic midline (Bovolenta and Mason, 1987; Godement et al., 1990). Axons that will not cross pause to extend multiple growth cone branches within a prescribed zone at the optic chiasm and then abruptly turn away from the midline and

reorient toward the ipsilateral side of the brain (Godement et al., 1990, 1994; Sretavan and Reichardt, 1993). Crossing axons pause, but cross the midline without undergoing the characteristic morphological change seen in uncrossed axons (Godement et al., 1994). These studies suggest that guidance cues located at the optic chiasm influence retinal axon morphology and pathfinding behavior, and importantly, operate differently on crossed versus uncrossed retinal axons. Interestingly, radial glia form a palisade at the optic chiasm where crossed and uncrossed axons diverge from one another (Marcus and Mason, 1995; Marcus et al., 1995). *In vitro*, crossed retinal fibers readily traverse clusters of chiasmatic neurons and glia, while uncrossed axons avoid them (Wang et al., 1995). Therefore, cues underlying the differential response patterns of retinal axons are likely localized within the population of midline cells encountered by retinal growth cones at the optic chiasm.

Changes in the growth cone cytoskeleton have been correlated with specific growth cone behaviors during axon growth and guidance. For instance, growth cones navigating the mammalian corpus callosum pause and undergo characteristic elaborations in morphology beneath their cortical targets (Halloran and Kalil, 1994). Interstitial axon branches form where the leading growth cones pause and elaborate *in situ* (Halloran and Kalil, 1994), and a corresponding sequence of growth cone pausing, elaboration, and branching occurs *in vitro* (Szebenyi et al., 1998). During branch formation *in vitro*, growth cones pause for many hours, elaborate, and form looped microtubules within their enlarged central regions (Dent et al., 1999). In transition regions of growth cones or at axon branch points, looped or bundled microtubules splay apart and F-actin accumulates at sites containing dynamic microtubules (Dent and Kalil, 2001). Disrupting the polymerization of either microtubules or F-actin inhibits axon

Neuron-glia interactions

Despite their prevalence in neural tissue and their remarkable morphological diversity across phyla, glia were historically thought of as nothing but support cells for neurons. Persistence by many glial researchers has falsified this notion, and clearly demonstrated that glia play vital roles in neural development, maintenance, and regeneration. Glial cells are far from passive, and cooperate interactively with neurons in seemingly every phase of brain function. For brevity, we will consider here only the roles ascribed to glia that are relevant to this thesis, namely their interactions with neurons during neural development.

Glial-cell involvement in growth cone guidance in the central nervous system

Considerable evidence suggests that glial cells of both vertebrate and invertebrate nervous systems act as intermediary targets in growth cone guidance and provide both permissive and restrictive substrates for axon growth. Not only do glia provide scaffolds for neuronal migration during cortical development (Rakic, 1978, 1991), but glial pathways in the vertebrate optic nerve and corpus callosum (Silver and Sapiro, 1981; Silver et al., 1982, 1987), and in the grasshopper and fly CNS (Bastiani and Goodman, 1986; Jacobs and Goodman, 1989), promote axon elongation and serve as instructive guides for pathfinding growth cones. Conversely, glia also play inhibitory roles during axon guidance, and act as barriers to restrict axon outgrowth. Astrocytes at the dorsal root and roof plate of the vertebrate spinal cord express growth inhibitory molecules, such as sulfated proteoglycans, and may prevent errant axon projections during development (Snow et al., 1990; Pindzola et al., 1993).

more axons cross the midline than wildtype, with normally ipsilateral axons misprojecting across the midline and commissural axons projecting more than once. Comm is transiently expressed by midline glia and is transferred to growth cones of commissural axons as they cross the midline (Tear et al., 1996). Robo belongs to a new subgroup within the IgG superfamily of cell surface receptors, and is expressed by all ipsilaterally projecting axons and by commissural axons after they cross the midline (Kidd et al., 1998a). Robo recognizes a repulsive cue at the midline, preventing ipsilateral projections from axons expressing high amounts of Robo, and preventing commissural axons from re-crossing the midline after Robo levels are upregulated *en passant* (Kidd et al., 1998b). After transfer of Comm to commissural growth cones, Robo levels are downregulated, leaving them immune to the negative cues that would otherwise restrict growth in midline territory. Other genes regulating axon guidance at the midline have also been identified. A midline glial specific gene, *slit*, encodes a secreted molecule containing multiple extracellular matrix protein motifs (Rothberg et al., 1988, 1990). Slit has been shown genetically (Kidd et al., 1999) and biochemically (Brose et al., 1999) to be a ligand for *robo*. Slit has subsequently been shown to be the midline repellent for Robo expressing axons. Robo normally interacts with Slit and repels axons from the midline, but after picking up Comm, commissural growth cones are no longer repelled by Slit. Instead, Netrin, yet another glia-derived midline cue, attracts commissural axons. Midline glia express *netrin A* and *netrin B* (Harris et al., 1996), which serve as chemoattractants to guide commissural axons expressing the netrin receptor Frazzled (Kolodziej et al., 1996) to the midline. After crossing the midline, commissural growth cones run out of Comm and re-express Robo, preventing them from re-crossing the midline because of repulsive interactions with Slit.

As in *Drosophila*, a specialized population of cells at the vertebrate midline, the floorplate of the spinal cord, regulates the proper growth behavior of contralaterally projecting axons. The vertebrate floorplate, like the fly midline, secretes the long-range chemoattractant netrin-1 (Kennedy et al., 1994; Serafini et al., 1994). Long-range guidance cues are insufficient, however, for the proper crossing of commissural axons at the vertebrate midline. Several mouse mutations, including the Dansforth's Short-tail (*Sd*) and homozygous null mutants for the transcription factor Gli2, lack a floorplate and display short-range axon guidance defects at the midline. In *Sd* mutants, commissural axons either reach the midline and stall or cross but misproject out of the correct longitudinal plane (Bovolenta and Dodd, 1991). In *Gli2* mutant mice, axons properly project to the ventral midline but terminate inappropriately where the floorplate would normally be located (Matise et al., 1998, 1999). These studies suggest that local guidance cues present at the vertebrate floorplate are necessary for commissural axon guidance. In chick embryos, an interaction of two cell adhesion molecules, axonin-1 on commissural axons and NrCam on floorplate cells, regulates short-range interactions at the vertebrate midline. NrCam provides a positive signal for axonin-1 expressing axons, allowing commissural axons to cross the midline. If the axonin-1/NrCam interaction is blocked *in vivo* or *in vitro* with specific antibodies, the floorplate is no longer permissive for growth, and commissural axons turn prematurely without projecting across the midline (Stoeckli and Landmesser, 1995; Stoeckli et al., 1997). Therefore, negative cues acting to repel axons at the floorplate are masked by normal axonin-1/NrCam interaction, allowing commissural axons to cross. Although repulsive signaling at the vertebrate midline has yet to be fully characterized, the Eph/ephrin signaling pathway

appears to be involved as the ligand ephrin B3 is strongly expressed at the floorplate (Bergemann et al., 1998).

The similarities between the vertebrate and invertebrate midline are striking. Both systems rely on a central population of specialized cells, the midline glia of *Drosophila* and the floorplate cells of the vertebrate spinal cord, to regulate the specificity of axon projections at a binary decision point for neural growth cones.

Peripheral glia in* Drosophila *and vertebrates

In grasshopper and fly embryos, glia act as intermediate targets during the formation of the intersegmental and segmental nerves of the peripheral nervous system (Auld, 1999). Axons forming the peripheral nerves encounter a series of immature glia, including segmental boundary cells, as they extend laterally across the longitudinal connectives. In grasshopper embryos, ablation of segmental boundary cells prevents pioneer motor axons from exiting the CNS (Bastiani and Goodman, 1986). Although axons also appear to follow glia out of the fly CNS, examination of the *glial cells missing* phenotype suggests that in contrast to grasshopper, segmental boundary cells are not required for the formation of peripheral nerves in *Drosophila* (Jones et al., 1995). The loss of peripheral glia located at the CNS/PNS border in *Drosophila*, however, results in defasciculation of the intersegmental and segmental nerve branches, and suggests that peripheral glia aid in axon fasciculation at the exit region of the embryonic CNS (Jones et al., 1995; Hosoya et al., 1995; Vincent et al., 1995; Sepp et al., 2001).

After motor axon pioneers have crossed into the PNS, peripheral glia located at the exit region of the embryonic fly CNS begin to migrate and extend cytoplasmic processes to enwrap the peripheral nerves (Sepp et al., 2000). Simultaneously, axons

of peripherally located sensory neurons project towards the CNS, and fasciculate with motor axons in the peripheral nerves. During embryogenesis, peripheral glia preferentially associate with sensory axons, and envelope the portion of the peripheral nerves bearing their axons; by the end of larval development, peripheral glia cover the entire extent of the peripheral nerves, including the distal-most lengths of the motor axons (Sepp et al., 2000). When peripheral glia are genetically ablated, sensory axons display deficits in axon growth and guidance, while motor axon trajectories remain relatively unaffected (Sepp et al., 2001). Interactions between peripheral glia and sensory axons may therefore be required for the development of sensory projections in the fly PNS.

Reciprocal neuron-glia interactions also regulate critical aspects of peripheral nervous system development in vertebrates. Neuron-produced neuregulins influence the differentiation, proliferation, and survival of peripheral Schwann cells, and Schwann cells in turn regulate axon fasciculation, maintenance of synapses, and ultimately, neuron survival (reviewed by Lemke, 2001). Schwann cells normally express the neuregulin receptors ErbB3 and ErbB2 (Meyer and Birchmeier, 1995; Meyer et al., 1997). In mice lacking those receptors, peripheral nerves are devoid of glia, axons have defects in fasciculation, and massive numbers of both sensory and motor neurons die (Riethmacher et al., 1997; Woldeyesus et al., 1999). Neuregulins can also induce the migration of Schwann cells, and together with the capacity of Schwann cells to provide trophic support for axons, might enhance nerve regeneration in the PNS (Mahanthappa et al., 1996). The low affinity neurotrophin receptor, p75, also plays a dual role in neural and glial development, and promotes both axon elongation and the migration of Schwann cells (Anton et al., 1994; Bentley and Lee, 2000). Time-lapse imaging of

growing axons and peripheral glia in zebrafish embryos demonstrates that axons and glia co-migrate with remarkable synchrony, and suggests that contact based axon-glia interactions might regulate the formation of peripheral nerves (Gilmour et al., 2002). By genetically misdirecting peripheral nerves, Gilmour and colleagues (2002) demonstrated that axons normally direct glial migration, and further, by ablating peripheral glia, showed that glia are required for axon fasciculation and the correct organization of peripheral nerve bundles.

Cell adhesion molecules in neuron-glia communication

Many neuron-glia interactions involve direct cell-cell contact, and cell adhesion plays critical roles in regulating these associations. Cultured glial cells typically provide good substrates for neuron growth and promote neurite elongation through adhesive interactions. Function-blocking experiments demonstrate that neurite outgrowth on cultured Schwann cells is regulated by the homophilic cell adhesion molecule L1 (Bixby et al., 1988; Kleitman et al., 1988; Seilheimer and Schachner, 1988). Extension on Schwann cells by motor neuron neurites not only depends on L1, but also on the calcium-dependent cell adhesion molecule N-cadherin, and on integrins (Bixby et al., 1988). In chick, N-cadherin function is necessary for axons of dorsal root ganglion (DRG) neurons to extend onto the upper surfaces of cultured Schwann cells (Letourneau et al., 1990). Similariy, N-cadherin and beta1-integrin regulate neurite elongation on CNS-derived astrocytes (Tomaselli et al., 1988; Neubauer et al., 1988). L1 also appears to promote neurite extension on astrocytes, since expression of recombinant L1 in rat astrocytes enhances cerebellar granule cell neurite extension *in vitro* (Yazaki et al., 1996). Müller cells, the principal glial cells of the retina, promote retinal neurite

outgrowth through intercellular interactions involving the adhesion molecules NCAM, L1, and N-cadherin (Drazba and Lemmon, 1990).

In addition to facilitating neurite elongation, the same set of adhesion molecules reciprocally influences Schwann cell behavior in response to sensory axons. L1 interactions regulate multiple steps in Schwann cell maturation, including the expression of myelin-specific components, and the linear alignment with and enwrapment of individual DRG axons (Seilheimer et al., 1989; Wood et al., 1990). N-cadherin has also been shown to mediate Schwann cell adhesion with and linear alignment along DRG axons (Letourneau et al., 1991; Wanner and Wood, 2002). Early events in Schwann cell-DRG interactions are mediated by the adhesion molecules axonin-1 and Nr-CAM, as application of antibodies against either disrupts their heterophilic binding and prevents the formation of contacts between co-cultured DRG neurites and Schwann cells (Suter et al., 1995). Moreover, the same adhesion molecules that regulate neurite extension on glial surfaces and glial association with axons regulate Schwann cell-Schwann cell adhesive interactions (Letourneau et al., 1991; Wanner and Wood, 2002).

Other molecuIs participate in similar neuron-glia interactions, as glial enwrapment of nerve tracts in *Drosophila* appears to depend on intercellular signaling involving the FGF pathway. Mutation in a *Drosophila* FGF receptor gene, *heartless*, prevents *heartless*-positive glia from migrating and enwrapping the longitudinal axon tracts of the embryonic fly CNS (Shishido et al., 1997). Likewise, a membrane-bound FGF-like signal triggers peripheral glia to ensheath axon tracts within the developing grasshopper CNS (Condron, 1999).

Olfactory system development

The neuroanatomical construction of olfactory systems differs dramatically from sensory systems that rely on topographical "mapping" of neural connections from sensory organs to CNS targets, such as the visual, somatosensory, and auditory systems (see Burd and Tolbert, 2000). Olfactory receptor neurons (ORNs), unlike other sensory cells, respond to molecular cues in their environment that, by their nature, do not contain spatial information. Discrimination of olfactory information begins at the level of ORNs, which are distributed in olfactory epithelia without respect to odor specificity. ORNs recognize unique molecular attributes of odorants, called odotopes (Shepherd, 1987), and ORNs that recognize the same odotope of an odorant presumably express the same odorant receptor protein. ORNs that express the same odorant receptor are widely distributed within olfactory epithelia. Their axons all converge on the same glomeruli within the brain, however, leading to the formation of an "odotopic" map (Vassar et al., 1994; Ressler et al., 1994; Mombaerts et al., 1996). Thus, odorant receptor expression by ORNs must be coordinated with the mechanisms that regulate glomerular targeting of olfactory axons, such that functional olfactory systems are successfully constructed.

Origin of ORNs

Across species, the cell bodies of bipolar ORNs are located in peripheral olfactory epithelia, and their axons extend into the CNS to synapse with dendrites of second-order neurons in spheriodal units of neuropil called glomeruli. During mammalian development, paired olfactory placodes located on each side of the embryonic midline invaginate to form olfactory pits, which give rise to the primary

olfactory epithelium and the vomeronasal organ (Cuschieri and Bannister, 1975). The vertebrate olfactory epithelium contains three major cell types: bipolar sensory neurons, support cells, and two distinct varieties of basal cells (see Farbman, 2000). The globose basal cells in mature vertebrate olfactory epithelia generate new ORNs (Graziadei and Monti Graziadei, 1978), which have relatively short life spans and are continually replaced throughout life (reviewed by Farbman, 1990). In insect antennae, cell bodies of ORNs are positioned with three types of support cells at the base of sensory organs called sensilla. In the moth *Manduca sexta*, rudimentary larval antennae are sloughed off at pupation when imaginal disks evaginate to form the pupal antennae, which subsequently develop into adult antennae during metamorphosis (Sanes and Hildebrand, 1976b). Shortly after evagination, adult ORNs are born in the olfactory epithelium of the pupal antennae (Sanes and Hildebrand, 1976), and immediately extend axons that grow toward the brain.

Olfactory mapping and axon guidance in olfactory systems

Olfactory system development occurs in several successive stages. In mammals, ORN axons first extend towards the presumptive olfactory bulb located at the ventral margin of the rostral telencephalon in mammals. Small fascicles of ORN axons extend from the olfactory epithelium to the brain in close association with migratory glial progenitors (Marin-Padilla and Amieva, 1989). A combination of growth-promoting factors expressed within the olfactory nerve pathway, such as laminin and heparin sulfate proteoglycans, and growth-inhibiting chondroitin sulfate proteoglycans in the surrounding mesenchyme, funnel the migrating cells and receptor axons toward the brain (Gong and Shipley, 1996; Whitesides and Lamantia, 1996; Treloar, et al. 1996;

Kafitz and Greer, 1997). The glial cells that accompany receptor axons to the brain, the olfactory ensheathing glia (Raisman, 1985), extend processes ahead of olfactory receptor axons during their migration (Tennent and Chuah, 1996), express growth-promoting molecules on their surfaces (Doucette, 1990; Gong and Shipley, 1996; Treloar et al., 1996), and are themselves attracted to soluble factors released from the bulb (Liu et al., 1995). Even though the distance from the olfactory epithelium to the presumptive bulb is relatively short in mammalian embryos, olfactory ensheathing glia may promote axon growth during the establishment of the olfactory pathway (reviewed by Chuah and West, 2002).

The second stage, the sorting of receptor axons into odor specific bundles, is perhaps the hallmark feature of olfactory system development, and is likely to occur as ORN axons follow a hierarchical set of guidance cues to ever-finer addresses within the olfactory pathway. The coarsest level of segregation occurs at the level of the olfactory epithelium, which can be divided into four zones in mammals, based on the expression patterns of odorant receptor genes (Ressler et al., 1993; Vassar et al., 1993). Differential expression of adhesion molecules has been proposed to regulate differential fasciculation of ORN axons, and thus the sorting of ORN axons into odor specific bundles. ORN axons and olfactory ensheathing cells express various adhesion molecules, including the embryonic form of N-CAM (Miragall et al., 1989; Whitesides and LaMantia, 1996), as they extend from the olfactory epithelium. A homophilic cell adhesion molecule identified by Kensaku Mori and colleagues, OCAM (olfactory cell adhesion molecule), is expressed by ORNs located in three of the four epithelial zones (Yoshihara et al., 1997). OCAM-positive axons segregate from OCAM-negative axons and terminate in the olfactory bulb in a zone specific manner, thus making OCAM a

candidate molecule for the broad grouping of zonally related ORNs (reviewed in Yoshihara and Mori, 1997; Mori et al., 1999). Subsets of ORNs also express cell-surface carbohydrates that have recently been proposed to function as axon-axon recognition molecules (Puche et al., 1996; St John and Key, 1999). The plant lectin, *Dolichos biflorus* agglutinin (DBA), labels a subset of ORN axons that selectively fasciculate upon entering the olfactory nerve layer and project to the dorsomedial bulb (Key and Akeson, 1993). Interestingly, DBA-reactive axons fail to terminate in caudal glomeruli in mice lacking galectin-1, an endogenous lectin that binds N-acetylactosamine (Puche et al., 1996). Galectin-1, which is expressed by olfactory ensheathing cells, could serve to cross link axons expressing molecules containing common glycoconjugate moieties (St John and Key, 1999). Subsets of ORN axons also express neuropilin-1, a guidance receptor that binds Sema3a (Kawakami et al., 1996; Takahashi et al., 1999). Sema3a is expressed by ensheathing cells in the olfactory nerve layer, and normally restricts neuropilin-1-positive axons from terminating in Sema3a-positive regions of the bulb. In mice lacking Sema3a, neuropilin-1-positive axons are misrouted and fail to terminate in the restricted pattern observed in wild-type animals (Schwarting et al., 2000). Therefore, semaphorins and their receptors also appear to regionally pattern axon projections in relatively broad areas of the olfactory bulb. In *Manduca sexta*, fasciclin II, a homophilic adhesion molecule related to N-CAM and O-CAM, is expressed by a large subset of ORN axons, and ORN axons sort into fasciclin II-positive and fasciclin II-negative bundles after encountering sorting zone glia at the entrance to the olfactory lobe (Rössler et al., 1999; Higgins et al., 2002). Olfactory ensheathing cells in mammals and sorting zone glia in *Manduca* may similarly enable the segregation of ORN axons into fascicles of like specificities.

Ultimately, the finest level of axon segregation is defined by expression of odorant receptors (ORs), which constitute large multigene families first identified in rat (Buck and Axel, 1991). ORNs are thought to selectively express a single OR out of around 1000 possible receptor subtypes in rodents (Strotmann et al., 1992; Sullivan et al., 1996; Malnic et al., 1999). Axons from ORNs expressing the same OR converge on the same one or two glomeruli in the bulb. This can be visualized either by using *in situ* hybridization to detect mRNA encoding a single odorant receptor subtype (Vassar et al., 1994; Ressler et al., 1994), or by using mice engineered such that ORNs expressing a particular OR are tagged with a reporter gene (Mombaerts et al., 1996; Wang et al., 1998). Recently, ORs have been identified in the fly by a combination of differential screening and analysis of *Drosophila* genomic databases (Clyne et al., 1999; Vosshall et al., 1999; Gao and Chess, 1999). Similar to the mouse, *Drosophila* ORs (DORs) are expressed by subsets of ORNs at the level of olfactory sense organs, and axons expressing the same DOR project to the same glomerulus in the brain (Vosshall et al., 2000; Gao et al., 2000). Since ORNs express OR genes before their axons reach the brain (Sullivan et al., 1995), ORNs must be pre-specified for both their odorant sensitivities and their glomerular targets. OR proteins themselves have been proposed to function as homophilic adhesion molecules, and enable selective fasciculation among receptor axons bearing the same OR proteins (Singer et al., 1995).

Finally, in the third stage, receptor axon bundles target discrete areas of neuropil and initiate the formation of glomeruli in the bulb. The chemical cues defining exact glomerular targets have yet to be identified. Do the synaptic partners of receptor axons, mitral/tufted cells in mammals, express target cues necessary for axon recognition? In moths, surgical removal of mitral-like target cells early in development does not prevent

glomerularization of the antennal lobe (Oland and Tolbert, 1998). Furthermore, topographic projection of ORN axons that express the P2 odorant receptor gene proceeds normally in transgenic mice lacking projection neurons or GABAergic interneurons after targeted gene disruption (Bulfone et al., 1998). These findings suggest that target cells of ORN axons do not influence glomerulus formation or the specification of glomerular targets. During receptor axon ingrowth, glial cells form a rind around the central neuropil of the moth antennal lobe (Oland and Tolbert, 1987), and radial glial endfeet form the glial limitans around the presumptive olfactory bulb in mammals (Valverde et al., 1992). Whether these glia provide positional information to ingrowing axons remains to be seen. There is genetic evidence, however, suggesting that ORs expressed by growing receptor axons play a role in target selection. Receptor-swap experiments in mice, where the coding region of P2 (OR gene) is replaced with a different OR subtype, M12, show that ORNs rely on OR expression for their correct topographic projection (Wang et al., 1998). When axons that normally express the P2 OR are forced to express M12, their axons fail to converge on either the P2 or the M12 glomerulus, but instead converge at an intermediate position. Moreover, both odorant specificity and glomerular targeting are regulated by OR subtype expression, such that swapping ORs shifts both the odorant sensitivities and the location of labeled glomeruli receiving innervation from the ORNs bearing the swapped OR transgene (Bozza et al., 2002). By removing 5' untranslated regions from OR transgenes, Vassalli and colleagues (2002) recently demonstrated that non-coding sequences located upstream of two separate OR genes confer zonal expression of ORs in the olfactory epithelium, and consequently, axon targeting in the olfactory bulb. ORNs expressing truncated

"minigenes" were not restricted to their normal zone in the olfactory epithelium, and their axons converged onto ectopic glomeruli in the bulb (Vassalli et al., 2002).

Second-order projection neurons extend their dendrites to synapse in glomeruli, and project their axons to higher olfactory centers in the brain. In the *Drosophila* olfactory system, the lineage and birth order of projection neurons appears to prespecify the anatomical positioning of their dendritic projections (Jefferis et al., 2001). This unexpected finding has led Jefferis and colleagues to hypothesize that cell-cell recognition molecules present on ORN axon terminals and projection neuron dendrites function to correctly match pre- and post-synaptic connections in specific glomeruli. Since glomerulus targeting is unaffected in mice lacking olfactory mitral/tufted cells (Bulfone et al., 1998), projection neurons might not direct axon targeting, but instead, as suggested in the fly, ensure reciprocal specificity in pre- and post-synaptic connections.

The role of odorant-evoked activity does not seem critical for glomerular targeting of ORN axons, since the pattern of glomerular convergence appears normal for M50 and P2 projections in mice lacking the olfactory cyclic nucleotide gated channel gene (Lin et al., 2000; Zheng et al., 2000). Subtle abnormalities were observed for the projections of M72-labeled axons in the same mutant background (Zheng et al., 2000). During the neonatal period, however, removal of olfactory input by unilateral naris closure leads to morphological changes in the deprived olfactory epithelium (Stahl et al., 1990) and in the olfactory bulb (Brunjes et al., 1994). Odorant-evoked electrical activity appears to regulate ORN survival and the persistence of axonal connections to the olfactory bulb, perhaps through activity-dependent competition for trophic factors present in the bulb (Zhao and Reed, 2001). In agreement with this hypothesis, removal of the olfactory bulb in adult rodents leads to massive ORN turnover and axon regrowth, however ORNs

eventually die and their axons degenerate without central targets (Schwob et al., 1992), suggesting that olfactory bulbs provide trophic support for ORNs.

Manduca sexta ***as a model for studying olfactory system development***

Insects have been used to great advantage in the field of developmental neurobiology, with each model taxon having unique attributes that lends itself for study. Large holometabolous insects, including the hawkmoth *Manduca sexta*, are particularly well suited for studies involving experimental manipulation due to the animals' large size and hardy nature. In *Manduca*, a massive postembryonic wave of development occurs during metamorphosis of the juvenile caterpillar into the adult moth, when both sensory and central olfactory structures are readily accessible.

The entire adult olfactory system of *Manduca* is generated during metamorphic development. ORNs located in the antennae arise independently of, and are physically separated from, their postsynaptic targets in the brain (Figure 1.2), allowing for the two populations of neurons to be manipulated separately. Though composed of fewer numbers, the cellular organization of the primary olfactory center in *Manduca* is very similar to that of the vertebrate olfactory lobe (Boeckh and Tolbert, 1993; Hildebrand and Shepherd, 1997). Both are organized into discrete functional units of neuropil called glomeruli, where terminals of ORN axons synapse with dendrites of second-order target neurons (63 glomeruli in *Manduca*; around 2000 in the mouse). Insect and vertebrate glomeruli are sites of extensive axon convergence, are served by uniglomerular output neurons, and have conspicuous round shapes that are delimited by glial envelopes.

A complex pattern of intercellular communication between ORN axons, target cell dendrites, and central glia operate to form the adult olfactory system of *Manduca* (Figure

1.3). During metamorphic development, ingrowing axons begin to arrive at the antennal (olfactory) lobe late in stage 3 (18 stages ~ 1day each). The cell bodies of post-mitotic target neurons are clustered in discrete cell-body packets located outside of the antennal lobe neuropil, which contains their branching neurites. At stage 3, a continuous border of glial cells surrounds the antennal lobe neuropil. As they arrive in the antennal lobe, ORN axons pierce the glial rind and encircle the central neuropil just beneath the glial layer before terminating in a fringe. Beginning at late stage 5 and proceeding throughout stage 6, ORN axon terminals segregate into nodules called protoglomeruli, which glial cells then migrate to enwrap. Dendrites of projection neurons extend into protoglomeruli almost as soon as they form (Malun et al., 1994), whereas dendrites from interneurons extend to meet axon terminals only after glial cells have enwrapped their boundaries (Oland et al., 1990). The last ORN axons arrive by stage 9, and the antennal lobe is morphologically indistinguishable from the adult lobe by stage 12. Arrival of ORN axons triggers antennal lobe development, as removal of sensory input prevents the formation of glomeruli in the antennal lobe (Hildebrand et al., 1979). Without afferents, dendrites of target neurons fail to arborize in characteristic tufts (Oland and Tolbert, 1990), and antennal lobe glia fail to migrate into the coarse neuropil (Oland and Tolbert, 1987).

Furthermore, antennal lobe glia actively mediate the construction of glomeruli. Reduction of glial cell number results in the formation of an aglomerular antennal lobe that is similar in appearance to lobes deprived of antennal innervation (Oland et al., 1988; Oland and Tolbert, 1988). In addition, glial cells occupying the sorting zone mediate the segregation of ORN axons into glomerulus specific bundles. ORN axons expressing the cell adhesion molecule *Manduca* fasciclin II (MFas II) are normally distributed throughout the antennal nerve, yet as they traverse the sorting zone, MFas II$^+$

axons converge into large fascicles that project to a subset (14-21) of glomeruli (Higgins et al., 2002). When glia are reduced in number, MFas II$^+$ axons travel down the antennal nerve normally, but fail to sort into MFas II$^+$ fascicles after passing through the sorting zone (Rössler et al., 1999). These findings suggest that glial cells are required for proper olfactory system development in *Manduca*.

Much less is known about the glial cells of the antennal nerve. Antennal nerve glia arise in the periphery (Rössler et al., 1999), and enwrap bundles of ORN axons in the mature nerve (Sanes and Hildebrand, 1976). Antennal nerve glia migrate from the antenna to invest the intracranial antennal nerve, distal to the sorting zone, after most ORN axons have reached the brain (Figure 1.3). A set of nerve glia express the GPI-linked isoform of MFas II during late stages of axon ingrowth (Higgins et al., 2002), suggesting the possibility for axon-glia interactions involving homophilic adhesion molecules. The cellular and molecular interactions between ORN axons and glial cells of the olfactory nerve and the antennal lobe remain largely unknown.

Electrical activity does not appear to regulate the organization of the primary olfactory neuropil in *Manduca*. Odorant-evoked electrical activity is not detectable in the antenna until late in metamorphic development, just a few days before the emergence of the adult moth (Schweitzer et al., 1976). Extracellular field-potentials can be recorded from the antennal nerve during development, however, indicating the presence of spontaneous neural activity in the moth olfactory system. Blockade of Na^+-based action potentials with tetrodotoxin during metamorphic development does not effect glomerulus formation; thus antennal lobe development proceeds normally in moths lacking tetrodotoxin-sensitive currents (Oland et al., 1996).

Purpose and significance of studies

Glial reduction experiments in *Manduca sexta* implicate glia as important mediators of axon sorting and glomerulus formation, two critical steps in the development of olfactory systems. Although less direct information is available, glial cells in vertebrates are thought to play similar roles. The following studies aim to characterize the effects of particular glia, known to play critical roles *in vivo*, on the behavior of individual ORN axons *in vitro*. By utilizing the advantages of an insect model system, the following studies provide insight into key cellular interactions that are likely critical to olfactory development in both vertebrate and invertebrate species.

Furthermore, many neuronal connections within the nervous system are formed without spatial topography dictating the patterning of axon projections, but the manner by which these projections form during development is poorly understood. Olfactory systems, being constructed odotopically rather than topographically, provide a model for studying the mechanisms regulating non-topographic map formation in developing nervous systems. In *Manduca*, sorting zone glia mediate the non-topographic sorting of ORN axons into glomerulus-specific bundles. In mammals, ensheathing cells occupying the olfactory nerve layer of the main olfactory bulb are in position to orchestrate the same event. Thus, studying cellular and molecular interactions between ORN axons and sorting zone glia can provide clues to the process of olfactory map formation, which might be similar in all olfactory systems, and additionally, may provide insight into how non-topographic mapping occurs during brain development in general.

Figure 1.1 Schematic diagram illustrating the principal components of the neuronal growth cone. The axon shaft contains microtubules (red) and intermediate filaments (not shown). Microtubules splay apart, loosing their parallel orientation, at the base of the growth cone. The flattened lamellipodium contains a meshwork of actin filaments (green). Filopodial spikes extend from the lamellipodium and are comprised of F-actin bundles. Lamellipodial veils often extend between filopodia in the preferred direction of growth cone advancement.

The neuronal growth cone

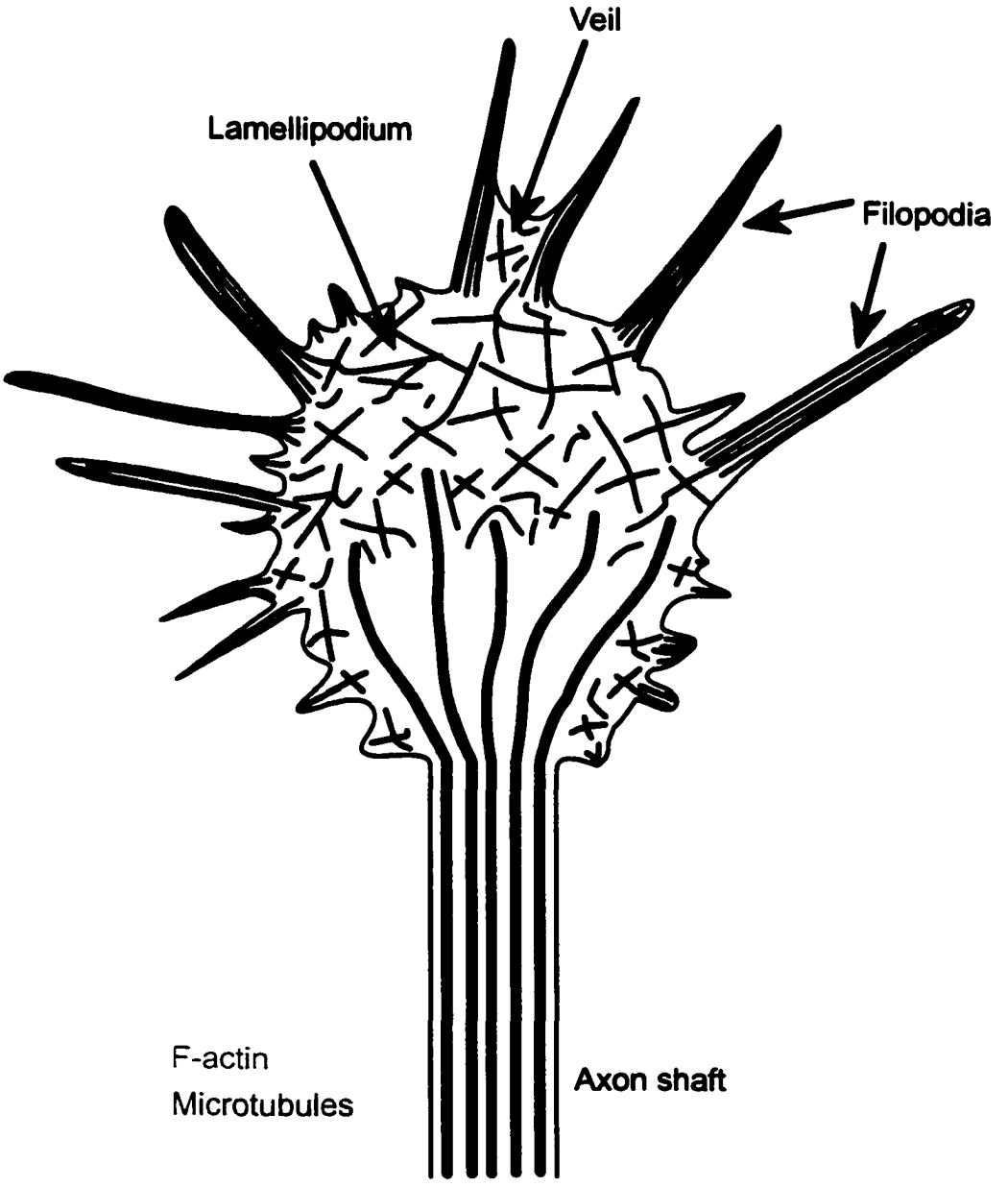

Figure 1.2 Diagrams of the mature antennal (olfactory) system of *Manduca sexta*. **A.** Long antennae extend distally from the head. ORNs in the antenna project axons toward the brain along the antennal nerve, and synapse with the dendrites of second-order neurons in the antennal lobe. **B.** Bundles of ORN axons, traveling in parallel down the antennal nerve, are ensheathed by antennal nerve glia. ORN axons cross and form bundles in the glia-rich sorting zone, and terminate in glomeruli in the antennal lobe. Intrinsic antennal lobe neurons are clustered in cell body packets outside of the antennal lobe neuropil. Dendrites of interneurons and projection neurons extend into glomeruli, which are delimited by glial envelopes.

The primary olfactory pathway of *Manduca sexta*

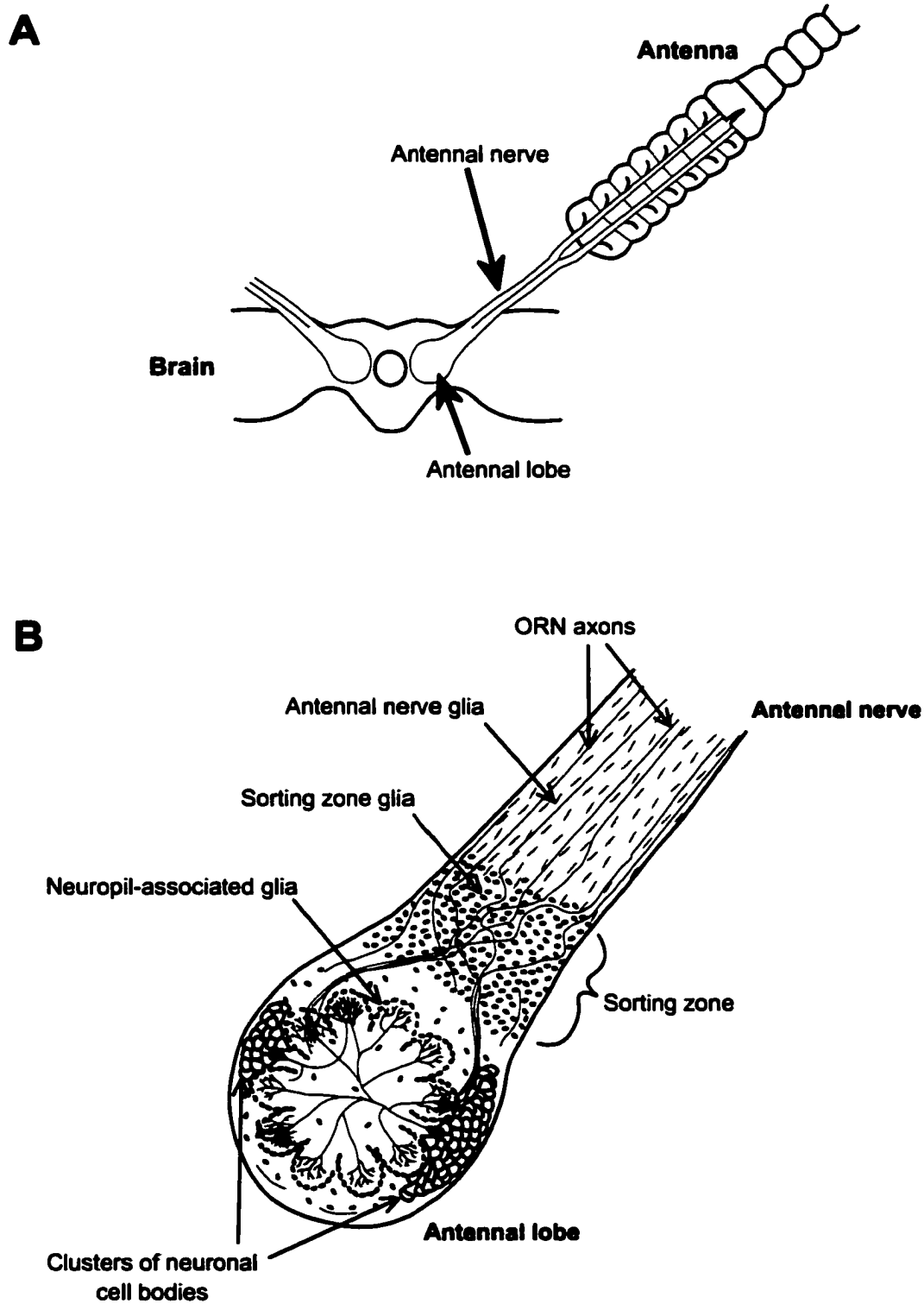

Figure 1.3 Development of the antenna and antennal lobe in *Manduca sexta*. Shortly after their birth, ORNs in the antenna extend axons toward the brain. The first ORN axons reach the antennal lobe at stage 3, after growing from the antenna along the pupal nerve (gray lines). After reaching the brain, ORN axons trigger the proliferation and migration of sorting zone glia (red) to the base of the antennal nerve. Subsequent ORN axons sort into fascicles after encountering sorting zone glia. ORN axons terminate in protoglomeruli in the antennal lobe and trigger the migration of neuropil-associated glia (green) to the borders of nascent glomeruli. Antennal nerve glia (purple) are born in the antenna after stage 3, and migrate down the antennal nerve and enwrap bundles of ORN axons.

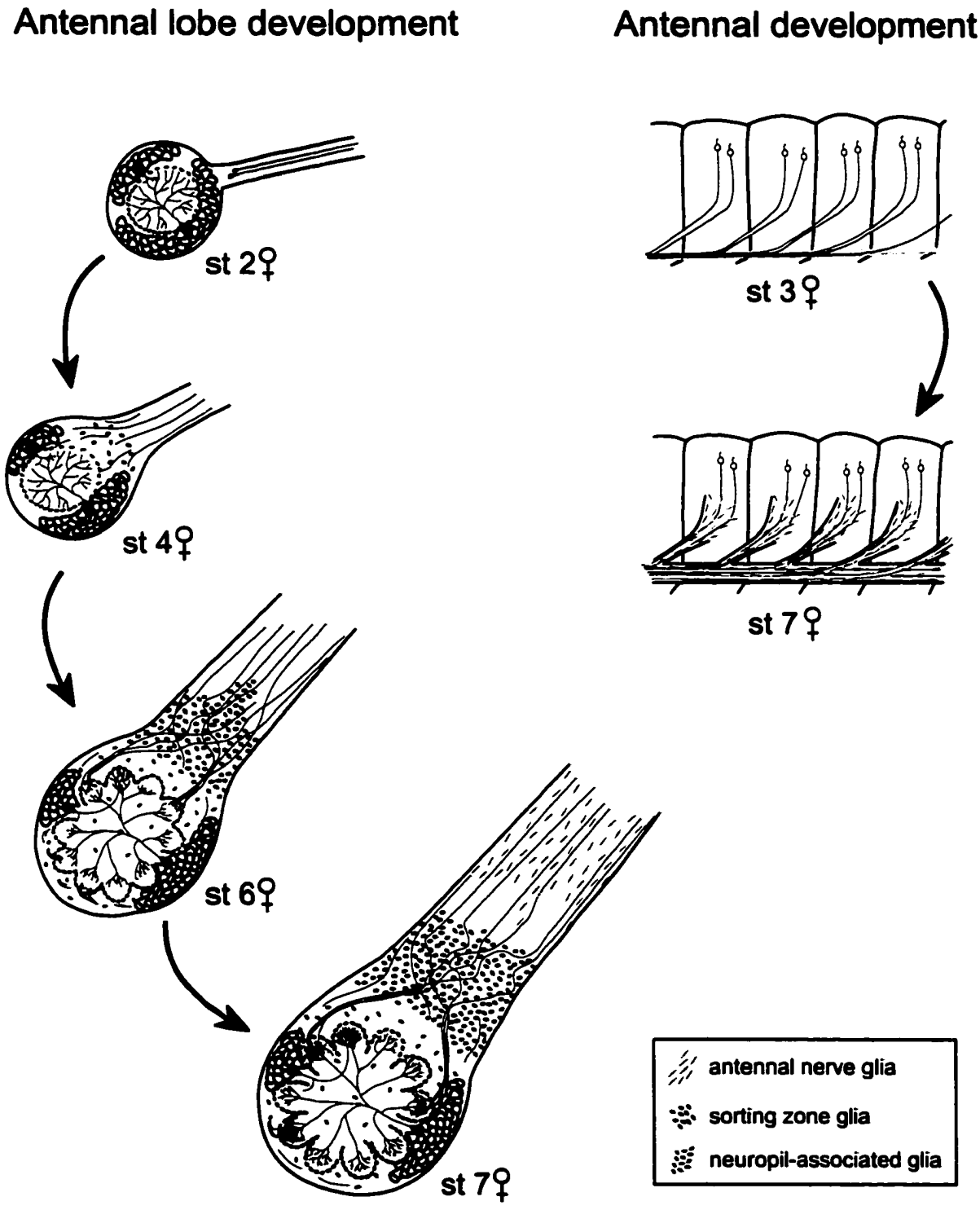
Antennal lobe development
Antennal development
st 2♀
st 3♀
st 4♀
st 7♀
st 6♀
st 7♀
antennal nerve glia
sorting zone glia
neuropil-associated glia

CHAPTER 2: *IN VITRO* ANALYSES OF INTERACTIONS BETWEEN OLFACTORY RECEPTOR GROWTH CONES AND GLIAL CELLS THAT MEDIATE AXON SORTING AND GLOMERULUS FORMATION

INTRODUCTION

Developing olfactory pathways provide models for studying growth cone guidance in systems where the targeting of sensory axons does not depend absolutely on the location of sensory neurons in the periphery. The cell bodies of olfactory receptor neurons (ORNs) that express the same odorant receptor are widely distributed within broad zones of olfactory epithelia (Ressler et al., 1993; Vassar et al., 1993; Clyne et al., 1999; Vosshall et al., 1999), yet their axons converge on the same glomerular targets in the brain (Vassar et al., 1994; Ressler et al., 1994; Mombaerts et al., 1996; Vosshall et al., 2000; Gao et al., 2000). The initial segregation of olfactory information is therefore dependent on the proper sorting of ORN axons. Genetic swapping of odorant receptors in mice leads to the mistargeting of ORN axons and demonstrates that odorant receptors are involved in axon pathfinding (Mombaerts et al., 1996; Wang et al., 1998; Bozza et al., 2002). However, axon targeting in olfactory systems also appears to depend on the coordinated expression of many different cell-surface (Puche et al., 1996; Treloar et al., 1997; Yoshihara et al., 1997; St. John and Key, 1999, 2001; Mori et al., 1999; Walz et al., 2002) and extracellular guidance molecules (Gong and Shipley, 1996; Treloar et al., 1996; Schwarting et al., 2000).

While our understanding of olfactory axon guidance has grown, many of the intercellular interactions that regulate axon guidance and target selection remain largely unknown. The olfactory system of the moth *Manduca sexta* shares many neuroanatomical and physiological similarities with vertebrate olfactory systems (Hildebrand and Shepherd, 1997) and is well suited for studies that examine the cellular mechanisms that underlie critical aspects of olfactory pathway development (Oland and Tolbert, 1996; Hildebrand et al., 1997). In *Manduca*, glial cells are required for sorting

METHODS

Animals

Manduca sexta (Lepidoptera:Sphingidae) were reared on an artificial diet under a long day photoperiod (17 h light, 7 hr dark) in environmental chambers maintained at 25°C and 50-60% relative humidity. Under these conditions, adult metamorphic development occurs over 18 stages, each lasting 1-4 days, starting at pupation and ending at eclosion to the moth. Pupae were staged by examining morphological changes in external adult structures visible beneath the pupal cuticle after fiber-optic illumination (Tolbert et al., 1983; Oland and Tolbert, 1987; Dubuque et al., 2001).

Removal of antennal input

In some animals, one antennal anlage was removed during the first stage of adult metamorphic development, before the birth of olfactory receptor neurons that reside in the antennal receptor epithelium (Sanes and Hildebrand, 1976). An opening was made in the cuticle covering the base of the antenna and the exposed antennal anlage was excised with forceps. The inner surface of the antennal trough was then scraped clean and the opening to the head plugged with melted wax, preventing axons from the surviving distal antennal segments from reaching the brain. Operated pupae were allowed to develop in an environmental chamber until they reached early stage 7 of adult metamorphic development. In *Manduca*, antennal innervation of the primary olfactory system is strictly ipsilateral and the removal of one antennal anlage does not lead to aberrant innervation from the contralateral antenna (Sanes et al., 1977; Kent, 1985). Therefore, this surgical procedure completely deprives the antennal lobe on the operated side of its normal antennal (olfactory) input, leaving only minor sensory inputs from the labial palp unperturbed (Kent et al., 1986, 1999).

Preparation of cultures

Explants of olfactory receptor epithelium. Whole antennae were removed from the antennal troughs of stage-4 female pupae and placed into a 35-mm dish containing sterile PBS. Antennae were filleted along a line that visibly marked the border between the olfactory receptor and non-receptor epithelia. Dissected olfactory receptor epithelia were transferred to a sterile polystyrene test tube containing approximately 400 µl of PBS on ice. Receptor epithelium was subjected to mild enzymatic digestion in a Ca^{2+} and Mg^{2+}-free Hanks' balanced salt solution (21250-014, Gibco, Grand Island, NY) containing 0.05 mg/ml collagenase (LS004196, Worthington, Freehold, NJ) and 0.2 mg/ml dispase II (165859, Boehringer Mannheim, Mannheim, Germany). The enzyme-treated antennal tissue was gently triturated with a fire-polished Pasteur pipette, layered onto 6 ml of Culture Saline, and allowed to settle by gravity. Large bits of antennal tissue were removed, leaving behind pieces approximately 100-200 µm in diameter. Culture Saline was then aspirated, leaving aggregated tissue behind, and the step was repeated first with Culture Saline and again with Culture Medium. Explants were evenly suspended in fresh Culture Medium and plated in 100 µl aliquots into the wells of pre-made culture dishes. One antenna provided sufficient explants for three wells. Culture-dish wells were made by attaching coverslips beneath 8-mm diameter holes drilled into the bottoms of 35-mm Falcon dishes. Dish wells were coated with a solution containing 400 µg/ml concanavalin A (C2010, Sigma, St. Louis, MO) and 4 µg/ml laminin (40232, Collaborative Research, Bedford, MA) and rinsed thoroughly with a stream of sterile water prior to cell plating. After plating of explants, culture dishes were sealed with

Parafilm to prevent evaporation and incubated in a 26°C humidified incubator with room air.

Glial cell cultures and co-cultures. Acutely isolated glial cells were prepared using essentially the same methods described previously by Lohr et al. (2002). Briefly, female pupae from stages late 6 to early 7 of metamorphic adult development were cooled on ice, and brains were dissected into 35-mm culture dishes containing sterile Dissecting Medium. Antennal lobes were desheathed, the neuronal cell-body packets were removed, and the antennal lobes were separated from the antennal nerve, leaving only glia and presumably a small number of tracheolar cells intact. Differential dissection was then used to yield one or more of the three distinct populations of olfactory glia (see Fig. 1): 1) sorting zone (SZ) glia, 2) antennal lobe neuropil (NP) glia, or 3) antennal nerve (AN) glia. Tissue was digested with 0.1 mg/ml papain (5125, Calbiochem, La Jolla, CA) in Simple Salt Solution for 4 min at 37°C prior to trituration. Dissociated cells in suspension were then layered onto Recovery Solution in a 15-ml Falcon tube, and 200 units of DNase (D4263, Sigma) in Simple Salt Solution were added to the top layer of suspended cells. Cells were centrifuged at 500 g in a tabletop centrifuge for 4 min. The resultant pellet was resuspended in Culture Medium and centrifuged as above. Cells were again resuspended in Culture Medium and plated into 8-mm wells (100 µl/well) constructed in 35-mm petri dishes. One animal was used per dish of glial cells plated.

For co-cultures, glial cells were resuspended in Culture Medium and added to explant cultures previously grown for one day *in vitro* (1 DIV). For each dish, 50 µl of Culture Medium was removed from the 100-µl bubble of medium overlying the cultured explants, and then gently replaced with 50 µl of the glial suspension. After cell plating,

the culture dishes were sealed with Parafilm and incubated for 2 hrs. Cultures were then flooded with at least 1 ml of Culture Medium.

Unafferented antennal lobes, from animals that had antennal anlagen surgically removed at stage 1, were dissected as above at early stage 7 on the day of the experiment. Afferented antennal lobes were removed from the unoperated side of experimental animals, differentially dissected to obtain NP tissue, and dissociated and plated separately from the unafferented lobes.

Tissue culture solutions

Culture Saline: (Oland et al., 1996): 149.9 m*M* NaCl, 3 m*M* KCl, 3 m*M* $CaCl_2$, 0.5 m*M* $MgCl_2$, 10 m*M* TES, 11 m*M* D-glucose, 3 g/L lactalbumin hydrosylate (11800-026, Gibco), 2.5 g/L TC yeastolate (255772, Difco, Detroit, MI), 10% fetal bovine serum (FBS; HyClone, Logan, UT), 100 U/ml penicillin, 100 µg/ml streptomycin, pH 7.0, 360 mOsm.

Culture Medium: (supplemented Leibovitz's L-15 culture medium, Lohr et al., 2002): The following ingredients were added to 500 ml L-15: 50 ml FBS, 185 mg α-ketoglutaric acid, 200 mg D-(–)-fructose, 350 mg D-glucose, 335 mg DL-malic acid, 30 mg succinic acid, 1.4 gm lactalbumin hydrosylate, 1.4 gm TC yeastolate, 0.1 mg niacin, 30 mg imidazole, 500 µg 20-hydroxyecdysone (H5142, Sigma), 100 U/ml penicillin, 100 µg/ml streptomycin, and 2.5 ml stable vitamin mix (SVM). A 5 ml stock solution of SVM consisted of 15 mg aspartic acid, 15 mg cystine, 5 mg β-alanine, 0.02 mg biotin, 2 mg vitamin B_{12}, 10 mg inositol, 10 mg choline chloride, 0.5 mg lipoic acid, 5 mg p-aminobenzoic acid, 25 mg fumaric acid, 0.4 mg coenzyme A, 15 mg glutamic acid, 0.5

mg phenol red. The pH was adjusted to 7.0 and the osmolarity was raised to 390 mOsm with D-glucose prior to sterile filtration.

Simple Salt Solution: 160m*M* NaCl, 6 m*M* KCL, 78.8 m*M* D-glucose, 10 m*M* HEPES, 100 U/ml penicillin, 100 µg/ml streptomycin, pH 7.0, 420 mOsm.

Recovery Solution: 50% (v/v) Culture Saline and 50% (v/v) Simple Salt Solution, pH 7.0, 380 mOsm.

Dissecting Medium: 50% Leibovitz's L-15 (41300-039, Gibco), 25% (v/v) Culture Saline, 25% Simple Salt Solution with 5 m*M* EDTA, and 18 m*M* D-glucose, pH 7.0, 360 mOsm.

Live-cell microscopy

Explant cultures grown for 1 DIV or co-cultures grown for 2 hrs after the plating of glial cells were used for time-lapse differential-interference-contrast (DIC) imaging experiments. Before being imaged, cultures were flooded with 3 ml of Culture Medium and placed on a temperature-controlled microscope stage to equilibrate. The imaging system included a fixed-stage microscope (BX50WI, Olympus, Tokyo, Japan) equipped with DIC and epifluorescence optics, long-working-distance water-immersion objectives, Uniblitz (Vincent Associates, Rochester, NY) shutters, a Ludl motorized z-drive, a cooled CCD camera (KAF1400, Photometrics, Tucson, AZ), and a Pentium III 550 MHz computer with dual 17-inch monitors and SimplePCI (Compix Inc., Cranberry Township, PA) acquisition and analysis software. A 12V/100W halogen bulb filtered by a green

optical lens (543 nm) was used for bright-field illumination during DIC imaging. A constant dish-temperature of 25°C was maintained with the aid of a temperature controller (TC202A, Harvard Apparatus, Holliston, MA) combined with an open perfusion micro-incubator (PDMI-2, Harvard Apparatus). An insulated chamber enclosed the microscope stage and provided a humidified internal environment that limited disturbances caused by ambient temperature fluctuations and air currents.

After an area within the dish was selected for imaging, a thin layer of canola oil was applied over the Culture Medium surface to prevent evaporation of the culture medium and to provide thermal insulation throughout the imaging experiment. High-magnification images were collected with a 60x objective at 20-min intervals for up to 24 hours. To overcome the small drift in focus that occurred over the imaging period, a series of 5 images at successive focal planes 1 μm apart were collected at each time point. Only the in-focus images at each time point were used.

Rate analysis

Time-lapse movie sequences were used to measure the distances that individual axons grew. Five axons from each co-culture condition were selected for measurement provided they met the following criteria: 1) each axon could clearly be identified as an individual, 2) the growth of the axon could be monitored before and after contact with glial cells, and 3) at least one image from each z-series was in focus for every time point of the movie sequence. Reference markers were placed at the distal tip of growing axons for each time point of the collection and the distances between consecutive markers were measured in microns using SimplePCI (see Fig. 5). Distances, positive for growth and negative for retraction, were recorded between adjacent frames of the

recording and summed over all frames to yield the cumulative distances traveled. Cumulative distances were plotted as a function of time for each measured axon. Growth rates were determined by calculating the slope of regression lines fit to pre-contact and post-contact curves for each plot.

Immunocytochemistry, phallotoxin staining, and confocal microscopy

Labeling of microtubules and F-actin was performed following a slightly modified version of a protocol previously developed for cultured motoneurons from *Manduca* (Matheson and Levine, 1999). Briefly, cultures were rinsed with microtubule-stabilizing buffer (K-PIPES buffer; 80mM PIPES-KOH, pH 6.8, 5 mM EGTA, 2 mM $MgCl_2$) and then fixed and extracted for 30 min in K-PIPES buffer containing 0.5% glutaraldehyde and 0.1% Triton X-100. Autofluorescence was quenched by rinsing cultures three times five minutes each in PBS containing 1 mg/ml $NaBH_4$. Cultures were then rinsed and blocked for 1 hr in PBS containing 0.2% fish skin gelatin and 0.1% Triton X-100 (blocking buffer), and incubated with primary antibody (anti-α-tubulin; T9028, Sigma) diluted 1:800 in blocking buffer for 2 hrs at room temperature. After rinsing, cultures were incubated for 1.5 hrs in a 1:1000 dilution of secondary antibody (goat anti-mouse Cy3; Jackson Immunoresearch, West Grove, PA) in blocking buffer containing approximately 2.5 U/ml, or 83 nM, Alexa-488 conjugated phalloidin (A-12379, Molecular Probes, Eugene, OR), to simultaneously label microtubules and F-actin. Cultures were then rinsed and mounted with coverslips in an aqueous polyvinyl alcohol (PVA)-based medium that included 1,4-diazobicyclo[2,2,2]octane (DABCO) to limit photobleaching. Controls for non-specific labeling were performed by omitting the primary antibody.

by-two contingency tables containing total numbers of simple and complex growth cones from each experimental condition were constructed and tested for statistical differences by Fisher's exact test (Fisher, 1925). Qualitative variables from tested conditions were defined as statistically different at probability value of $p < 0.05$.

Data from preliminary experiments were used to determine that approximately 30 images/dish provided an adequate sample size (number of growth cones) for studies of appropriate power. Five independent experiments that included at least 2 SZ co-culture dishes gave identical results to the experiment analyzed in full detail in Figure 8.

RESULTS

Development of the sorting-zone glial cells and the generation of explant-glial cell co-cultures

In *Manduca*, the first cohort of ORN axons extends into the antennal (olfactory) lobe during stage 3 of adult metamorphic development (Sanes and Hildebrand, 1976; Oland and Tolbert, 1987) and triggers the localized proliferation and migration of a group of central glia away from the antennal lobe neuropil to the most proximal portion of the antennal nerve, called the sorting zone (SZ) (Rössler et al., 1999). Glial cells rapidly fill the SZ during the ensuing developmental stages (Fig. 1*A*) and subsequently influence the fasciculation patterns of ORN axons *en route* to developing glomeruli within the antennal lobe (Rössler et al., 1999). Neuropil (NP) glia, apparently derived from the same set of central precursors in the antennal lobe, are initially confined to a rind surrounding the antennal lobe neuropil. They respond to ORN axon ingrowth by migrating and extending processes to surround "protoglomeruli" formed by the ORN axons (Fig. 1*A*; Oland and Tolbert, 1987).

The anatomical positioning of glial cells within the SZ and the antennal lobe, together with the absence of neuronal cell bodies in the neuropil, makes it possible to establish highly pure glial cultures by differential dissection and dissociation (Figure 1*B*). Glial cells were harvested for culture at early stage 7, when glial density within the SZ nears its peak and before peripheral glial cells migrating down the antennal nerve from the antenna reach the distal edge of the SZ (Fig. 1*A;* Rössler et al., 1999). For co-cultures, dissociated glial cells were introduced to previously plated explants of olfactory receptor epithelium that had been isolated from stage-4 antennae and grown for 24 hrs *in vitro* (Fig. 1*B*).

Behavior and morphology of ORN axons *in vitro*

In vitro, hundreds of olfactory receptor axons extend radially from cultured explants of developing olfactory receptor epithelium (Fig. 1*C*). The robust nature of axonal outgrowth, particularly within the first 48 hours of culture, allowed us to study dynamic changes in axon behavior. Since a dense meshwork of axonal processes surrounded explants, individual axons were distinguishable only at the outermost fringe of axon outgrowth (Fig. 1*C*, *box*). Time-lapse imaging showed that axons elongated while extending and retracting fine branches from their growth cones (not shown). Thin filopodial processes became engorged with cytoplasm during the advancement of motile branches, while non-motile branches were retained but left with little remaining cytoplasm. Most axons had simple, bullet-shaped growth cones (Fig. 1*D*, arrows). Infrequently, large, flattened growth cones were seen at the tips of growing axons (Fig. 1*D*, arrowheads). Multiple branches often arose from the periphery of flattened growth cones. One or two nascent branches would subsequently extend away from the growth cone, leaving the lamellar region behind.

Glial cells from the SZ and antennal lobe neuropil (NP) had very similar morphologies *in vitro*. Glial cell bodies were relatively small (~15μm) and had thin processes with a range of branching patterns (Figs. 1*E-G*). Their small size and distinctive morphologies allowed for easy identification and distinction from ORNs and ORN axons.

Axon behavior after contact with SZ-derived glial cells

Co-cultures containing explants of olfactory receptor epithelium and either SZ or NP glial cells were prepared by differentially dissecting antennal lobes, separately collecting and dissociating SZ and NP tissue, and separately adding SZ or NP glial cells to pre-plated explant cultures. In co-cultures, receptor axons that did not encounter glial cells grew in a pattern indistinguishable from axons of explants grown alone. Single filopodial contact with isolated SZ glial cells, however, was sufficient to markedly influence growth cone morphology and axon behavior. Growth cones contacting SZ glial cells often developed large, lamellar profiles at the point of axon contact (Fig. 2*A*). Elaboration of growth cones began within minutes of glial contact and continued for many hours (Fig. 2*A*, *arrowheads*). Small branches often extended from glial-cell-contacting growth cones (Fig. 2*A*, *open arrowheads in frames 5-7*), but the flattened growth cone morphologies were usually retained. Lamellar processes extended on, but never past, glial processes or cell bodies (Fig. 2*A*, *arrowheads*). Although growth cone flattening was the predominant response to glial-cell contact, glia-mediated alterations in growth cone morphology were variable. Some growth cones branched near their base, while others remained simple after contacting SZ glial cells (Table 1). Contact-mediated branching often resulted in the formation of highly branched growth cones (Fig. 2*B*). Axon branching usually occurred at the point of glial-cell contact, but was not restricted to the growth cone tip (Fig. 2*B*, *arrowhead*). Axon branching continued for several hours after contact, and growth cones usually remained closely associated with the glial cells that they encountered (Fig. 2*B*).

Regardless of the morphological response, the majority of encounters (88%) between individual axons and SZ glial cells resulted in the cessation of growth cone

advancement (Fig. 2*A*, Table1). Growth cones often remained active after glial contact by extending and retracting filopodia, lamellar processes, and/or growth cone branches, yet they routinely failed to advance. A relatively small percentage of axons (12%) did continue to elongate past SZ glial cells (Fig. 2*B*, Table 1), but those axons never had flattened growth cones. Thus after contact with glial cells, growth cones that stopped either flattened, branched or remained simple, whereas growth cones that advanced remained simple or branched, but never flattened. Elongating axons occasionally branched after glial contact before extending over or around the impeding glial cells (Fig. 2*B*). Axons that branched but continued to elongate were counted as "elongating" axons in Table 1. In all recordings analyzed, axons that did not encounter glial cells continued to elongate in close proximity to axons that stalled following glial contact. This finding precludes the possibility that growth cone motility was unintentionally compromised during the process of time-lapse imaging and underscores the importance of glial-cell contact in the alteration of growth cone behavior.

Axon behavior after contact with NP-derived glial cells

NP glial cells evoked the same range of morphological and behavioral changes in ORN axons as SZ glial cells did (Table 1). Again, ORN growth cones flattened (Fig. 3*A*), branched (Fig. 3*B*; Fig. 3C, *open arrow* and *open arrowheads*), or remained simple in morphology (Fig. 3C, *arrow and arrowheads*) following contact with NP glial cells. The distributions of growth cone responses to SZ and NP glial cells were not significantly different ($P = 0.132$) when compared by chi-squared analysis. The contact-mediated formation of flattened growth cones occurred identically to such formation following SZ glial-cell contact, with lamellar processes extending rapidly from stabilized sites of axon-

glial-cell contacts. Elaboration again occurred in direct apposition to the processes or the cell bodies of NP glial cells, often resulting in extension onto but not past NP glial cell processes (Fig. 3*A*, *arrowhead*). Axons that branched following NP glial contact appeared similar in morphology to those branching after SZ glial contact. As with SZ contacts, growth cone branches extended both on and away from the surfaces of NP glial cells (Fig. 3*B*). Axons typically remained closely associated with glial processes while branching (Fig. 3*B*, *arrowheads*; Fig. 3*C*, *open arrowheads*). Some axons remained tipped with simple, bullet-shaped growth cones after contacting SZ (not shown) and NP (Fig. 3*C*, *arrowheads*) glial cells. These simply tipped axons maintained their pre-contact morphology but occasionally engorged with cytoplasm, becoming thicker in appearance following glial cell contact.

Encounters between growth cones and glial cells were long-lived, often lasting many hours after the initial filopodial contact. Most axons (87%) that contacted NP glial cells failed to elongate beyond the contacted glial cells during our recordings. As with SZ contacts, the cessation of growth cone advancement following contact with NP glial cells was not strictly correlated with specific changes in growth cone morphology (Figs. 3*A-C*). The overall percentage of axons stopping after contact with glial cells was nearly identical for SZ (88%) and NP (87%) encounters. Thus contact with SZ and NP glial cells similarly influenced growth cone motility.

Receptor axons respond differently to antennal nerve glial cells

The axonal responses to SZ and NP glial cells were not generalized reactions to cell contact, but rather specific axon behaviors triggered by contact with centrally derived glial cells. Peripheral glial cells from the antenna elicited an entirely different behavior in

ORN axons after growth cone contact (Fig. 4). Antennal nerve glial cells were separated from SZ and NP glia by isolating and culturing the distal portion of early stage-7 antennal nerves. Antennal nerve glial cells had distinctive morphologies including oblong cell bodies and long, stout processes (Fig. 4*A*, *asterisk*). Antennal nerve glial processes were motile and often contacted ORN axons before axonal growth cones extended toward the glial cells (Fig. 4*B*, *double arrowheads*). After contact with antennal nerve glial cells, ORN axons elongated in direct apposition with glial cell processes (Fig. 4*C-F*, *arrowheads*) or elongated on the substrate adjacent to antennal nerve glial cells (Fig. 4*C-F*, *open arrowheads*) without significant changes in growth cone morphology. The ORN axon shown in the inset of Figure 4*F* extended for 40 μm in close apposition to the glial process. In contrast, growth cones that advanced after contact with SZ and NP glial cells never maintained direct associations with glial processes. Therefore, growth cone contact with antennal nerve glial cells affected growth cone motility and morphology differently than contact with SZ and NP glial cells.

Rate Analysis

To analyze contact-induced changes in axon elongation, sample recordings were selected from SZ and NP co-cultures and the distances that individual axons grew were measured and plotted as a function of time. Ten consecutive frames from a NP co-culture recording illustrate how axon elongation was analyzed in the current study (Fig. 5). The cumulative distance that an individual axon grew was determined by summing the distances between markers placed at the growth cone tip in consecutive movie frames (Fig. 5, *black dots*). Additionally, a reference point corresponding to the original position of the axon tip was placed in each frame to aid visualization of axon growth.

The same strategy was used to measure growth cone branches (Fig. 5, *white dots*), provided they unambiguously arose from their parent axon and they persisted for longer than one hour after formation.

Contact with SZ (Fig. 6*A*) and NP (Fig. 6*B*) glial cells usually prevented forward axon progression past the point of contact (Fig. 6, *arrows*), making the rate of axon elongation markedly different before and after encounters with glial cells (Figs. 6*A-B*, *tables*). Axons behaved similarly whether growth cones flattened (Fig. 6*A*, *axon #1-4*; Fig. 6*B*, *axons #2* and *3*), branched (Fig. 6*A*, *axon #5*; Fig. 6*B*, *axon #3*), or remained simple (Fig. 6*A*, *axon #4b*; Fig. 6*B*, *axons #1*, *4*, and *5*) after contacting SZ and NP glial cells. The initial growth seen immediately following glial cell contact usually represented the expansion of lamellar processes or the formation of growth cone branches. About half of the analyzed axons branched during the recording, some before and some after contact with glial cells. Growth rates were reported only for those branches that formed prior to glial-cell contact (Fig. 6*A*, *axons #4 and 5*) so that before and after comparisons could be made. Axon #3 of the NP plots (Fig. 6*B*) represents the complete measurement of the axon-glial cell encounter depicted in Figure 5. The saw-toothed pattern appearing in the plot after glial contact (Fig. 6*B*, *axon #3*, arrow) corresponded to the extension and retraction of the axon tip seen following contact (Fig. 5, *arrowhead*). The branch that formed after contact (Fig. 5, *white dots*) temporarily continued to advance, while the original axon tip stalled (Fig. 5, *black dots*; Fig. 6*B*, *axon #3*). On average, the rate of axon elongation after SZ glial contact was 2.8% of the average pre-contact rate (Fig. 6*A*, *table*). Similarly, axon elongation slowed to an average of 9.1% of the original rate following contact with NP glial cells (Fig. 6*B*, *table*).

In stark contrast, growth cone motility was essentially unchanged following contact with antennal nerve glial cells (Fig. 6*C*). Axon branches were measured for the encounter depicted in Figure 4. In this recording, glial contact occurred at the 1-hour time point (Fig. 4*B*, *double arrowhead*; Fig. 6*C*, *downward arrow*). After contact, the axon branched and continued to elongate. One branch contacted a glial cell process (Fig. 4*C*, *arrowhead*; Fig. 6*C*, *upward arrow*) and subsequently extended in contact with the process (Figs. 4*C-F*, *arrowheads*; Fig. 6*C*, *branch b*) while the second branch elongated adjacent to the glial cell (Figs. 4*C-F*, *open arrowheads*; Fig. 6*C*, *branch a*). Axon branch "b" became obscured by the glial cell after the five-hour time point (Fig. 4*F*), and therefore was not measured further. Branch "a" was measured until the end of the recording. The average rate of axon elongation following glial contact for branches "a" and "b" was 61% of their pre-contact rate. Branch "b" actually advanced at a faster rate while growing on the glial process than before it had contacted the glial cell. The rate of axon elongation after contact with an antennal nerve glial cell was markedly different from the elongation rates seen following contact with SZ and NP glia.

Morphological diversity of ORN growth cones

To analyze many more growth cones than was possible with live-cell imaging, we used cytoskeletal staining in fixed cells to evaluate growth cone morphology. Images of the entire perimeter of randomly selected explants were collected on the confocal microscope, and all isolated growth cones were qualitatively scored according to their morphological appearance. Axons grown without glia were tipped with growth cones that exhibited a range in morphological diversity (Fig. 7). All growth cones could be grouped into two broad categories, those with "simple" and those with "complex"

morphologies. Simple growth cones had either unbranched or branched microtubule-based processes, and were tipped by filopodial spikes (Fig. 7*A*). Complex growth cones had lamellar regions containing splayed microtubules, and were surrounded by a dense fringe of short, F-actin-based filopodia (Fig. 7*B*). Size was not a determinant for categorization, as complex growth cones in particular varied in both their length and width. The vast majority of growth cones (~85%) in glia-free cultures had simple morphologies (Figs. 8*I* and 9*I*).

Glial contact mediated change in growth cone morphology

Co-cultures containing either SZ or NP glial cells were simultaneously prepared using differentially dissected tissue from the same experimental animals. After immunocytochemistry, dish identity was coded so that observers were blind to glial cell origin during confocal microscopy and growth cone scoring. Three experimental dishes were prepared and analyzed for each condition. Dishes from the same experimental group were summed after confirmation of their statistical similarity.

In SZ and NP co-cultures, growth cones not in contact with glial cells were predominantly simple, and had a distribution of growth cone morphologies that closely matched those of growth cones grown without glial cells (Figure 8*I*). The distributions of growth cone morphologies were not statistically different between any of the non-contacting conditions. Figure 8 shows examples of growth cones contacting SZ and NP glial cells falling into the simple (Figs. 8*A*,*B* and *E*,*F*) and complex (Figs. 8*C*,*D* and *G*,*H*) categories. The frequency of complex growth cones was statistically significantly higher among growth cones that contacted either SZ (Fig. 8*J*) or NP glial cells (Fig. 8*J*) compared with those that did not contact glia ($P = 0.004$ for SZ and $P < 0.001$ for NP co-

cultures). Growth cone morphology was equally affected by contact with SZ and with NP glial cells. Since growth cone morphology changed only in axons contacting glial cells, the possibility that a long-range soluble factor influenced growth cone morphology was discounted.

In summary, the fixed-cell cytoskeletal staining approach used to examine growth cone morphology recapitulated results obtained with live-cell imaging: growth cones that contacted both SZ and NP glial cells showed a greater degree of morphological complexity than growth cones that did not contact glial cells.

Glial cells deprived of ORN axon ingrowth can influence growth cone morphology

Reciprocal communication between ORN axons and glial cells has been hypothesized to underlie several processes that are critical to the formation of the moth primary olfactory system. First, early-arriving ORN axons trigger migration of glial cells to the sorting zone. SZ glial cells then influence the behavior of subsequently arriving receptor axons (Rössler et al., 1999). Second, the arrival of ORN axons influences the morphogenesis of NP glia by triggering the extension of glial processes into the neuropil and the migration of glial cell bodies to surround the developing glomeruli (Oland and Tolbert, 1987). The normal proliferation and migration of NP glial cells subsequently serve to stabilize clusters of receptor axon terminals, called protoglomeruli, and partition the antennal lobe neuropil into functional glomerular units (Oland and Tolbert, 1988; Oland et al., 1988; Baumann et al., 1996). Thus communication between ORN axons and glial cells could conceivably lead to changes in gene expression that in turn modify subsequent cellular behavior.

To test whether interactions with ORN axons were required for SZ and NP glial cells to develop the ability to influence growth cone morphology *in vitro*, glial cells were allowed to develop without olfactory input before being harvested for co-culture. Unilaterally unafferented animals were produced and allowed to develop until early stage 7 (see Methods). Each experimental animal contained one normally afferented and one unafferented antennal lobe. Although SZ glia are not produced, NP glia continue to proliferate normally in the absence of receptor axon innervation (Oland and Tolbert, 1989). Therefore a direct comparison between NP glial cells from normal and unafferented antennal lobes could be made. The neuropil regions of unafferented and control antennal lobes were dissected, dissociated, and introduced to explant cultures separately. The fixed-cell cytoskeletal staining approach was used to permit statistical analysis of large numbers of growth cones across multiple experimental dishes. The observers were again blind to glial cell origin during confocal microscopy and scoring of growth cone morphologies.

Growth cones from co-cultures containing NP glial cells isolated from afferented (NP/Aff-AL) and unafferented antennal lobes (NP/Unaff-AL) displayed the same range of morphological diversity as growth cones in explant only, normal SZ, and normal NP co-cultures (Figs. 7 and 8*I*). The non-contacting axons from NP/Aff-AL and NP/Unaff-AL co-cultures had nearly identical distributions of growth cone morphologies as axons grown without glial cells (Fig. 9*I*). Contacting axons in NP/Aff-AL or NP/Unaff-AL co-cultures were categorized as having either simple (Figs. 9*A,B* and *E,F*) or complex (Figs. 9*C,D* and *G,H*) growth cone morphologies. Regardless of whether their parent antennal lobes had been exposed to sensory axons, growth cones contacting glial cells were less likely to be simple and more likely to be complex. Axons that contacted NP glial cells

from unafferented antennal lobes behaved identically to the axons that contacted NP glial cells from afferented lobes (Fig. 9*J*), as the distributions of growth cone morphologies were statistically equivalent between contacting axons in NP/Aff-AL and NP/Unaff-AL co-cultures ($P > 0.999$). The distributions of growth cone morphologies were significantly different between contacting and non-contacting axons, both in NP/Aff-AL ($P < 0.001$) and in NP/Unaff-AL ($P < 0.001$) co-cultures, indicating that previous interaction with ORN axons was not necessary for glia to develop the ability to affect growth cone behavior.

DISCUSSION

Previous studies indicated that SZ and NP glia influence ORN axons in the developing olfactory system of *Manduca sexta*. In the present paper, we have demonstrated that contact with individual SZ and NP glial cells alters the behavior of individual ORN axons *in vitro*. Live-cell imaging showed that contact with SZ and NP glial cells typically caused ORN growth cones to increase in morphological complexity and cease advancement. Analysis of growth cones in fixed preparations demonstrated that contact with SZ and NP glial cells had a statistically significant effect on growth cone complexity, regardless of whether glial cells had previously been exposed to ingrowing ORN axons *in vivo*. Finally, ORN axons that contacted peripherally-derived antennal nerve glial cells did not stop but continued to elongate, suggesting that contact-mediated growth cone responses to SZ and NP glial cells were specific behaviors and not generalized reactions to cell contact.

Growth cone responses to SZ and NP glial cells

During development axon behavior dramatically changes in the glia-rich sorting zone, where axons sort into fascicles (Rössler et al., 1999), and in the antennal lobe, where axons branch and form protoglomeruli that are stabilized by NP glial cells (Baumann et al., 1996). Proper axon behavior in the sorting zone and antennal lobe depends on the presence of adequate numbers of glial cells (Oland and Tolbert, 1988; Oland et al., 1988; Baumann et al., 1996; Rössler et al., 1999), suggesting that interactions with glia are responsible for region-specific changes in axon behavior.

In vitro, however, SZ and NP glial cells exert nearly identical influences on the behavior and morphology of ORN growth cones, implying that similar mechanisms may

mediate these responses. Similarities in growth cone behavior could reflect the common central origin of SZ and NP glia from a set of cells outlining the neuropil of the young antennal lobe (Rössler et al., 1999). SZ and NP glia may continue to share many molecular properties after terminal differentiation. These shared properties may govern what occurs in the simplified environment of tissue culture, where we examined only the first growth cone encounters with glial cells. *In vivo*, the history of glial encounters might be critical, and progression of ORN axons through the sorting zone might "prime" growth cones for later encounters with NP glia.

We report in the current paper that centrally derived glial cells did not require interactions with ORN axons *in vivo* in order to induce contact-dependent changes in ORN growth cone morphology *in vitro*. This finding suggests SZ and NP glia have an axon-independent ability to influence ORN growth cone morphology and behavior. An interesting question is whether the heterogeneity in growth cone behavior observed after contact with SZ and NP glial cells is due to intrinsic differences among individual ORN axons, or alternatively, intrinsic differences among individual glial cells. Although examples are limited, individual glial cells do not appear to impart identical changes in growth cone behavior, as exemplified in Figure 3C, where two ORN axons respond differently to contact with the same glial cell.

Changes in growth cone adhesive properties may alter growth cone behavior

Our findings that ORN growth cones elaborate and stop advancing after contacting SZ and NP glial cells *in vitro* are consistent with the possibility that growth cone adhesive properties are altered following contact with glial cells. Classic *in vitro* studies demonstrated that growth cones with flattened, lamellar morphologies were

strongly attached to the underlying substrate (Letourneau, 1975). Subsequent work indicated that growth cones were large, flat, more adherent, and slower growing when extending on cell adhesion molecules and were small, filopodial, less adherent, and faster growing when extending on extracellular matrix proteins (Payne et al., 1992; Lemmon et al., 1992; Drazba et al., 1997). In the present studies, growth cones that adopted flattened morphologies had presumably increased adhesion to the underlying concanavalin A/laminin substrate.

Changes in axon adhesion might well regulate the behavior of ORN axons *in vivo*. After encountering SZ glia, ORN axons change associations by sorting into new axon fascicles (Oland et al., 1998). Adhesive properties must change as axons become less adherent to their neighbors and more adherent to axons of similar olfactory specificity. Support for this hypothesis comes from observations that a subset of ORN axons expressing the homophilic cell adhesion molecule *Manduca* fasciclin II are initially dispersed in the antennal nerve and undergo glia-dependent sorting into fasciclin II-positive bundles in the SZ before targeting a subset of glomeruli (Rössler et al., 1999; Higgins et al., 2002). Adhesive interactions among like ORN axons might also regulate axon behavior in the antennal lobe. After ORN axons grow through glia surrounding the antennal lobe neuropil, they abruptly branch and spread out to form a fringe of terminal processes (Oland et al., 1998). Eventually, terminal arbors of like ORN axons coalesce into discrete nodules called protoglomeruli (Oland et al., 1990, 1998). Adhesion among like axons could prevent the intermingling of dissimilar axon terminals and confine the arborization of later arriving axons to territories that are occupied by terminal branches of like identity.

Contact with glial cells may therefore increase the quantity, the quality, or the availability of molecules that affect cell adhesion at growth cone surfaces. Whereas changes in cell-surface adhesion molecules *in vitro* generally might lead to growth cone flattening and adherence to the underlying substrate, changes in the same molecules *in vivo* might lead to region-specific changes in growth cone behavior.

Functional consequences of cytoskeletal rearrangements within growth cones

Another possibility is that contact-dependent signaling cascades act to regulate cytoskeletal dynamics in glial-cell contacting growth cones. The Rho family of small GTPases could mediate shape change and loss of motility, since they directly affect growth cone behavior by regulating the actin cytoskeleton through associated kinases (Nikolic, 2002), and since they are downstream targets of activated cell-surface guidance receptors (Dickson, 2001; Grunwald and Klein, 2002). Ephrins and semaphorins can alter the growth cone cytoskeleton by differentially regulating small GTPases (Shamah et al., 2001; Hu et al., 2001), leading to the collapse of growth cones that express their cognate receptors (Luo et al., 1993; Drescher et al., 1995; Xu et al., 2000).

Microtubule reorganization also changes growth cone form and behavior. For instance, microtubule looping has been described in a wide variety of neuronal growth cones and appears to be correlated with extended periods of decreased neuritic outgrowth (Tsui et al., 1984; Lankford and Klein, 1990; Tanaka and Kirschner, 1991; Sabry et al., 1991; Roos et al., 2000) and growth cone branching (Dent et al., 1999). In the present study, fixed ORN growth cones from *Manduca* are large and preferentially contain splayed microtubules when contacting SZ and NP glial cells; this morphology is

correlated with extensive periods of growth cone stalling. Microtubule rearrangements underlie turning behaviors in growth cones (Sabry et al., 1991; Lin and Forscher, 1993; Tanaka et al., 1995), and may cause *Manduca* ORN growth cones to turn after contacting SZ glia *in vivo*. In addition, axon contact with NP glia within the antennal lobe may induce microtubule reorganization and initiate terminal branching.

A model for glia-mediated changes in axon behavior

We propose that the alteration of growth cone adhesion and/or rearrangements of the growth cone cytoskeleton are involved in mediating ORN growth cone responses to contact with SZ and NP glia (Fig. 10). We hypothesize that: 1) Contact with SZ glia transiently leads to growth cone enlargement and the exploration of their local environments. Also, as growth cones enlarge, microtubules splay apart and reorganize to initiate turning. 2) Interaction with SZ glia leads to the increased expression of particular adhesion molecules at growth cone surfaces, enabling them to adhere to axons of like identity. 3) Contact with NP glia initiates terminal branching, and 4), as axonal arbors coalesce into protoglomeruli, cell-surface adhesion molecules aid in the segregation of like axon terminals into nascent glomeruli.

Comparisons to glia in the mammalian olfactory system

Increasing evidence suggests that mammalian glia, like glia in *Manduca*, participate with neurons to fashion the developing primary olfactory center. Olfactory ensheathing cells migrate from the olfactory placode and enwrap bundles of ORN axons in the olfactory nerve and in the nerve layer of rodent olfactory bulbs (Marin-Padilla and Amieva, 1989; Doucette, 1989, 1991). Olfactory ensheathing cells display a blend of

Schwann cell and astrocyte properties (Raisman, 1985; Ramon-Cueto and Avila, 1998; Bartolomei and Greer, 2000), and promote neurite growth (Ramon-Cueto and Valverde, 1995; Kafitz and Greer, 1999). Ensheathing cells also express molecules that influence the growth, sorting, and targeting of ORN axons (Puche et al., 1996; St. John and Key, 1999; Tisay et al., 2000; Schwarting et al., 2000). Despite their distinctly different origins, *Manduca* SZ glia and mammalian olfactory ensheathing cells may play functionally equivalent roles (Valverde, 1999; Key and St. John, 2002). Likewise, mammalian astrocytes delineate glomerular boundaries and perhaps play a role similar to *Manduca* NP glia in glomerular stabilization (Valverde et al., 1992; Gonzalez and Silver, 1994; Treloar et al., 1999; Valverde, 1999).

In conclusion, glial cells isolated from the developing sorting zone and antennal lobe neuropil of *Manduca sexta* directly influence the motility and the morphology of ORN growth cones in a well-defined culture system. We suggest that glia-mediated alterations in growth cone behavior *in vitro* reflect changes in growth cone adhesive properties and the cytoskeleton, and that those changes enable ORN axons to sort into fascicles, reorient during steering, slow growth, form branches, and segregate into protoglomeruli *in vivo*. Future studies will examine the molecular bases of growth cone-glial cell interactions and relate *in vitro* findings to the behavior of individually labeled ORN axons *in situ*.

Table 2.1: ORN growth cone responses to contact with sorting zone and neuropil-associated glial cells.

Growth cone behavior	SZ glia (n=50)	NP glia (n=40)
Flatten and stop	60%	40%
Branch and stop	18%	20%
Stay simple and stop	10%	27%
Elongate	12%	13%

Time-lapse microscopy revealed four categories of growth cone behaviors that followed contact with sorting zone (SZ) and neuropil-associated (NP) glial cells. The total number of growth cone encounters (n) is indicated for each glial cell type.

Figure 2.1 Generation of cultures containing explants of olfactory receptor epithelium and glial cells from the olfactory pathway of *Manduca sexta*. **A.** Schematic diagram illustrating changes in glial number and position that occur during development. After the first ORN axons arrive, sorting zone glia (red) proliferate and migrate to fill the base of the antennal nerve. Glia surrounding the antennal lobe neuropil (green) proliferate, migrate, and extend processes to envelop nascent glomeruli. Antennal nerve glia (blue), born in the antenna, migrate toward the antennal lobe and fill the antennal nerve. **B.** Summary diagram of co-culture methods. On day 1, stage-4 antennae are dissociated to yield explants of olfactory receptor epithelium. On day 2, tissue from the sorting zone (*SZ*), antennal lobe (*AL*), or antennal nerve (*AN*), is dissociated from early stage-7 brains, and the resulting glial cells are plated onto explant cultures. **C.** Low magnification view of an explant grown for 24 hrs *in vitro*. **D.** High magnification view of the boxed region in C showing the distal fringe of ORN axon outgrowth. *Arrows* indicate simple growth cones; *arrowheads* indicate flattened growth cones. **E-G.** Freshly cultured SZ glial cells. Scale bars: C, 100 μm; D, E, 20 μm. Scale bar in E applies to F,G.

Figure 2.2 ORN growth cone encounters with SZ glial cells. **A.** Frames from a movie sequence showing a typical growth cone response to contact with SZ glial cells. Shortly after contact (3:20), the growth cone flattens, elaborates, and stops advancing. **B.** Movie frames showing a less frequent type of response following contact with SZ glial cells. Growth cone branches after contact (2:20), pauses, then continues to advance over and around the pair of glial cells. *Asterisks* indicate glial cell bodies. *Arrows* mark axon shaft and *arrowheads* mark axon tip. *Open arrowhead* in A marks the tip of a growth cone branch. Time stamps are in hours and minutes. Scale bars: A, B, 10 μm.

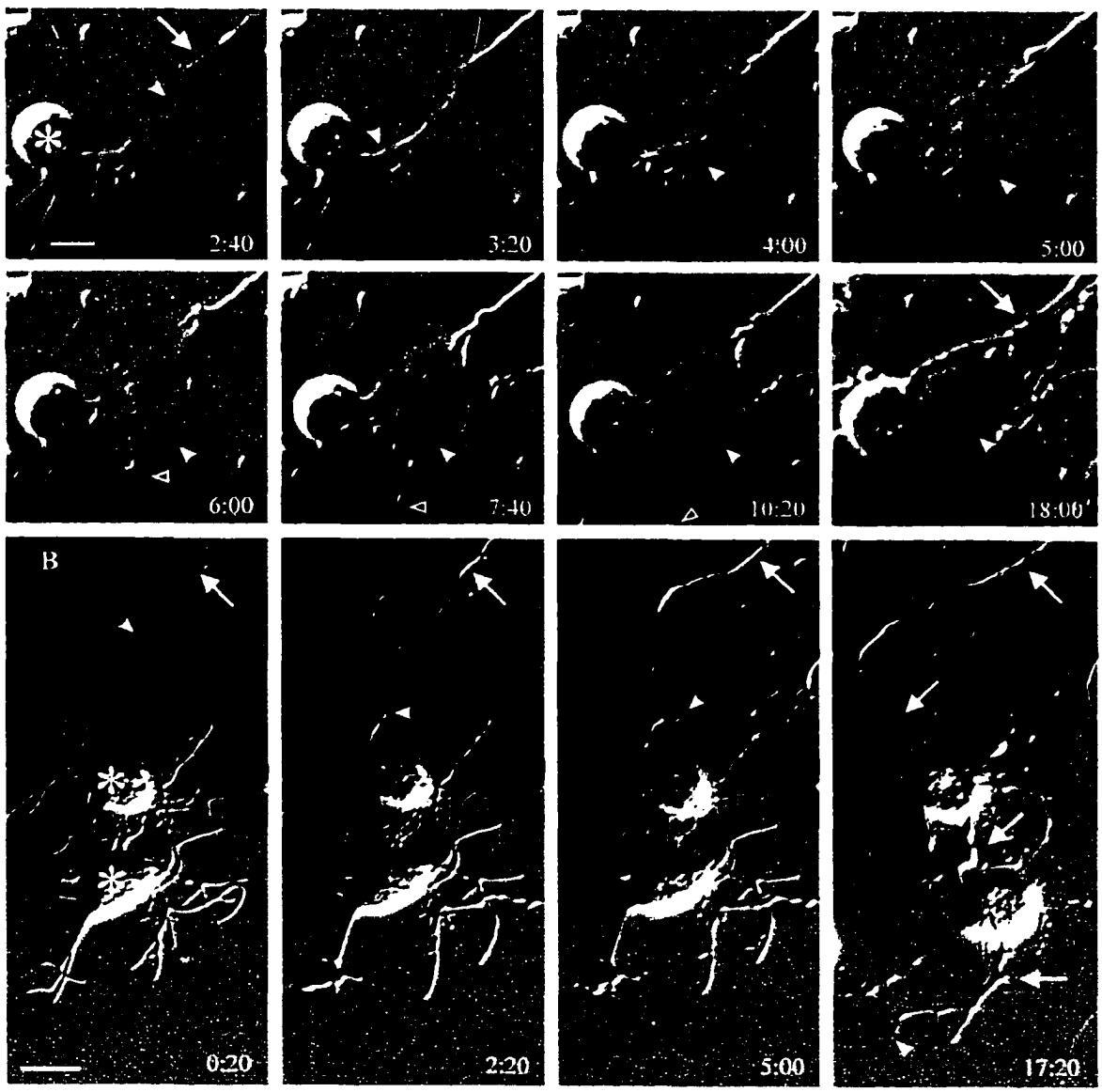
2:40
3:20
4:00
5:00
6:00
7:40
10:20
18:00
B
0:20
2:20
5:00
17:20

Figure 2.3 ORN growth cone encounters with NP glial cells. **A.** Movie frames showing an ORN growth cone that flattened and stopped advancing after contacting a NP glial cell (6:00). *Arrow*, axon shaft; *arrowhead*, axon tip. **B.** A growth cone extends toward and contacts a glial cell process (8:40), branches, and remains associated with the surface of the glial process. *Arrow*, axon shaft; *arrowheads*, tips of growth cone branches. **C.** Two growth cones extending from separate axon shafts (*arrow; open arrow*) contact the same glial cell. First growth cone (*arrowhead*) contacts the glial cell (9:20) and remains simple in morphology for the duration of the recording. Second growth cone (*open arrowhead*) contacts the glial cell (15:20) and branches. Scale bar: A, 10 μm, applies to all.

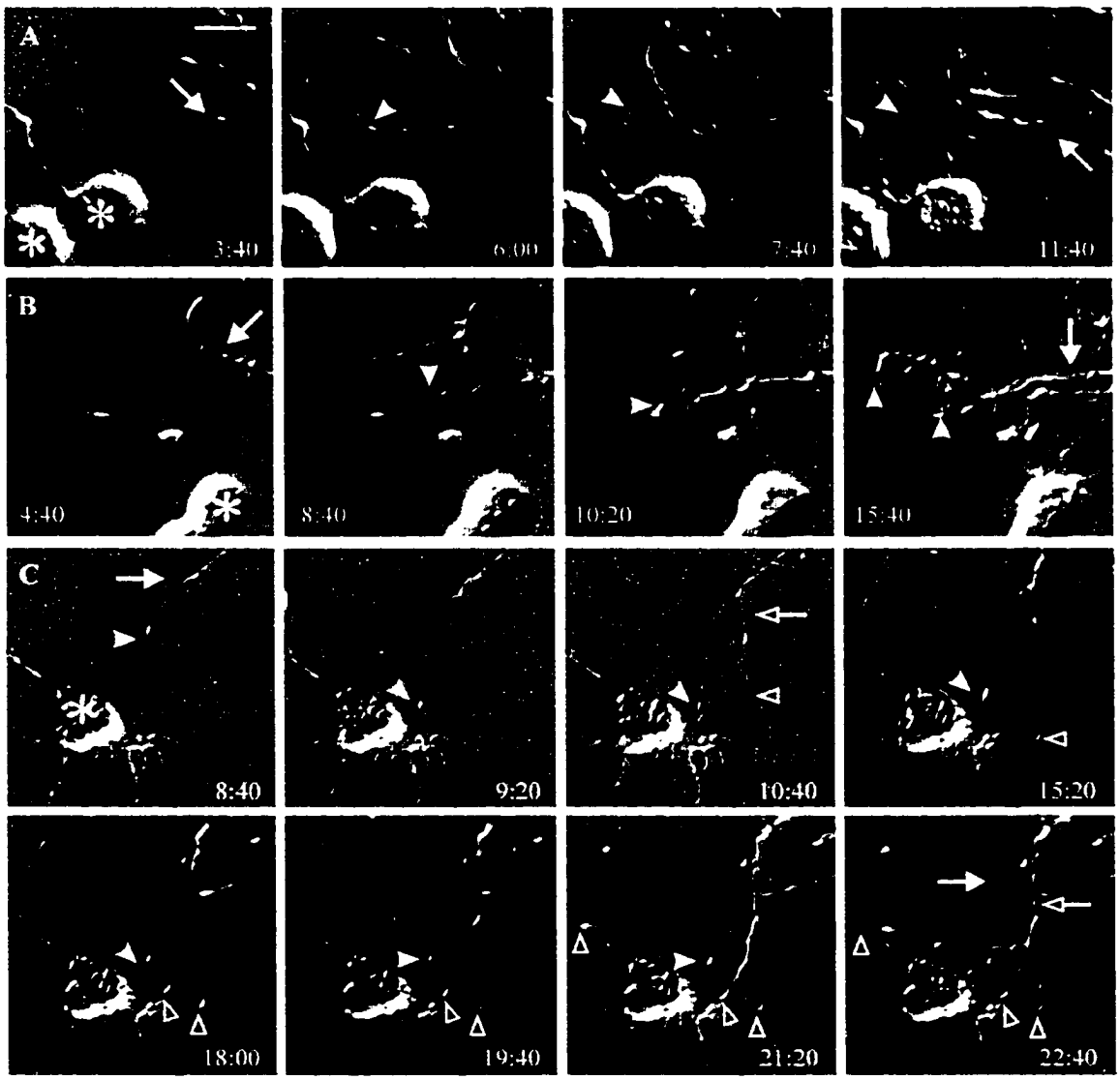
A
3:40
6:00
7:40
11:40
B
4:40
8:40
10:20
15:40
C
8:40
9:20
10:40
15:20
18:00
19:40
21:20
22:40

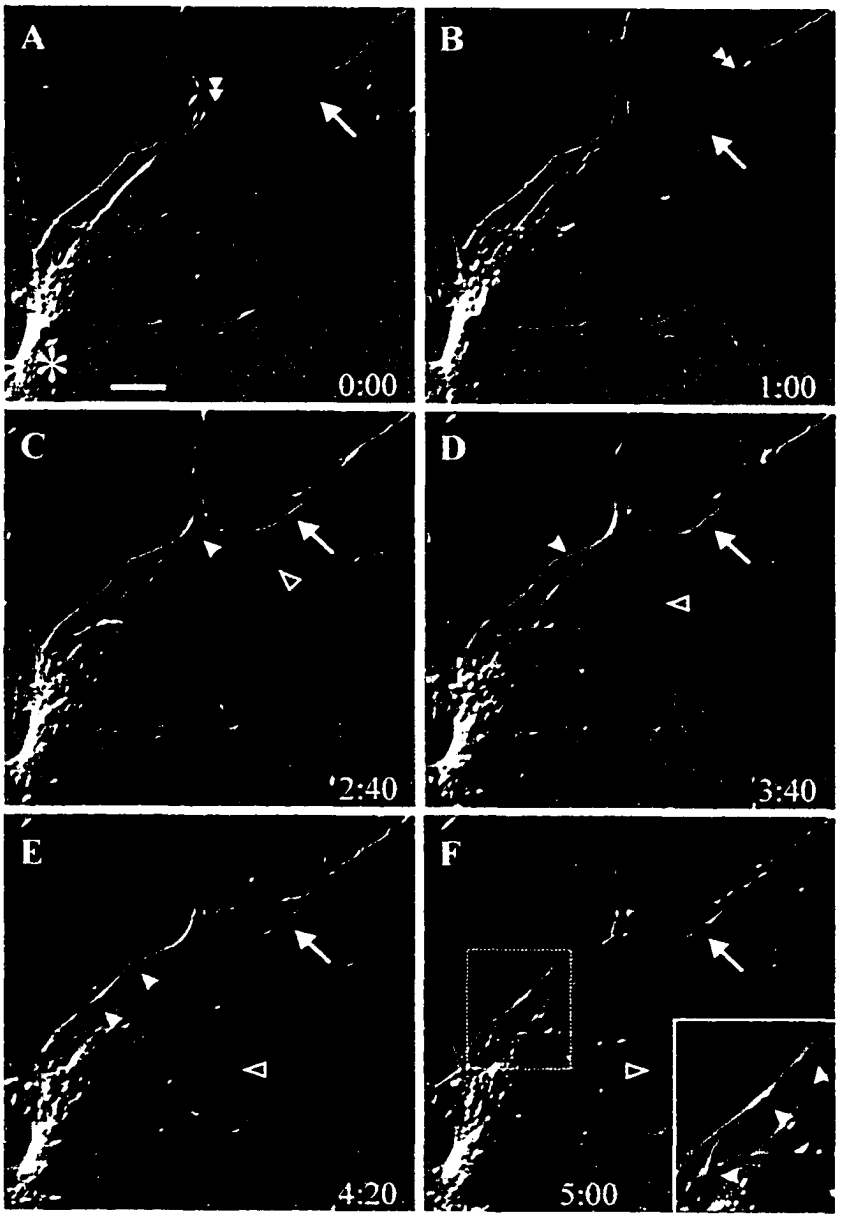
A
0:00
B
1:00
C
2:40
D
3:40
E
4:20
F
5:00

Figure 2.5 Sequential frames from a time-lapse recording illustrating how distance measurements were obtained. In the first frame (600 min), a reference mark (*black dot*) was placed at the tip of the advancing growth cone. As the growth cone advanced or retracted, a new marker was placed at its tip in every frame. The distances between markers in adjacent movie frames were measured in microns, and summed across all frames to yield the net distance that the axon grew. This growth cone branched (7:20 min), and the branch was marked (*white dot*) and measured using the same strategy. *Arrowhead* denotes growth cone contact with the glial cell. Scale bar = 10 μm.

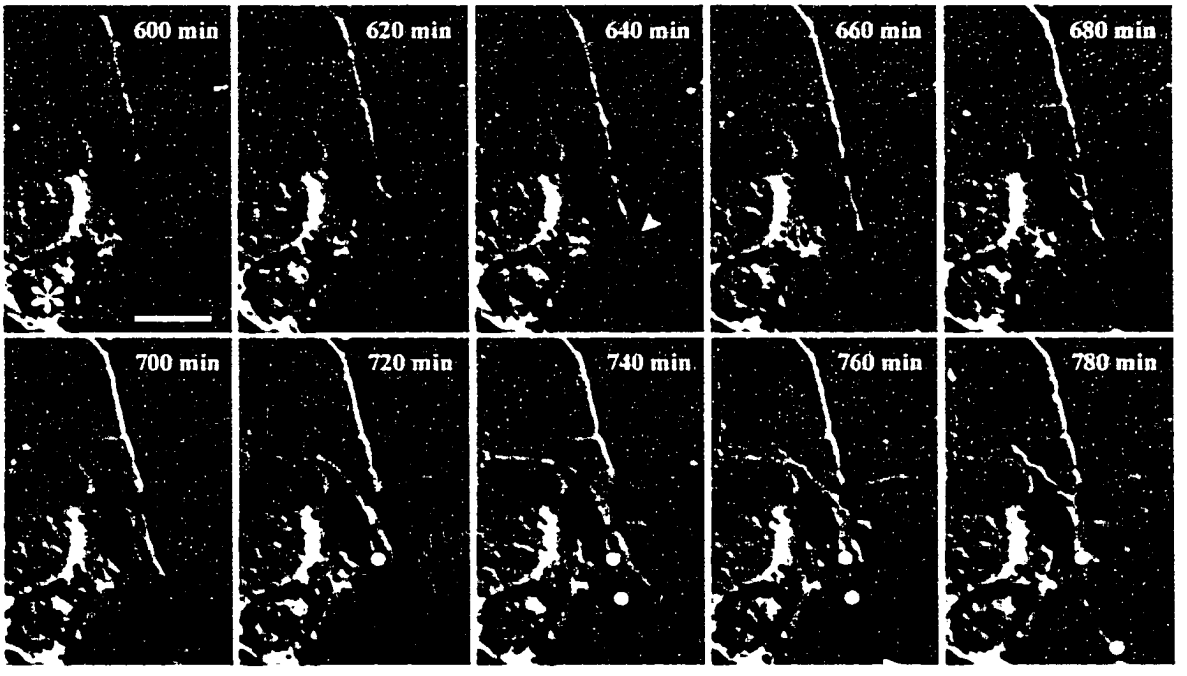
600 min
620 min
640 min
660 min
680 min
700 min
720 min
740 min
760 min
780 min

Figure 2.6 ORN growth cones cease advancement following contact with SZ and NP glial cells. Plots represent total distances that axons grew before and after contact with glial cells. *Arrows* mark the moment of glial cell contact. *Dotted lines* indicate distances that axon branches grew. Tables include rates of axon elongation before and after contact. **A.** Growth cone contact with SZ glial cells halts axon elongation in five independent cases. **B.** Similar growth arrest is seen in cases of encounters with NP glial cells. **C.** Single plot of an encounter with a peripherally derived antennal nerve glial cell. Branch "a" extended on the substrate adjacent to the glial cell, whereas branch "b" extended directly in contact with a glial process.

A

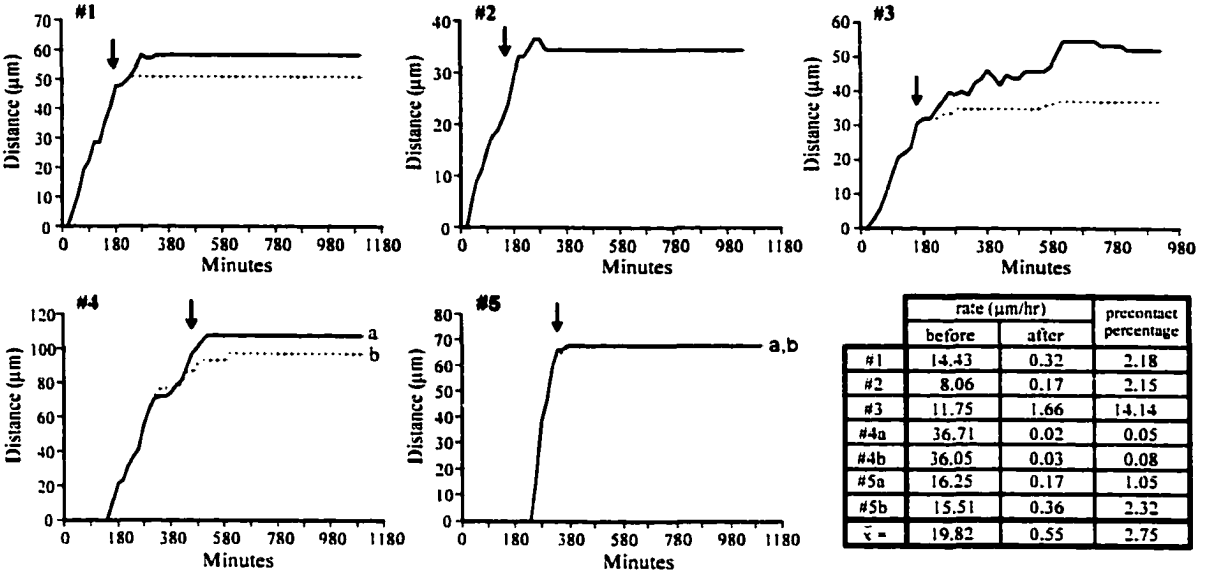

	rate (µm/hr)		precontact percentage
	before	after	
#1	14.43	0.32	2.18
#2	8.06	0.17	2.15
#3	11.75	1.66	14.14
#4a	36.71	0.02	0.05
#4b	36.05	0.03	0.08
#5a	16.25	0.17	1.05
#5b	15.51	0.36	2.32
$\bar{x}$ =	19.82	0.55	2.75

B

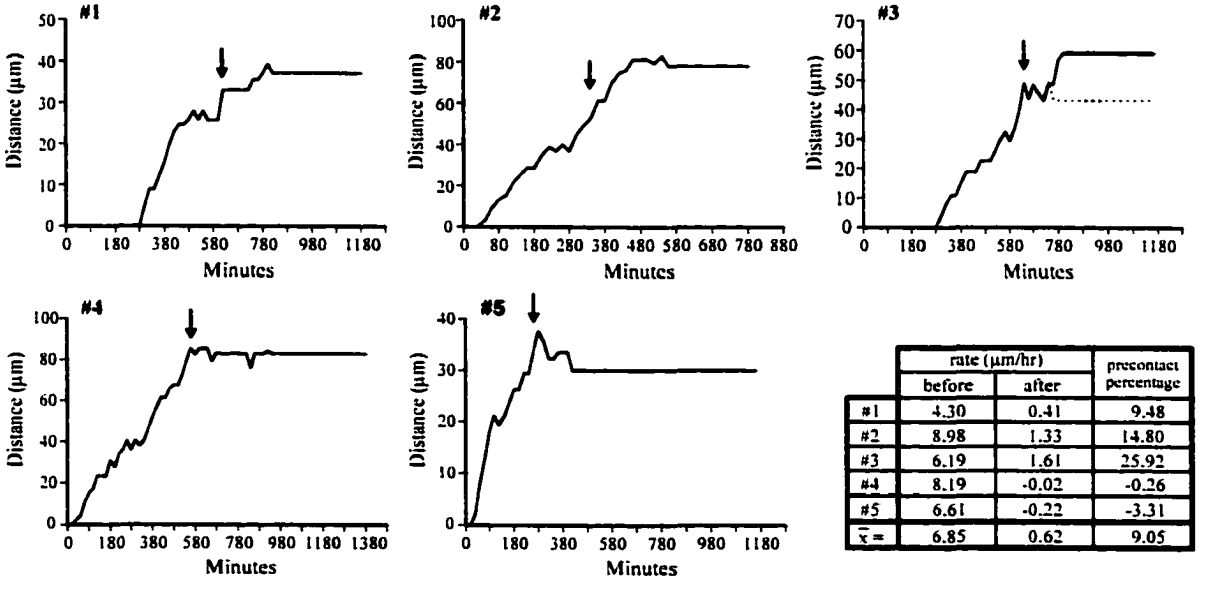

	rate (µm/hr)		precontact percentage
	before	after	
#1	4.30	0.41	9.48
#2	8.98	1.33	14.80
#3	6.19	1.61	25.92
#4	8.19	-0.02	-0.26
#5	6.61	-0.22	-3.31
$\bar{x}$ =	6.85	0.62	9.05

C

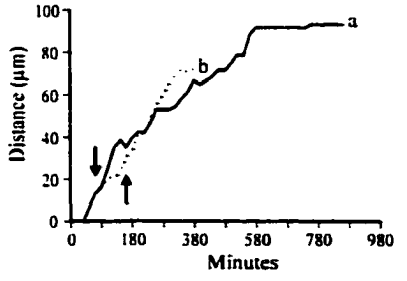

	rate (µm/hr)		precontact percentage
	before	after	
a	18.93	5.70	30
b	10.38	12.24	117
$\bar{x}$ =	14.64	8.97	61

Figure 2.7 Confocal micrographs of isolated ORN growth cones stained to reveal microtubules (red) and actin filaments (green). Images represent the normal range of ORN growth cone morphologies *in vitro*. **A.** Simple growth cones, having either unbranched or branched microtubule domains tipped by actin rich filopodia. **B.** Complex growth cones, having flattened regions with splayed microtubules surrounded by a dense fringe of actin-based filopodia. Scale bar = 10 μm, applies to all.

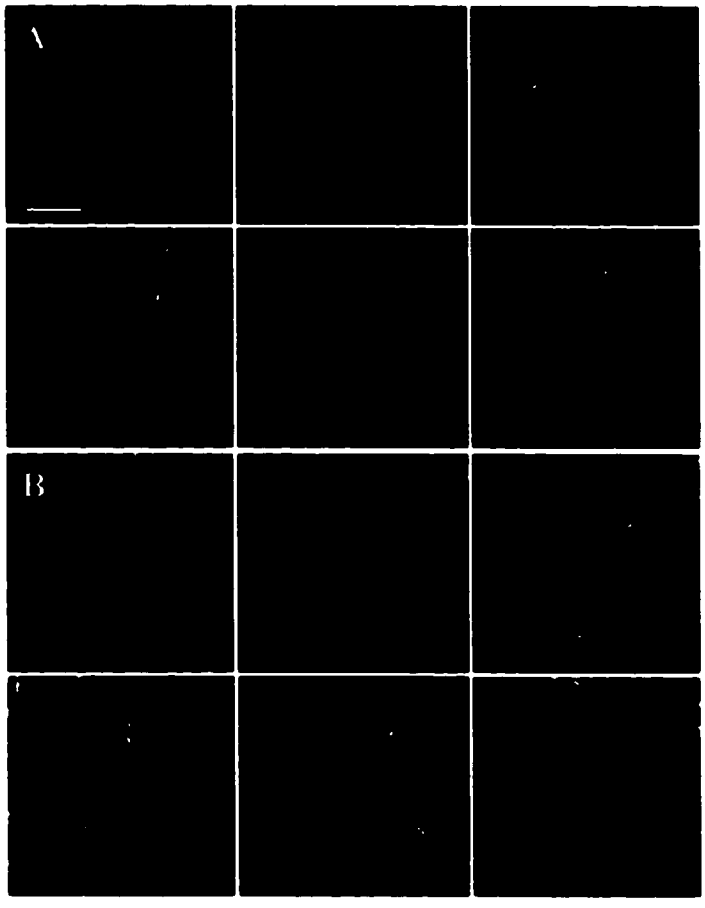
A
B

Figure 2.8 Contact with SZ and NP glial cells leads to an increase in growth cone complexity, in cultures stained to reveal tubulin (red) and actin (green). **A-H.** Isolated growth cones (*arrows*) in contact with glial cells (*asterisks*). **A-D.** Growth cones contacting SZ glial cells. A,B, simple; C,D complex. **E-H.** Growth cones contacting NP glial cells. E,F, simple; G,H, complex. **I.** Distribution of growth cone morphologies. Whether grown alone (*black bars*), with SZ glia (*medium gray bars*), or with NP glia (*light gray bars*), growth cones not contacting glial cells have predominantly simple morphologies. **J.** Growth cones contacting SZ glial cells (*yellow bars*) and NP glial cells (*red bars*) have statistically significantly different proportions of simple and complex growth cones (SZ: $P = 0.004$; NP: $P < 0.001$) than growth cones not contacting glial cells (*gray bars*) in the same cultures. Scale bar: A, 10 μm, applies to A-H.

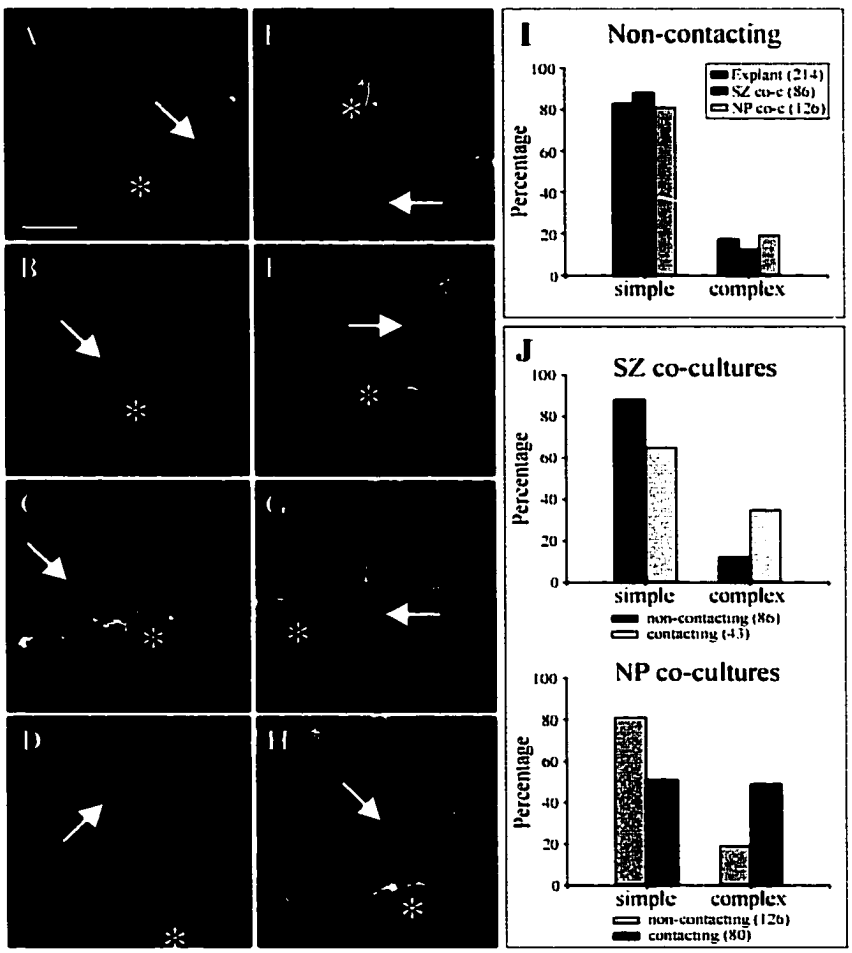
I
Non-contacting
Explant (214)
SZ co-c (86)
NP co-c (126)
Percentage
100
80
60
40
20
0
simple
complex
J
SZ co-cultures
Percentage
simple
complex
non-contacting (86)
contacting (43)
NP co-cultures
Percentage
simple
complex
non-contacting (126)
contacting (80)

Figure 2.9 Glial cells do not require exposure to afferent axons to elicit ORN growth cone elaboration *in vitro*. Red, tubulin; green, actin. **A-H.** Isolated growth cones (*arrows*) in contact with glial cells (*asterisks*). **A-D.** Growth cones contacting glial cells from normally afferented antennal lobes. A,B, simple; C,D complex. **E-H.** Growth cones contacting glial cells from unafferented antennal lobes (see Methods). E,F, simple; G,H, complex. **I.** Distribution of growth cone morphologies. The proportions of simple and complex growth cones are nearly equivalent between growth cones cultured without glia (*black bars*), and with glia from normally afferented (*medium gray*), and unafferented (*light gray*) antennal lobes. **J.** Axons contacting glial cells from normally afferented lobes (*red bars*) and unafferented lobes (*blue bars*) have statistically significantly different distributions of growth cone morphologies (Aff-AL: $P < 0.001$; Unaff-AL: $P < 0.001$) from growth cones not contacting glial cells (*gray bars*) in the same cultures. The proportions of complex growth cones contacting glial cells are statistically identical between Aff-AL and UnAff-AL co-cultures ($P > 0.999$). Scale bar: A, 10 μm, applies to A-H.

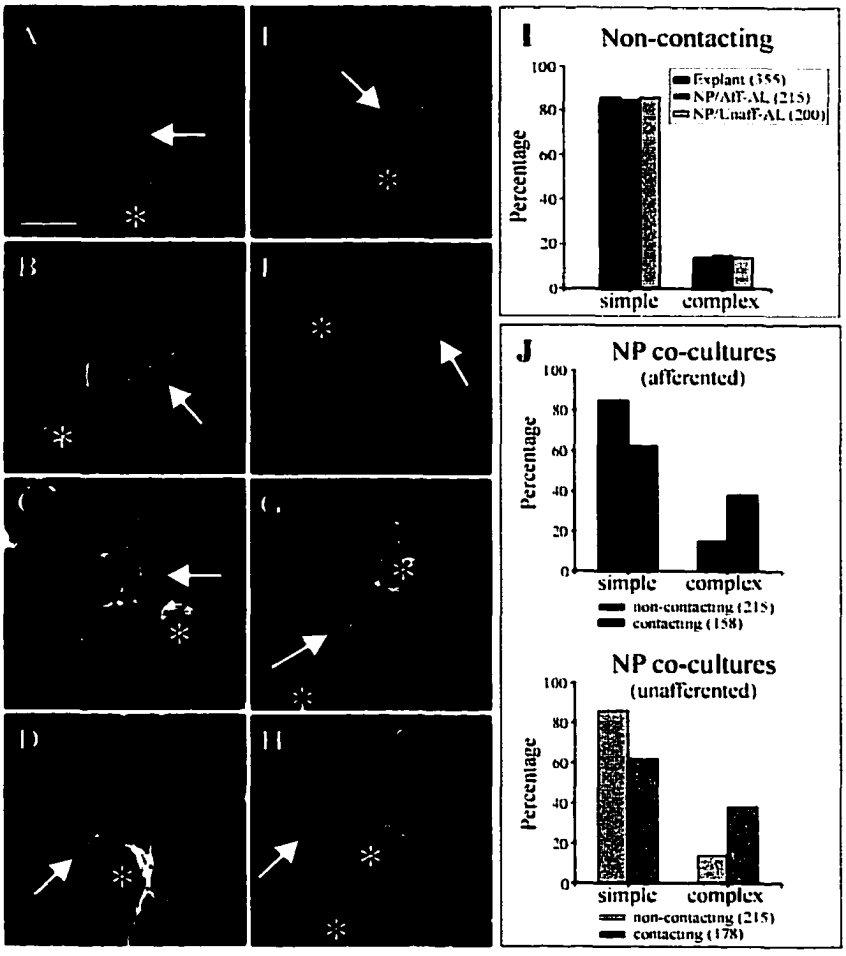
I
Non-contacting
Explant (355)
NP/Aff-AL (215)
NP/Unaff-AL (200)
Percentage
simple
complex
J
NP co-cultures
(afferented)
Percentage
simple
complex
non-contacting (215)
contacting (158)
NP co-cultures
(unafferented)
Percentage
simple
complex
non-contacting (215)
contacting (178)

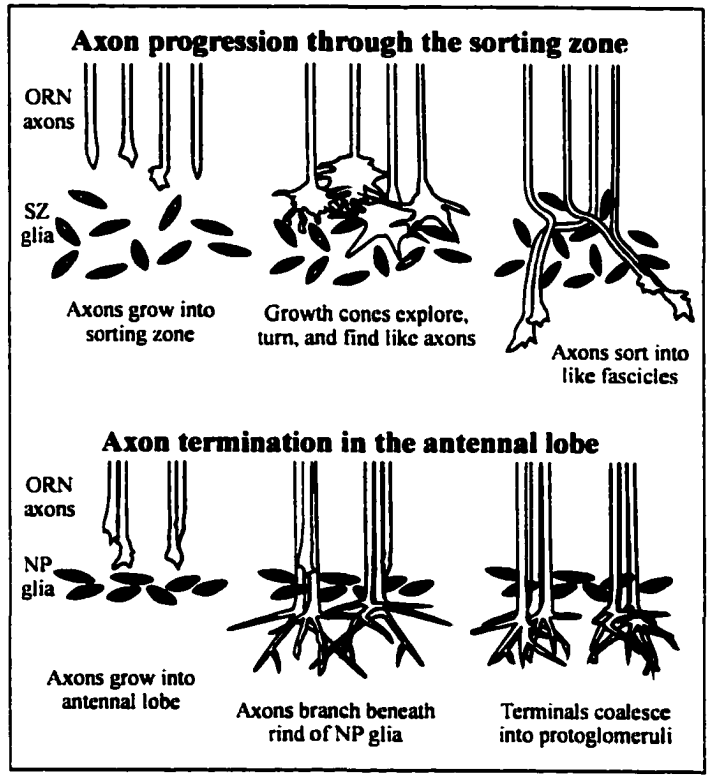
Axon progression through the sorting zone
ORN axons
SZ glia
Axons grow into sorting zone
Growth cones explore, turn, and find like axons
Axons sort into like fascicles
Axon termination in the antennal lobe
ORN axons
NP glia
Axons grow into antennal lobe
Axons branch beneath rind of NP glia
Terminals coalesce into protoglomeruli

CHAPTER 3: RECIPROCAL INTERACTIONS BETWEEN OLFACTORY RECEPTOR AXONS AND OLFACTORY NERVE GLIA CULTURED FROM THE DEVELOPING MOTH *MANDUCA SEXTA*

ABSTRACT

In olfactory systems, neuron-glia interactions have been implicated in the growth and guidance of olfactory receptor axons. In the moth *Manduca sexta*, developing olfactory receptor axons encounter several types of glia as they grow into the brain. Antennal nerve glia are born in the periphery and enwrap bundles of olfactory receptor axons in the antennal nerve. Although their peripheral origin and relationship with axon bundles suggests they share features with mammalian olfactory ensheathing cells, the developmental roles of antennal nerve glia remain elusive. When co-cultured with antennal nerve glial cells, olfactory receptor growth cones readily advance along glial processes without displaying prolonged changes in morphology. In turn, olfactory receptor axons induce antennal nerve glial cells to form multicellular arrays through proliferation and process extension. In contrast to antennal nerve glia, centrally derived glial cells from the axon sorting zone and antennal lobe never form arrays *in vitro*, and growth-cone glial-cell encounters with these cells halt axon elongation and cause permanent elaborations in growth cone morphology. We propose that antennal nerve glia play roles similar to olfactory ensheathing cells in supporting axon elongation, yet they differ in their capacity to influence axon guidance, sorting, and targeting, roles that could be played by central olfactory glia in *Manduca*.

populate the base of the developing nerve; these glial cells, which we call "sorting zone glia," in turn play a strategic role in sorting ORN axons into fascicles that are destined to terminate in particular glomeruli in the antennal lobe (Rössler et al., 1999). Their role in axon sorting suggests that sorting zone glia share certain similarities with the mammalian olfactory ensheathing cells. A second type of glial cell associated with the antennal-lobe neuropil is required to stabilize the borders of developing glomeruli (Oland and Tolbert, 1988; Oland et al., 1988; Baumann et al., 1996). In addition to having an influence on the behavior of ORN axons *in vivo*, we have recently shown that sorting zone and neuropil-associated glial cells have dramatic influences on ORN axons *in vitro* (Tucker et al., 2000, 2001). Using co-cultures containing explants of olfactory receptor epithelium and glial cells, we demonstrated that contact with sorting zone and neuropil-associated glial cells leads to robust elaborations in ORN growth cone morphology and the rapid loss of ORN growth cone motility.

A third type of glial cell that ORN axons encounter, the antennal nerve (AN) glia, arise in the periphery and eventually enwrap bundles of ORN axons after they migrate down the antennal nerve to the distal margin of the sorting zone (Rössler et al., 1999). Little is known about the roles that AN glia play during development, yet their peripheral origin and relationship with ORN axons suggest they, too, may share features with olfactory ensheathing cells. The current paper presents *in vitro* experiments that explore cellular interactions between ORN axons and AN glial cells. Results indicate that, without undergoing long-lasting changes in morphology, ORN growth cones typically continue to advance after contacting AN glial cells. ORN axons often travel directly on the surfaces of glial processes, indicating that AN glial cells provide a permissive substrate for axon extension. Moreover, the behavior of AN glial cells is itself changed

METHODS

Animals

Manduca sexta (Lepidoptera:Sphingidae) were reared from eggs in environmental chambers maintained at 25°C and 50-60% relative humidity under a long day photoperiod (17 h light, 7 hr dark). Under these laboratory conditions, adult metamorphic development occurs over 18 stages, each lasting 1-4 days, starting at pupation and ending with the emergence of the adult moth. Pupae were staged by examining morphological changes in external structures visible beneath the pupal cuticle after fiber-optic illumination (Tolbert et al., 1983; Oland and Tolbert, 1987; Dubuque et al., 2001). Before use, experimental animals were anesthetized on ice.

Preparation of cultures

Explants of olfactory receptor epithelium. Antennae were removed from stage-4 female pupae, placed in a Petri dish containing sterile PBS, and filleted along a visible border between the olfactory receptor and non-receptor epithelia. The olfactory receptor tissue was incubated for 2 min at 37°C in a Ca^{2+} and Mg^{2+}-free Hanks' balanced salt solution (21250-014, Gibco, Grand Island, NY) containing 0.05 mg/ml collagenase (LS004196, Worthington, Freehold, NJ) and 0.2 mg/ml dispase II (165859, Boehringer Mannheim, Mannheim, Germany). After enzymatic digestion, the tissue was gently triturated with a fire-polished Pasteur pipette, layered onto 6 ml of Culture Saline, and allowed to settle by gravity. The aggregated tissue was rinsed twice more, first with Culture Saline and then with Culture Medium. Explants of olfactory receptor epithelium were evenly suspended in fresh Culture Medium and plated in 100-µl aliquots into the wells of pre-made culture dishes. Culture-dish wells were made by attaching coverslips

beneath 8-mm diameter holes drilled into the bottoms of 35-mm Falcon dishes. Dish wells were coated with a solution containing 400 µg/ml concanavalin A (C2010, Sigma, St. Louis, MO) and 4 µg/ml laminin (40232, Collaborative Research, Bedford, MA), and rinsed with sterile water prior use. After plating, culture dishes were sealed with Parafilm to prevent evaporation and incubated in a 26°C humidified incubator with room air.

Glial cell cultures and explant-glia co-cultures. For isolation of antennal nerve (AN) glia, whole brains with attached partial antennae from stage early-7 female pupae were dissected into a Petri dish containing ice-cold, sterile Dissecting Medium. Antennal lobes were exposed, and the attached antennae were filleted. The antennal nerve branches were cut close to the first antennal segment, and the perineural sheath was simultaneously removed from the antennal lobes and antennal nerves. The antennal nerves were then cut distal to the sorting zone, such that the entire intracranial portion of the antennal nerve and a small amount of antennal nerve from inside the antenna were saved. Antennal nerve tissue was digested with 0.1 mg/ml papain (5125, Calbiochem, La Jolla, CA) in Simple Salt Solution for 4 min at 37°C prior to trituration. Dissociated cells were then layered onto Recovery Solution in a 15-ml Falcon tube, and 200 units of DNase (Sigma D4263) in Simple Salt Solution were added to the top layer of suspended cells. Cells were centrifuged at 500 g for 4 min, resuspended in fresh Culture Medium, and centrifuged again. For plating alone, cells were resuspended in Culture Medium and plated into 8-mm wells (100 µl/well) as above.

For explant-glia co-cultures, glial cells were resuspended in Culture Medium and added to explant cultures previously grown for one day *in vitro* (1 DIV). For each dish, 50 µl of Culture Medium was removed from the 100-µl bubble of medium overlying the

cultured explants, and gently replaced with 50 µl of the glial suspension. After plating, the culture dishes were sealed, incubated for 2 hrs, and flooded with at least 1 ml of Culture Medium.

For isolation of sorting zone and neuropil-associated glia, antennal lobes were dissected and desheathed as above, neuronal cell-body packets were removed, and the sorting zone and neuropil tissue were cut apart and saved separately from the antennal nerve tissue. Tissue from all three sources was processed simultaneously for tissue culture, but plated separately.

Tissue culture solutions

Culture Saline: (Oland et al., 1996): 149.9 m*M* NaCl, 3 m*M* KCl, 3 m*M* $CaCl_2$, 0.5 m*M* $MgCl_2$, 10 m*M* TES, 11 m*M* D-glucose, 3 g/L lactalbumin hydrosylate (11800-026, Gibco), 2.5 g/L TC yeastolate (255772, Difco, Detroit, MI), 10% fetal bovine serum (FBS; HyClone, Logan, UT), 100 U/ml penicillin, 100 µg/ml streptomycin, pH 7.0, 360 mOsm.

Culture Medium: (supplemented Leibovitz's L-15 culture medium, Lohr et al., 2002): The following ingredients were added to 500 ml L-15: 50 ml FBS, 185 mg α-ketoglutaric acid, 200 mg D-(–)-fructose, 350 mg D-glucose, 335 mg DL-malic acid, 30 mg succinic acid, 1.4 gm lactalbumin hydrosylate, 1.4 gm TC yeastolate, 0.1 mg niacin, 30 mg imidazole, 500 µg 20-hydroxyecdysone (H-5142, Sigma), 100 U/ml penicillin, 100 µg/ml streptomycin, and 2.5 ml stable vitamin mix (SVM). A 5 ml stock solution of SVM consisted of 15 mg aspartic acid, 15 mg cystine, 5 mg β-alanine, 0.02 mg biotin, 2 mg vitamin B_{12}, 10 mg inositol, 10 mg choline chloride, 0.5 mg lipoic acid, 5 mg p-aminobenzoic acid, 25 mg fumaric acid, 0.4 mg coenzyme A, 15 mg glutamic acid, 0.5

mg phenol red. The pH was adjusted to 7.0 and the osmolarity was raised to 390 mOsm with D-glucose prior to sterile filtration.

Simple Salt Solution: 160m*M* NaCl, 6 m*M* KCL, 78.8 m*M* D-glucose, 10 m*M* HEPES, 100 U/ml penicillin, 100 µg/ml streptomycin, pH 7.0, 420 mOsm.

Recovery Solution: 50% (v/v) Culture Saline and 50% (v/v) Simple Salt Solution, pH 7.0, 380 mOsm.

Dissecting Medium: 50% Leibovitz's L-15 (Gibco BRL 41300-039), 25% (v/v) Culture Saline, 25% Simple Salt Solution with 5 m*M* EDTA, and 18 m*M* D-glucose, pH 7.0, 360 mOsm.

Live-cell microscopy

Time-lapse differential-interference-contrast imaging was performed on explant cultures grown for 1 DIV or explant-glia co-cultures grown for 2 hrs after the plating of AN glial cells. The imaging system included an Olympus BX50WI upright microscope with water-immersion objectives, shutters, z-drive, 12V/100W halogen bulb filtered by a green optical lens (543 nm), cooled CCD camera, and computer with SimplePCI (Compix Inc., Cranberry Township, PA) acquisition and analysis software. Prior to imaging, cultures were flooded with 3 ml of Culture Medium and placed inside an insulated chamber enclosing the stage to equilibrate to 25°C in a temperature-controlled micro-incubator (TC202A/ PDMI-2, Harvard Apparatus, Holliston, MA).

To prevent evaporation, a thin layer of canola oil was applied over the Culture Medium surface prior to imaging. Images were collected with a 60x objective at 20-min intervals for up to 24 hours. To ensure that focus was maintained over these relatively long imaging periods, a series of 5-6 images at successive focal planes 1 μm apart were collected at each time point. Only the in-focus images were used.

Rate analysis

The distances that axons grew were measured as reported previously (Tucker et al., submitted). Axons from explant-glia co-cultures were measured provided they met the following criteria: 1) each axon could clearly be identified as an individual, 2) axon growth could be monitored before and after contact with glial cells or glial processes, and 3) at least one image from each z-series was in focus for every time point of the movie sequence. While stepping through the selected movie sequences, markers were placed at the distal tip of growing axons in each frame and the distances between markers in consecutive frames were measured in microns using SimplePCI. The net distance grown by each individual axon at each point in time was determined by summing all distances that were recorded up to that point. Branches that clearly arose from parent axons and continued to grow for longer than 1 hour after formation were also measured. All branches were measured from the time of their appearance to the end of the recording. Net distances were plotted as a function of time, and elongation rates were determined by calculating the slope of regression lines fit to the pre-contact and post-contact curves for the each plot.

Cytoskeletal staining, growth cone sampling, and statistical analysis

Microtubule and F-actin labeling were performed as previously described (Tucker et al., submitted). Cultures were rinsed with K-PIPES buffer (80mM PIPES-KOH, pH 6.8, 5 mM EGTA, 2 mM $MgCl_2$), then fixed and extracted for 30 min in K-PIPES buffer containing 0.5% glutaraldehyde and 0.1% Triton X-100. Cultures were rinsed in phosphate-buffered saline (PBS) containing 1 mg/ml $NaBH_4$ to quench autofluorescence, then rinsed and blocked for 1 hr in PBS containing 0.2% fish skin gelatin and 0.1% Triton X-100 (blocking buffer). Mouse anti-α-tubulin (T9028, Sigma) was diluted 1:800 in blocking buffer and applied for 2.0 hrs at room temperature. After rinsing, cultures were incubated for 1.5 hrs in a 1:1000 dilution of secondary antibody (goat anti-mouse Cy3; Jackson ImmunoResearch, West Grove, PA) in blocking buffer containing approximately 2.5 U/ml, or 83 nM, Alexa-488 conjugated phalloidin (A-12379, Molecular Probes, Eugene, OR). Cultures were then rinsed and mounted with coverslips in a polyvinyl alcohol (PVA)-based mounting medium that included 1,4-diazobicyclo[2,2,2]octane (DABCO) to limit photobleaching.

Tubulin and F-actin stained cultures were used to compare the morphological complexity of hundreds of growth cones across multiple dishes. At least three explants displaying radial growth and a high number of surrounding glial cells were randomly selected from each of three explant and three explant-glia dishes. The entire perimeters of the selected explants were sampled using a 60x objective, and images (~30 / dish) were saved. Unmanipulated confocal images were printed and all isolated growth cones were scored based on a qualitative scale of morphological complexity. Scoring accuracy was confirmed by comparing independent results from two separate observers. Dishes were summed only if growth cone scores were statistically similar between dishes within

the same experimental group. Two-by-two contingency tables containing total numbers of simple and complex growth cones from each experimental group were constructed and tested for statistical differences by Fisher's exact test (Fisher, 1925). Qualitative variables from tested conditions were defined as statistically different at a probability value of $p < 0.05$.

Labeling of GPI-linked Fasciclin II

Cultures were fixed for 1 hr in a 0.1 M phosphate buffer containing 4% paraformaldehyde (PFA), and then rinsed and blocked for 1 hr in PBS containing 4% normal goat serum (NGS). Antibodies raised to specifically recognize the GPI-linked isoform of *Manduca* Fasciclin II (Wright and Copenhaver, 2000) were diluted 1:10,000 in PBS with 4% NGS, applied to cultures, and incubated overnight at 4°C. Cultures were rinsed in PBS, and incubated for 1.5 hrs in goat-anti-guinea pig Cy3 secondary antibody (Jackson Immunoresearch) diluted 1:500 in PBS. Cultures were then rinsed into Tris-buffered saline (TBS), incubated for 20 min at RT in a 1:1500 dilution of the nucleic acid stain Syto 13 (S-7575, Molecular Probes) in TBS, rinsed, and mounted in PVA.

CellTracker and anti-Horse radish peroxidase (HRP) labeling

Prior to plating, AN glial cells were suspended in 500 µl loading buffer containing 5 µM CellTracker green (C-7025, Molecular Probes) and 0.01% Pluronic F-127 (P-6866, Molecular Probes) in standard insect saline (150 mM NaCl, 4 mM KCl, 2 mM $CaCl_2$, 1 mM $MgCl_2$, 10 mM HEPES buffer, 35.5 mM D-glucose, 40 mM mannitol, pH 7.0, 390 mOsm). Cells were incubated 10-20 min with slight agitation. Labeled cells were transferred to a tube containing 6 ml of Culture Medium, pelleted by centrifugation,

resuspended in Culture Medium, and plated with explant cultures grown for 1DIV. Explant-glia co-cultures were grown for 1 or 2 days *in vitro*, and then processed for anti-HRP immunocytochemistry. Antibodies against HRP specifically recognize cell-surface antigens on developing insect neurons (Jan and Jan, 1982). Cultures were fixed for 30 min in 0.1 M phosphate buffer containing 4% PFA, rinsed in PBS, and blocked for 1hr in PBS with 2% NGS, 2% bovine serum albumin (BSA), and 0.5% Triton x-100. Rabbit anti-HRP (323-005-021, Jackson ImmunoResearch) was diluted 1:1000 in PBS with 1% NGS and 1% BSA, added to cultures, and incubated overnight at 4°C. Cultures were then rinsed in PBS with 1% NGS, 1% BSA, and 0.25% Triton X-100, and incubated for 1 hr with goat anti-rabbit Cy3 secondary diluted 1:1000 in PBS with 1% NGS and 1% BSA. Cultures were rinsed in PBS with 0.25% Triton X-100, and then rinsed again with PBS before mounting in PVA.

Laser-scanning confocal microscopy

A Nikon PCM 2000 system equipped with a Nikon E800 microscope, a 50 mW argon laser, 4 mW green and 10 mW red HeNe lasers, and a computer running SimplePCI acquisition and analysis software, was used for confocal imaging. Appropriate dichromatic filters were used for multi-channel collection. Serial optical sections were taken at sequential depths, 0.3-1.0 μm apart depending on the depth of field of the required objective lens, and stored as stacks of optical images. If needed, confocal images were manipulated for brightness, contrast, and intensity with Photo Paint 9 or SimplePCI and prepared in figure format with Corel Draw 9.

Bromodeoxyuridine incorporation, immunocytochemistry, and analysis

The uridine derivitive, bromodeoxyuridine, can substitute for thymidine and incorporate into DNA during the S-phase of the cell-division cycle. To monitor glial proliferation *in vitro*, 5-bromo-2'-deoxyuridine (BrdU; B-9285, Sigma) was added to explant-glia co-cultures at a final concentration of 5 µg/ml. At the stage used to isolate glia, neuropil-associated glia (Oland and Tolbert, 1989; Kirschenbaum et al., 1995), some sorting zone glia (Rössler et al., 1999), and glia within the intracranial portion of the AN (unpublished observations), are dividing. Glial cells were cultured for 12 hrs before receiving BrdU to ensure that any cells in S-phase at the time of plating would exit this portion of the cell cycle and that all BrdU incorporation would be the result of DNA synthesis occurring *in vitro*. Explant-glia co-cultures were grown for 13.5 hrs in the presence of BrdU, and then fixed with 4% PFA in 0.1M phosphate buffer for 1 hr. Following fixation, cultures were rinsed in PBS, treated with 2N HCl in PBS for 30 min to denature DNA and facilitate antibody recognition, rinsed in PBS with 0.3% Triton X-100 (PBST), and blocked in PBST with 4% NGS for 1 hr. Mouse anti-BrdU (347580, Beckton Dickinson, San Jose, CA) was diluted 1:200 in PBS with 1% NGS, applied to cultures, and incubated for 2 days at 4°C. Cultures were then rinsed in PBS with 2% NGS, incubated in a 1:800 dilution of goat-anti-mouse Cy3 secondary in PBS with 2% NGS, rinsed in PBS, incubated for 10 min in a 1 µg/ml solution of 4',6-diamidino-2-phenylindole dihydrochloride (DAPI; D9542, Sigma) to counterstain all nuclei, rinsed, and mounted in PVA. Phase contrast and two-channel fluorescence images were collected using an inverted Olympus microscope with a Hammamatsu CCD camera and appropriate filter sets. Five non-overlapping images were collected with a 20x

planapochromat objective, covering the majority of each dish, and cell nuclei were counted in all fields provided they could be identified as glial cells in corresponding bright field images. After counting nuclei in each field and summing nuclei from similar dishes, BrdU-positive glial nuclei were expressed as a percentage of the total number of DAPI stained glial nuclei for each glial type.

Conditioned-medium experiments

Coverslips were glued beneath two physically separated 8-mm holes drilled into the bottoms of individual 35-mm Falcon dishes, and coated as described above. This technique has previously been used to prevent physical contact between cells cultured in the two adjacent wells, but allow for chemical communication between cells in the two wells through the 1 ml of culture medium that covers them after plating (Oland and Oberlander, 1994; Luedeman and Levine, 1996). AN glial cells were grown either alone (Fig. 10, condition 1), or physically separated from explants of olfactory epithelium (Fig. 10, condition 2). In a third condition, AN glial cells received medium conditioned by explant-glia co-cultures (Fig. 10, condition 3). In condition 3, glial cells were plated into both wells simultaneously, such that explant-glia cultures in well "A" were established at the same time glial cells were plated in well "B." During normal explant-glia co-culture preparation, AN glial cells were bathed for 2-3 hrs prior to flooding in a 100-µl bubble of Culture Medium that possibly contained a concentrated supply of diffusible factors released from explants. To replicate this, AN glial cells in conditions 2 and 3 were plated into explant conditioned medium prior to flooding. Three double-well dishes were prepared per condition described in Figure 10. For photography, slightly overlapping

phase-contrast images were collected down a central strip of well B in all dishes, creating a representative montage of the AN glial cells at 24 and 72 hours after plating.

RESULTS

Isolation and culture of antennal nerve glial cells and explants of olfactory receptor epithelium

In *Manduca*, glial cells of the sorting zone and antennal lobe neuropil arise from a common pool of CNS glia (Rössler et al., 1999). AN glia have a separate origin, however, and arise in the antenna. AN glia migrate down the antennal nerve and arrive at the distal edge of the sorting zone by stage 7 (Rössler et al., 1999; Fig. 1A). AN glia were harvested for culture from pieces of early stage-7 antennal nerves that were cut distal to the sorting zone and proximal to the second segment of the antenna. This dissection excluded the sorting zone glia, which occupy the most proximal portion of the antennal nerve, and the olfactory receptor neurons (ORNs), which are located in the olfactory receptor epithelium of the antenna starting in the third segment (Fig. 1A). *In vitro*, AN glial cells had either oblong (Figs. 1B-C) or discoid (Fig. 1D) cell bodies, and many long, stout processes.

AN glial cells were added to cultures containing explants of stage-4 olfactory receptor epithelium grown for 24 hrs *in vitro*. Before addition of glial cells, hundreds of ORN axons extended from explants and normally displayed a radial pattern of outgrowth (Fig. 1E). ORN axon outgrowth from olfactory receptor explants was robust, particularly within the first 48 hrs of culture, allowing for the observation of dynamic changes in axon behavior. Individual growth cones could be identified at the peripheral margin of explants, where the extent of axon overlap was minimal (Fig. 1F). Time-lapse observations showed that ORN axons elongated by extending and retracting fine branches that extended from their growth cones. Most axons had streamlined growth

After contact, some axons (13%) branched and continued to advance on the substrate adjacent to the contacted AN glial cells (Figs. 3A-F; Table 1). At the beginning of the sequence shown in Figure 3, axons extended from the upper right and contacted a process from the AN glial cell located at the bottom left of Figure 3A. One growth cone (Fig. 3B, arrowhead) advanced toward and contacted the glial process (Fig. 3C), enlarged, branched, and continued to advance (Figs. 3D-F). Axons that branched but continued to elongate typically extended one branch at a time; when a growing branch stopped elongating, a new branch would grow while the first was retained but left with little cytoplasm (Figs. 3E-F).

Other growth cones (13%) simply continued to advance across the AN glial cells or processes that they contacted, while a few growth cones (7%) ceased advancement after contact (Table 1). Growth cones that advanced across or stopped advancing remained simple in morphology, neither flattening nor branching following contact with AN glial cells (data not shown).

Rate Analysis

The net distances grown by individual axons selected from representative recordings were analyzed to study possible contact-mediated changes in axon elongation.

Whether growth cones branched and advanced (Fig. 4, axons #1 and #2), advanced on the substrate adjacent to AN glial cells (Fig. 4, axon #5a), or advanced in contact with the processes of AN glial cells (Fig. 4, axons #3, #4, and #5b), ORN axons continued to elongate long after growth cone contact with AN glia (Fig. 4, arrows). The bars above axons #3, #4, and #5b in Figure 4 correspond to the period of time during which their

growth cones extended on glial processes. The first three branches of axon #1 (Fig. 4) are shown in Figures 2D-F. Axon #4 (Fig. 4) is depicted in Figure 2, and was measured until the tip became obscured after reaching the glial cell body shortly after Figure 2F. The tip of axon #5b became obscured after it reached the cell body of the glial cell it had grown on, and could not be followed until the end of the recording.

After contacting glial cells, ORN axons continued to elongate, on average, at 59% (Fig. 4, table) of their pre-contact rate. In two recordings, the rate of axon elongation was actually greater on glial processes than before contact with AN glial cells (Fig. 4, axons #4 and #5b).

Statistical analysis of contact-mediated changes in growth cone morphology

To better characterize the influence that contact with AN glial cells had on ORN growth cone morphology, we used cytoskeletal labeling to analyze hundreds of growth cones from fixed cells. In confocal microscopic images of the entire perimeters of randomly selected explants, individual growth cones were scored qualitatively according to their morphological complexities. ORN growth cones had diverse shapes (Figs. 5A-D), yet they could be grouped into two broad categories: those with simple (Figs. 5A-B) and those with complex (Figs. 5C-D) morphologies. Simple growth cones had either unbranched or branched microtubule domains, and were usually tipped by a single F-actin-based filopodium. Complex growth cones had lamellar regions containing splayed microtubules, and were surrounded by short, dense fringes of F-actin-based filopodia. Growth cones also adopted simple (Figs. 5E-F) or complex (Figs. 5G-H) morphologies when they were in contact with AN glial cells. Growth cones were predominantly simple (~85 %) in morphology, regardless of glial cell contact (Figs. 5I-J). The distributions of

growth cone morphologies in non-contacting conditions were not statistically different from one another (P = 0.690), nor were there statistically significant differences between contacting and non-contacting growth cones in explant-glia co-cultures (P = 0.516), when analyzed by Fisher's exact test.

ORN axons and AN glial cells form close associations with each other

Live-cell recordings demonstrated that ORN axons and AN glial cells were often closely associated with one another. To better visualize the extent of neuron-glia inter-relationships, differential staining was used to separately label ORN axons and AN glial cells. AN glial cells were labeled with a vital fluorescent dye prior to plating with explants and the explant-glia co-cultures were grown for 24 or 48 hours, fixed, and then stained with antibodies against horseradish peroxidase (HRP) to label ORN axons. Anti-HRP antibodies specifically detect glycoproteins on the cell-surfaces of insect neurons (Jan and Jan, 1982; Sun and Salvaterra, 1995), including cultured moth ORNs isolated from developing antennae (Lucas and Nagnan-Le Meillour, 1997).

Confocal microscopy revealed many examples of ORN axons intimately associated with AN glial cells, both at the 24 hr (Figs. 6A-C) and 48 hr (Fig. 6D) time points. Interestingly, AN glial cells formed multicellular arrays that were linked together by processes (Figs. 6A-C, E). ORN axons readily grew on the AN glial cells they encountered, and their trajectories were noticeably influenced by the directional orientation of AN glial arrays (Fig. 6C). Axons grew for considerable distances along AN glial cells, sometimes shifting back and forth between glial surfaces and the adjacent substrate (Figs. 6A-D). Glial arrays often occurred between explants of olfactory epithelium (Fig. 6E; compare with Fig.7A), in territory close to explants but devoid of

ORN axons (Fig. 6F), indicating that axonal processes did not prefigure the formation of AN glial arrays.

AN glial cells form multicellular arrays on and near ORN axons

By taking phase-contrast photographs of the same fields of view on successive days in culture, we were able to characterize the behavior of individual glial cells during the formation of glial arrays. One such field of view is presented in Figure 7, which shows many AN glial cells distributed between several explants (Fig. 7A). Three hours after plating, AN glial cells were growing in no obvious pattern on and next to ORN axons that extended from nearby explants (Fig. 7B). At 24 hrs, processes grew from many glial cells, and the cells had formed the rudiments of arrays (Fig. 7C). Additional cell bodies appeared to accumulate along glial processes, suggesting that glial cells proliferated during array formation (Figs. 7B-E, arrowheads). By 48 hrs, glial cells had assembled into clearly recognizable arrays both on and next to ORN axons, with glial processes spanning between and interconnecting multiple glial cell bodies (Fig. 7D). By 72 hrs, the array had expanded further, with new additions of glial processes added to the array seen at 48 hrs (Fig. 7E). Although new additions to glial arrays were infrequent after 72 hrs, they were still present after 96 hrs of culture (Fig. 8A). Glial cells that did not incorporate into arrays apparently died, as no individual glial cells remained in isolation beyond 72 hrs.

When cultured in the absence of neurons, AN glial cells typically did not form arrays and died between 48-72 hrs *in vitro*. In rare cases, a small number of AN glial cells elongated and joined with several neighbors to form small glial aggregates that

survived past 72 hrs in culture, but these arrays were always less extensive than those formed near ORN axons in co-cultures.

AN glial arrays are immunoreactive for GPI-linked Fasciclin II

Fasciclin II is a homophilic cell adhesion molecule in the immunoglobulin superfamily that is involved in the fasciculation and guidance of certain axons in developing insect nervous systems (Bastiani et al., 1987; Harrelson and Goodman, 1988; Grenningloh et al., 1991). *In vivo*, a large subset of ORN axons expresses the transmembrane isoform of *Manduca* Fasciclin-II (MFas II), and a set of AN glial cells distal to the sorting zone express the GPI-linked isoform of MFas II (GPI-MFas II) (Higgins et al., 2002). Interactions between isoforms of MFas II could underlie cellular interactions between ORN axons and AN glial cells, both *in vivo* and *in vitro*. To test if arrays of AN glial cells were GPI-MFas II-positive, explant-glia co-cultures were fixed after 96 hrs of glial growth and labeled for GPI-MFas II. All of the AN glial cells in randomly chosen arrays were immunoreactive for GPI-MFas II (Fig. 8). As expected, ORN axons were GPI-MFas II-negative (Fig. 8B). The multicellular nature of glial arrays was apparent after counterstaining with a fluorescent nucleic acid stain. At the higher magnification shown in the boxed region in Figure 8B, multiple nuclei were observed within the GPI-MFas II-positive array of AN glial cells (Figs. 8C-E).

AN glial cells proliferate *in vitro*

To determine whether AN glial cells were mitotically active *in vitro*, bromodeoxyuridine (BrdU) was used to label cells in the S-phase of the cell-division cycle in 12-hour explant-glia co-cultures. Before cell counts were made, glial cells were

identified in phase-contrast images (Figs. 9A,E,I). All nuclei were counterstained with DAPI, such that the total number of neuropil-associated (Fig. 9B), sorting zone (Fig. 9F), and AN (Fig. 9J) glial cells per field of view could be counted. For the experiment presented in Figure 9, neuropil-associated (Figs. 9A-D), sorting zone (Figs. 9E-H), and AN glia (Figs. 9I-L) were grown and examined separately, and the numbers of BrdU-positive neuropil-associated (Figs. 9C,D), sorting zone (Figs. 9G,H), and AN (Figs. 9K,L) glial nuclei were counted in each field and summed across similar dishes. Less than 2% of neuropil and sorting zone glia were BrdU-positive, while approximately 16% of glial nuclei in AN co-cultures incorporated BrdU (Fig. 9M). Explants contained a few BrdU-positive nuclei (Figs. 9K,L open arrows), presumably from non-neuronal cells, but these labeled cells were not counted.

Long-range diffusible factors fail to promote the formation of AN glial arrays

The formation of AN glial arrays depended on the presence of explants of olfactory epithelium, but since arrays often formed on the dish substrate between explants (Figs. 6E-F, Fig. 7), it was unclear whether contact with ORN axons was required for their formation. To test whether a soluble signal released from explants could influence the development of glial arrays, we used two-well culture dishes that allowed cells in the two wells to be in chemical communication with one another. This paradigm allowed us to test the effect of culturing AN glial cells alone (condition 1), culturing AN glial cells with medium conditioned by explants (condition 2), and culturing AN glial cells with medium conditioned by explants and AN glial cells (condition 3). Condition three was included to test whether a diffusible signal that could influence the formation of AN glial arrays was generated in explant-glia co-cultures. Photographs

were taken at 24 and 72 hrs after glial addition. Arrays of AN glial cells did not form in well B of condition 1 (Fig. 10B), in well B of condition 2 (Fig. 10C), or in well B of condition 3 (Fig. 10D), suggesting that a long-range diffusible signal did not stimulate array construction. The small glial aggregates that were occasionally seen in the absence of explants were not present in any of the three conditions. In well A of condition 3, however, AN glial cells that were grown with explants of olfactory epithelium did form arrays (Fig. 10E), suggesting that AN glia were competent to form arrays, but required the local presence of explants to do so.

DISCUSSION

Axon-glia interactions underlie critical developmental events in the formation of the adult olfactory system in the moth *Manduca sexta*. In the present *in vitro* study, we characterized reciprocal interactions between ORN axons and glial cells isolated from the developing antennal nerve of *Manduca*. Contact with AN glia overwhelmingly led to continued axon elongation, without causing dramatic or long-lasting changes in growth cone complexity. In addition, growth cones preferentially extended along glial surfaces, indicating that AN glial cells provided a permissive substrate for axon elongation. AN glial cells were active during interactions with ORN axons; they often initiated encounters by extending processes to meet advancing growth cones. Furthermore, glial cells proliferated and actively organized into multicellular arrays on and near ORN axons. Arrays rarely developed when AN glia were grown alone, and those that did form were always considerably smaller than those that formed in explant-glia co-cultures. Exposing AN glial cells to conditioned medium from explants or explant-glia co-cultures failed to induce the formation of glial arrays, indicating that this glial behavior was dependent on short-range interactions with ORN axons. We hypothesize that AN glial cells provide permissive but not instructive cues for growing ORN axons *in vivo*, and in turn, that ORN axons stimulate changes in the behavior of AN glia that allow them to migrate and enwrap small bundles of ORN axons in the nerve.

ORN axons respond differently to sorting zone and neuropil-associated glial cells

In marked contrast to the findings reported here for AN glial cells, the glial cells that populate the sorting zone and antennal lobe neuropil have been found to induce extensive contact-dependent elaborations in growth cone morphology and cause the

cessation of ORN axon elongation (Tucker et al., 2000, 2001). Unlike AN glia, which arise in the periphery, sorting zone and neuropil-associated glia arise from precursors in the CNS and are present at key decision regions of the olfactory pathway during early stages of ORN axon ingrowth. We have shown that both have decisive influences on the behavior of ORN axons *in vivo* (Oland and Tolbert, 1988; Oland et al., 1988; Baumann et al., 1996; Rössler et al., 1999). In the glia-rich sorting zone, ORN axons lose associations with neighboring axons, abruptly change trajectories, and join with axons of like identity to form new fascicles that terminate in particular glomeruli (Oland et al., 1998; Rössler et al., 1999; Higgins et al., 2002). In the neuropil, axons make terminal branches that coalesce into protoglomeruli after passing through the shell of neuropil-associated glia (Oland et al., 1990; Oland et al., 1998). The dramatic differences seen *in vitro* in growth cone responses to AN glial cells versus sorting zone and neuropil-associated glial cells likely have functional consequences *in vivo*; AN glia may provide a permissive substrate for axon elongation, whereas sorting zone and neuropil-associated glia may provide cues necessary for axon sorting, targeting, and branching.

Potential roles for AN glia *in vivo*: Glial influences on axon behavior

AN glia are born peripherally in the antennal epithelium, and migrate to populate the entire length of the antennal nerve distal to the sorting zone (Rössler et al., 1999). The AN glia first appear in the intracranial portion of the antennal nerve at stage 6, label with antibodies against the GPI-linked isoform of *Manduca* Fasciclin II (GPI-MFas II), and have longitudinally oriented processes that extend to the distal margin of the sorting zone (Higgins et al., 2002). AN glia completely invest the intracranial portion of the

antennal nerve by mid-stage 7, after most ORN axons have reached the brain (Rössler et al., 1999). Since AN glia do not accompany early growing ORN axons to the brain, AN glia are unlikely to influence axon outgrowth or guidance during the initial establishment of the antennal pathway. The AN glia could, however, provide a permissive substrate for later growing ORN axons, which continue to arrive through stage 9 of adult development (Sanes and Hildebrand, 1976).

Our current *in vitro* findings suggest that growth cones readily traverse AN glial surfaces, without prolonged changes in growth cone morphology or dramatic alterations in the rates of axon elongation. Time-lapse movie sequences and differential labeling of fixed preparations demonstrated that ORN axons formed intimate associations with AN glial cells, an observation corroborated by electron microscopy (L.A. Oland, unpublished observations). We hypothesize that cell-cell and/or cell-matrix adhesion molecules mediate axon-glia interactions and allow ORN axons to elongate on glial processes *in vitro*.

Potential roles for AN glia *in vivo*: Axon influences on glial behavior

AN glia are intimately associated with ORN axons in the mature antennal nerve, where glial processes enwrap fascicles that include 10-70 ORN axons (Sanes and Hildebrand, 1976). Results from the current and previous studies suggest that the development of this arrangement may require both physical and chemical communication between AN glial cells and ORN axons.

First, ORN axons likely provide a substrate for glial migration *in vivo*, as AN glia course down the antennal nerve along axons. We report in the current study that before forming arrays, AN glial processes were often seen extending toward, adhering to, and

growing along ORN axons. Intimate associations between ORN axons and AN glial cells were therefore formed mutually, with both axons and glial cells contributing to the response. We hypothesize that contact-dependent processes similar, if not identical, to those predicted to regulate axon extension on glial surfaces, underlie the association of AN glial processes with ORN axons.

Second, nitric oxide (NO) signaling appears to regulate glial migration in the developing primary olfactory system of *Manduca*. A calcium-dependent NO synthase (NOS) gene has been cloned in *Manduca*, and is strongly expressed in the antenna (Nighorn et al.,1998). The spatial location of NOS immunoreactivity in ORN axons changes during development, such that at stage 5, NOS-positive axons are restricted to the region of nerve adjacent to the rootlets, and at stage 7, NOS-positive axons are distributed throughout the entire width of the antennal nerve (Gibson and Nighorn, 2000). The distribution of glial cells in the antennal nerve also changes developmentally, and coincides spatially and temporally with the location of NOS-positive ORN axons (Gibson and Nighorn, 2000). Treatment of developing animals with agents that block NO signaling disrupts the migration of AN glia in the antennal nerve, suggesting that NO released from ORN axons could either directly or indirectly stimulate glial migration (Gibson et al., 2001).

In the current study, AN glial cells preferentially formed arrays in cultures containing explants of olfactory epithelium, but they often did so adjacent to, not directly on, ORN axons. This suggests that direct physical contact with axons is not necessary for array formation. Since potential long-range soluble factors presented through conditioned medium did not substitute for the absence of explants, the simplest hypothesis is that short-range secreted signals, either diffusible or substrate-bound, act

to stimulate the formation of glial arrays *in vitro*. An intriguing possibility is that NO, which has a short half-life and thus a spatially discrete sphere of influence (Philippides et al., 2000), induces the formation of AN glial arrays after being released from NOS-positive ORN axons.

The axon-induced formation of multicellular glial arrays *in vitro* likely represents a 2-D reflection of more complex changes in glial behavior that normally occur *in vivo*. Array formation could represent an *in vitro* response to a signal that normally leads to glial elongation and migration along axons *in vivo*. In addition, AN glial association with and alignment near ORN axons could represent an *in vitro* behavior that reflects the process of glial enwrapment of axon fascicles *in vivo*.

Reciprocity in vertebrate neuron-glia interactions

The current study describes reciprocal interactions between cultured ORN axons and AN glial cells from *Manduca*. Such two-way interactions between cultured neurons and glia have been studied in considerable detail in vertebrates. *In vitro*, cellular behaviors including neurite elongation on glial cells and glial enwrapment of axons have been well characterized, and are dependent on the proper function of cell-cell and cell-matrix adhesion molecules. Across vertebrate species, function-blocking experiments demonstrate that the outgrowth of motor and sensory neurites on cultured Schwann cells is regulated by a variety of glycoproteins, including integrins and the homophilic adhesion molecules L1 and N-cadherin (Bixby et al., 1988; Kleitman et al., 1988; Seilheimer and Schachner, 1988; Letourneau et al., 1990). Adhesion molecules and integrins also regulate neurite elongation on CNS-derived astrocytes and Müller cells (Tomaselli et al., 1988; Neubauer et al., 1988; Drazba and Lemmon, 1990; Yazaki et al.,

1996). Furthermore, L1 and N-cadherin act reciprocally to mediate axon-induced changes in Schwann cell behavior, including the linear alignment along, adhesion to, and enwrapment of individual axons (Seilheimer et al., 1989; Wood et al., 1990; Letourneau et al., 1991; Wanner and Wood, 2002). Heterophilic adhesion molecules also mediate neuron-glia interactions and allow for the formation of contacts between DRG neurites and Schwann cells during the early stages of glial enwrapment (Suter et al., 1995). Like vertebrate neuron-glia interactions, adhesive interactions between moth ORN axons and AN glial cells likely promote bi-directional changes in cellular behavior that lead to axon extension on glial surfaces and glial process association with ORN axons.

Comparison of AN glia and ensheathing cells of the mammalian olfactory system

The arrangement of glia within the primary olfactory pathway of mammals has been studied in considerable detail, in part because the adult olfactory bulb retains the ability to support the continuous ingrowth of axons from the periphery. This ability has been attributed to a specialized population of glia, the olfactory ensheathing cells, that display a blend of Schwann cell and astrocyte characteristics (Barber and Lindsay, 1982; Raisman, 1985; Doucette, 1990; Ramón-Cueto and Avila, 1998). AN glia and olfactory ensheathing cells have certain similarities and some key differences, highlighted by: 1) their anatomical locations within their respective olfactory pathways, 2) their roles in promoting neurite growth, and 3) their roles in axon guidance.

During development, olfactory ensheathing cells arise from the olfactory placode (Chauh and Au, 1991) and accompany the first ORN axons to the presumptive olfactory bulb (Marin-Padilla and Amieva, 1989; Doucette, 1989; Valverde et al., 1992). Olfactory

and provide trophic support for ORN axons during development and in normal adult-turnover (Key et al., 1996; Woodhall et al., 2001; Martin et al., 2002). Although it remains possible that AN glia display similar trophic interactions with ORN axons during development, ORN turnover is not likely to occur in *Manduca* due to its brief adult lifespan.

In mice, olfactory ensheathing cell processes envelop fascicles of ORN axons in the olfactory nerve and outer olfactory nerve layer of the adult olfactory bulb (Au et al., 2002). Olfactory ensheathing cells express molecules known to influence the growth, sorting, and targeting of ORN axons as they extend from the olfactory nerve layer to the underlying glomerular layer of the olfactory bulb (Puche et al., 1996; St John and Key, 1999; Tisay et al., 2000; Crandall et al. 2000; Schwarting et al., 2000; Gilbert et al., 2001). Ensheathing cells of a different molecular profile, coined olfactory ensheathing cell-like cells, loosely associate with ORN axons in the inner olfactory nerve layer, and may play a role in axon reorganization and targeting (Au et al., 2002). Instead of sorting in the nerve layer that circumscribes the olfactory neuropil, ORN axons in *Manduca* reorganize extensively within the sorting zone before reaching target glomeruli within the antennal lobe (Oland et al., 1998; Rössler et al., 1999). Since AN glia arrive late and do not enter the sorting zone, they are unlikely to mediate axon sorting or targeting. Instead, the centrally derived glia that reside in the sorting zone could play functionally equivalent roles to the ensheathing cells that reside in the nerve layer of the olfactory bulb (Valverde, 1999; Key and St. John, 2002).

Summary

Glial cells play critical roles during the development of the adult moth olfactory system. The results of the current *in vitro* study suggest that reciprocal interactions between ORN axons and AN glial cells could influence axon-glia interrelationships *in vivo*. AN glia support the elongation of ORN axons *in vitro*, and, although they are not required for the initial growth or guidance of axons *in vivo*, AN glia may promote the growth of late-arriving ORN axons. In addition, ORN axons have the capacity to influence the behavior of AN glial cells, by triggering the formation of multicellular arrays *in vitro*, and by triggering the migration of AN glia *in vivo*. The intimate relationships seen between ORN axons and AN glial cells *in vitro* likely reflect the mutual associations that are required to support glial migration, glial enwrapment of axon bundles, and axon elongation on glial processes *in vivo*. Future studies will more closely examine the interdependence of ORN axon and AN glial cell behavior *in vivo*, and probe the molecular bases of neuron-glia interactions *in vitro*.

Figure 3.1 Establishment of cultures containing ORN axons and antennal nerve (AN) glial cells. **A.** Diagram illustrating the anatomical locations of AN, sorting zone (SZ), and neuropil-associated (NP) glial cells in the primary olfactory pathway of *Manduca sexta* at stage 7 of adult metamorphic development. **B-D.** Differential interference contrast (DIC) images of freshly cultured glial cells from the antennal nerves of early stage-7 animals. **E.** Low magnification phase contrast image of an explant of olfactory receptor epithelium cultured for 1 DIV. ORN axons extend in a radial pattern from explant. **F.** High magnification DIC image of ORN axons at the peripheral margin of axon outgrowth form an explant. Open arrow, flattened growth cone; closed arrow, simple growth cone. Scale bars: B, 25 μm, applies to C, D; F, 25 μm; E, 100 μm.

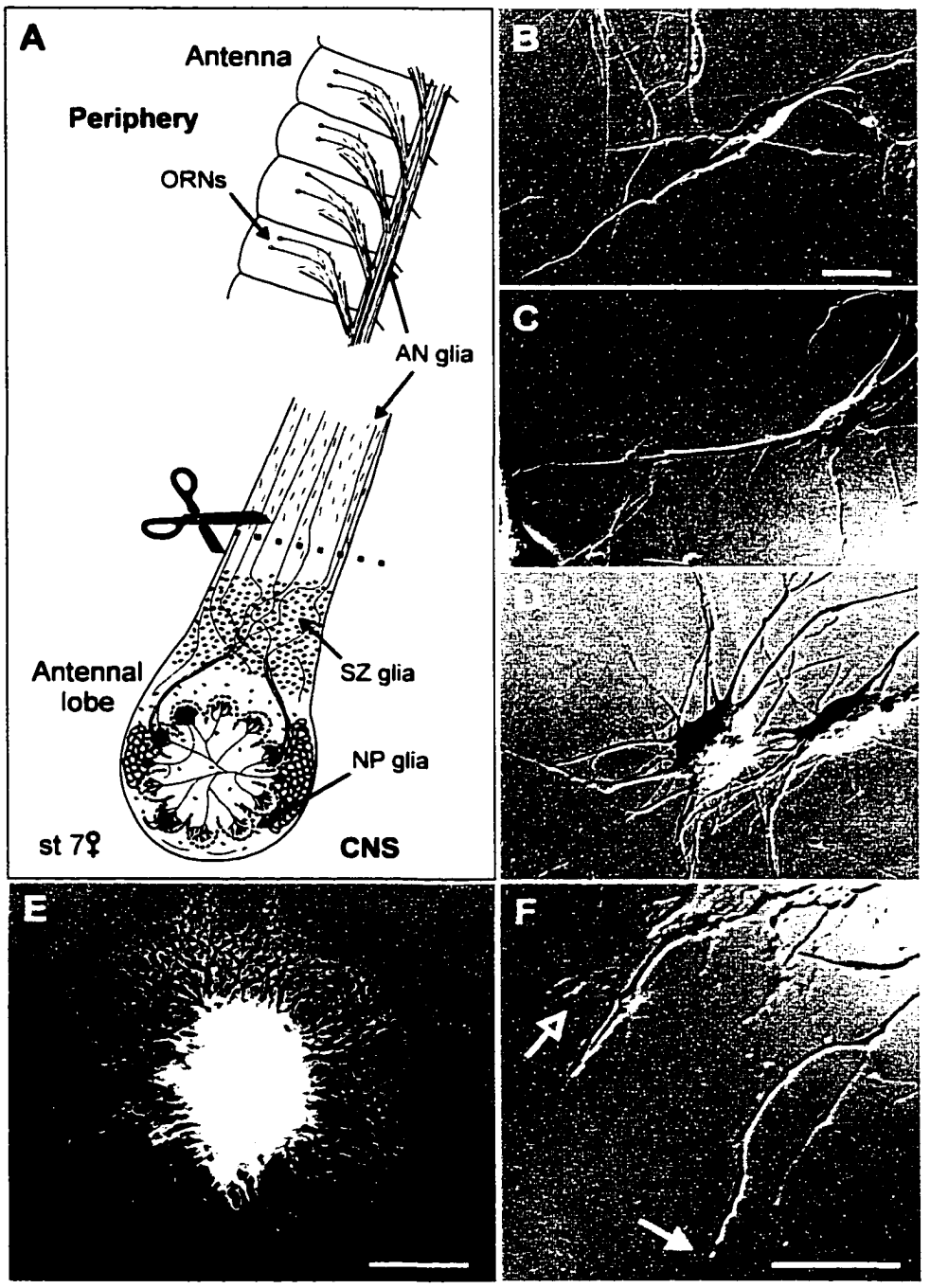
A
Antenna
Periphery
ORNs
AN glia
Antennal lobe
SZ glia
NP glia
st 7♀
CNS
B
C
E
F

Figure 3.2 After contact with AN glial cells, ORN growth cones sometimes elaborate before advancing along glial processes. **A-F.** DIC images from time-lapse recording (top), and traces (bottom) of growth cone at arrow (light gray) and glial processes at open arrow (dark gray). Glial processes grow in from lower left; ORN growth cone enters from upper right. **A, B.** Glial process extends toward and contacts growth cone. **C.** Growth cone flattens and extends along glial process. **D.** Flattened growth cone has elaborated while remaining intimately associated with glial process. **E-F.** Growth cone remodels, becoming simpler, and advances along glial process. Arrows indicate axon shaft; arrowheads indicate axon tip. Time stamps are in hours and minutes. Scale bar: 10 μm, applies to all.

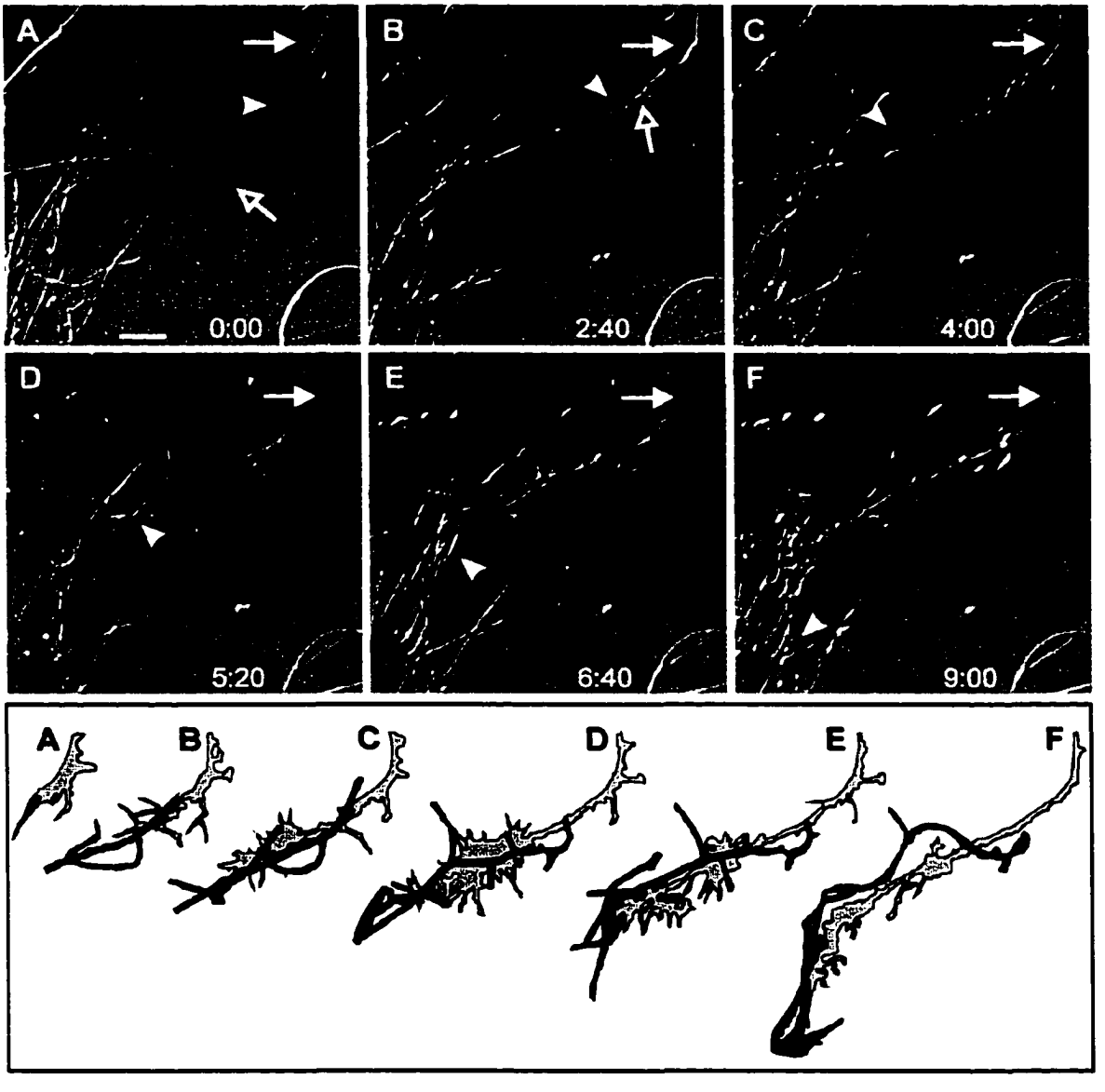
A
0:00
B
2:40
C
4:00
D
5:20
E
6:40
F
9:00
A
B
C
D
E
F

Figure 3.3 Two other axon behaviors following growth cone contact with an AN glial cell. **A.** Entire field of view at time zero. Cell body of AN glial cell (asterisk), bottom left; ORN axon (arrow) extends from an explant outside the field to the upper right. **B-F.** Digital zoom of area outlined in A, showing axon branching and elongation following contact with glial process (asterisk). **C.** Growth cone contacts glial process at arrowhead. **D.** Growth cone enlarges (star) and a small branch (arrowhead) emerges from left edge. **E.** Branch continues to grow to its furthest extent. **F.** New branch (open arrowhead) extends upwards as old one (arrowhead) is maintained. **G-I.** Area highlighted by oval in F, showing elongation of a different axon on a glial process. Growth cone tip (arrowhead) extends along glial process (asterisk). Double arrowhead in F indicates the ORN axon that elongated along glial process in G-I. Time stamps are in hours and minutes. Scale bars: A, 25 μm; B-I, 10 μm.

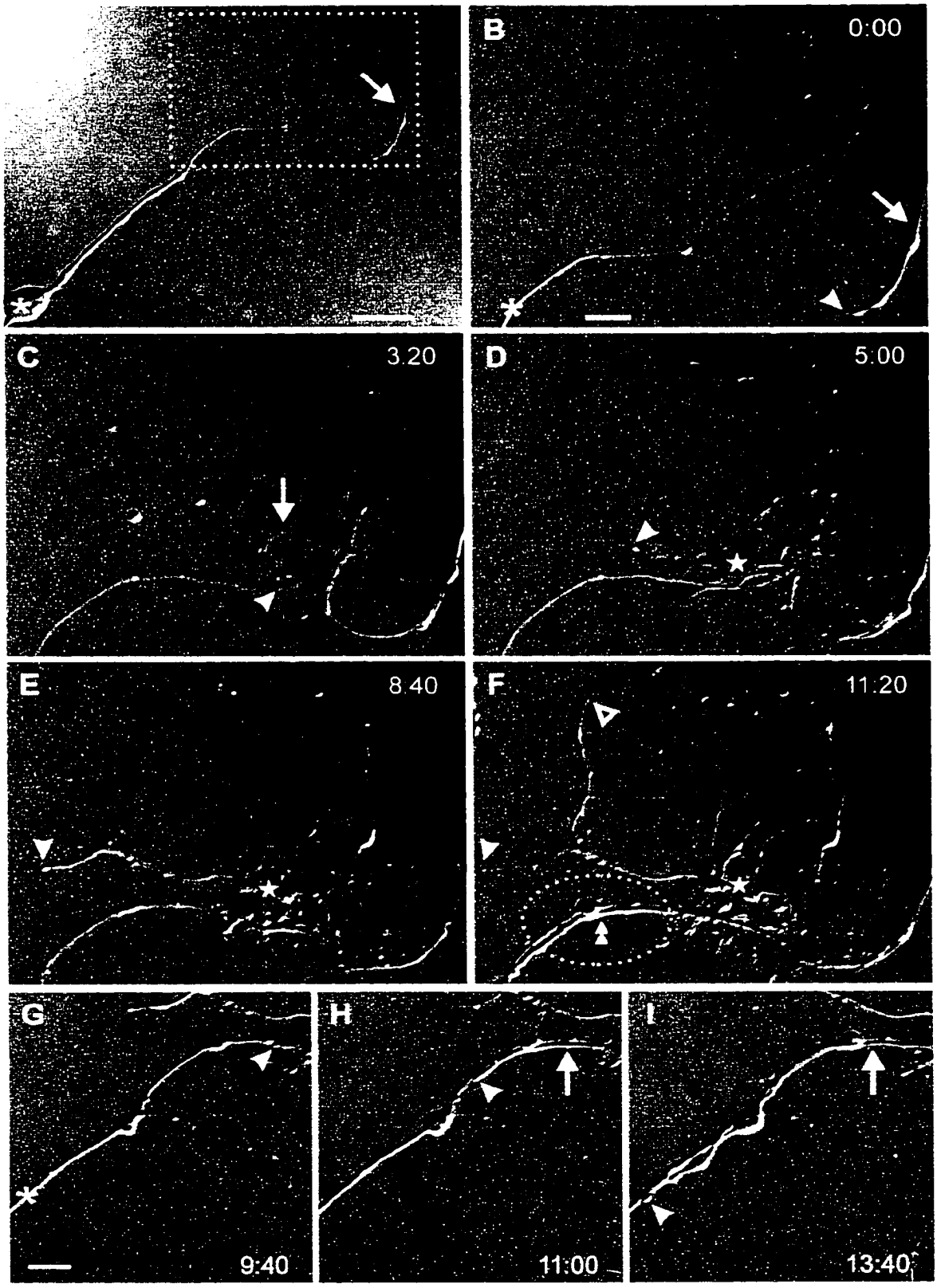
B
0:00
C
3.20
D
5:00
E
8.40
F
11:20
G
9:40
H
11:00
I
13:40

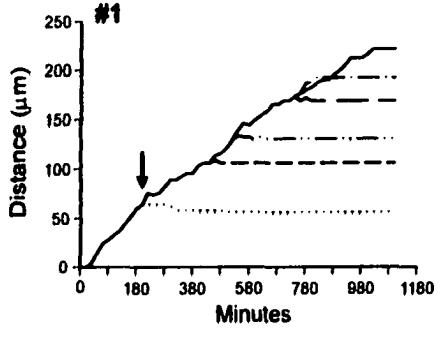

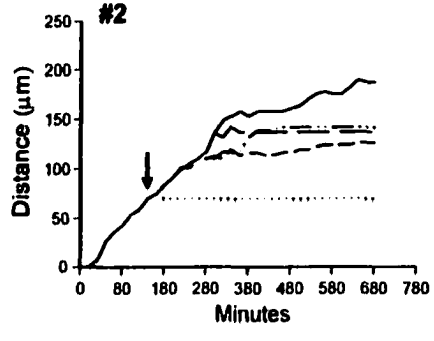

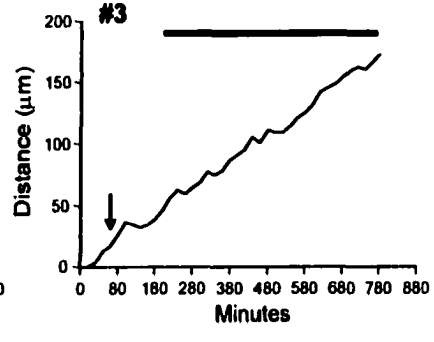

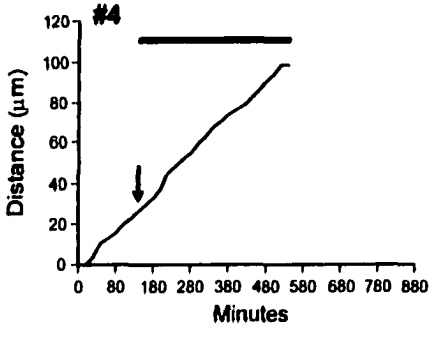

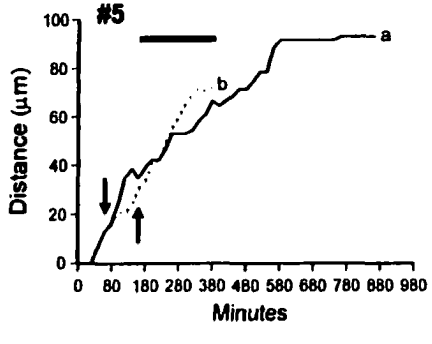

	rate (µm/hr)		precontact percentage
	before	after	
#1	19.19	11.07	58
#2	30.12	12.14	40
#3	20.47	12.70	62
#4	10.47	10.89	104
#5a	18.89	5.70	30
#5b	10.38	12.24	118
$\bar{x}$ =	18.26	10.79	59

Figure 3.5 Contact with AN glial cells does not elicit statistically significant changes in growth cone complexity. Cultures were fixed and stained to visualize microtubules (red) and F-actin (green). **A-D.** Confocal micrographs showing morphological differences between simple (A-B) and complex (C-D) ORN growth cones. **E-F.** Simple growth cones (arrows) contacting AN glial cells (asterisks). **G-H.** Complex growth cones (arrows) contacting AN glial cells. Growth cones exhibit the full range of morphologies, regardless of whether they contact glial cells. **I.** Non-contacting growth cones were predominantly simple, and proportions of simple and complex growth cones were not statistically different between explant only and explant-glia co-cultures. **J.** Proportions of simple and complex growth cones were not statistically different between growth cones that contacted glial cells (green bars) and growth cones that did not (blue bars) in explant-glia co-cultures. Scale bars: A, 10 μm; E, 20 μm, applies to F-H.

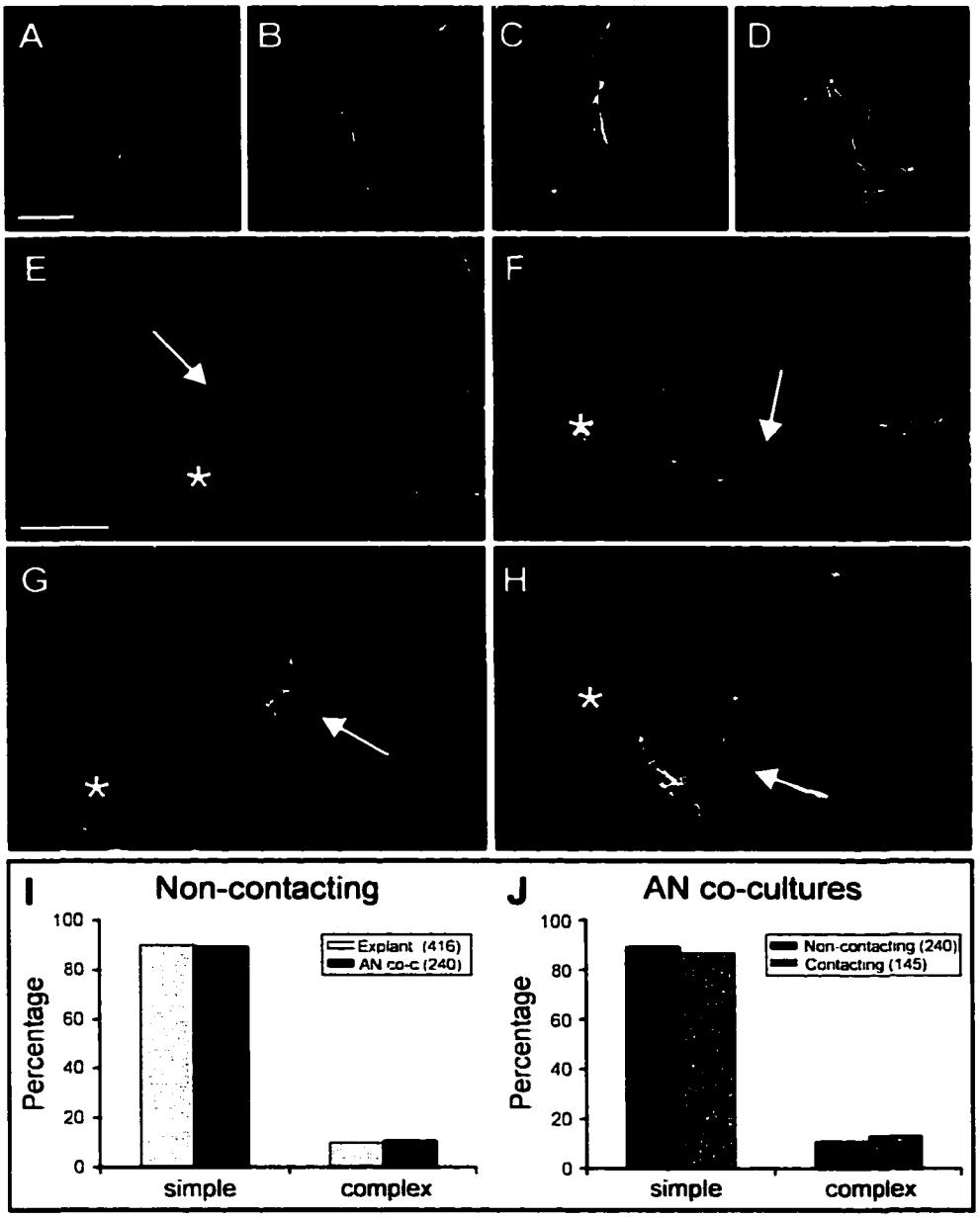
A
B
C
D
E
F
G
H
I
Non-contacting
Explant (416)
AN co-c (240)
Percentage
100
80
60
40
20
0
simple
complex
J
AN co-cultures
Non-contacting (240)
Contacting (145)
Percentage
100
80
60
40
20
0
simple
complex

Figure 3.6 ORN axons and AN glial cells form close associations. ORN axons (green) labeled with antibodies against horseradish peroxidase after 1 (A-C) and 2 days *in vitro* (D-F), and glial cells (red), labeled with a vital fluorescent dye prior to culturing. ORN axons, arrows; AN glial cell bodies, asterisks. **A.** Single axon in close association with several AN glial cells in an array. **B.** Aggregated glial cells extend process into an area of dense axon outgrowth. One axon (arrow) extended along the AN glial process, while others extended across or alongside the array. **C.** ORN axons grew along the curvature of an AN glial array. **D.** Individual ORN axon on the surface of a glial process, which was elevated from the substrate. **E.** Low magnification view, showing a glial array between several explants. **F.** High magnification view of boxed region in E, showing that ORN axons are absent from the array. Scale bars: A-C, F, 10 μm; E, 100 μm; width of D, 8 μm.

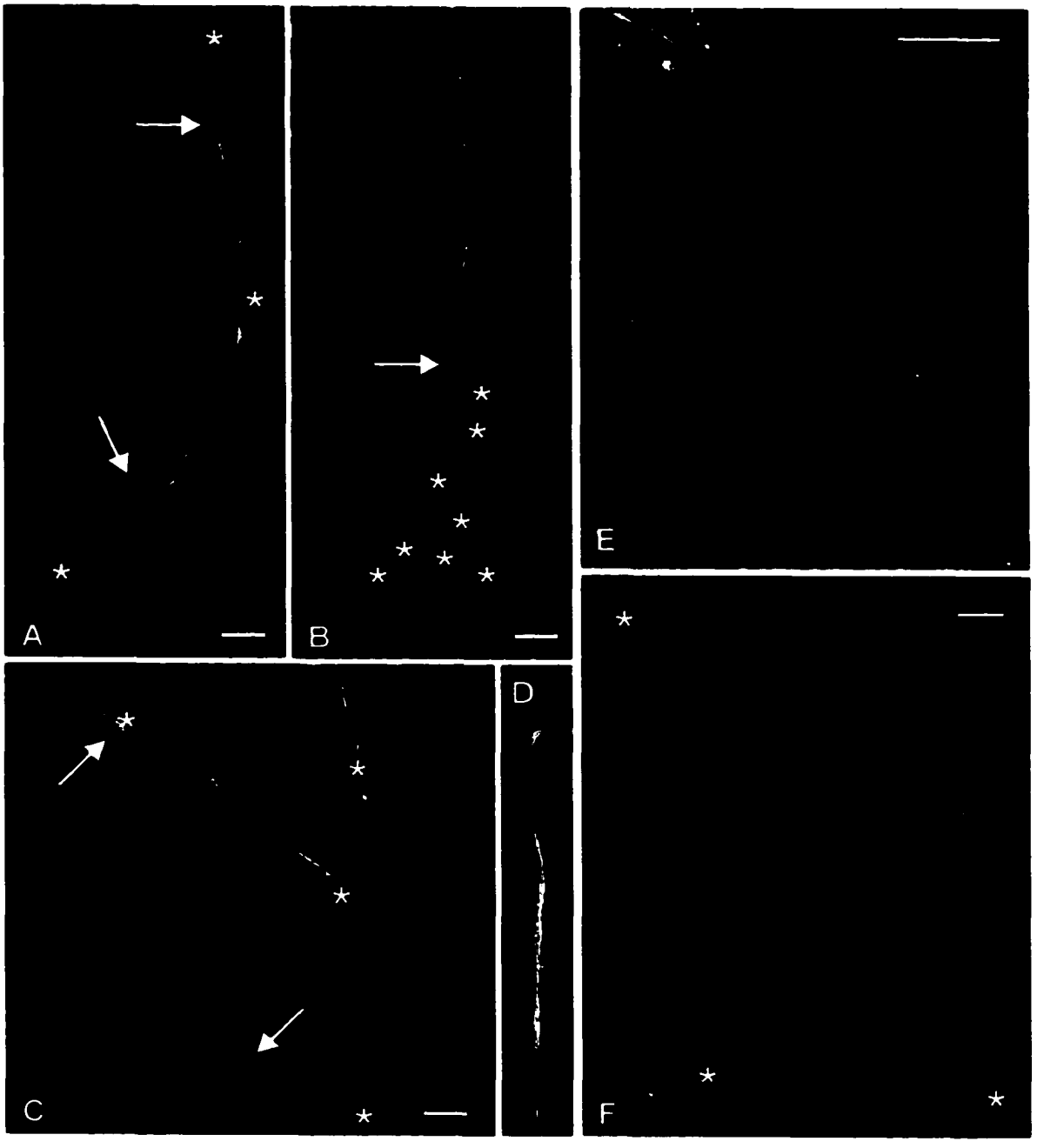
A
B
C
D
E
F

Figure 3.7 AN glial cells link to form multicellular arrays near ORN axons. **A.** Phase contrast image showing AN glial cells situated between explants at 24 hrs of co-culture. **B-E.** Sequential photographs showing changes in glial distribution that occurred over time within the boxed region of A. **B.** 3 hrs after addition to explant cultures, glial cells appeared disorganized. **C.** After 24 hrs, some glial cells died (short arrow), while others (open and closed arrows) grew processes. New phase-bright cell bodies (arrowheads) were occasionally added along glial processes, here and in D. **D.** By 48 hrs, many glial processes extended to join neighboring glia to form arrays. **E.** Arrays continued to become more pronounced, reaching their maximal size around 72 hrs *in vitro*. Scale bars: A, 200 μm; B-E, 100 μm.

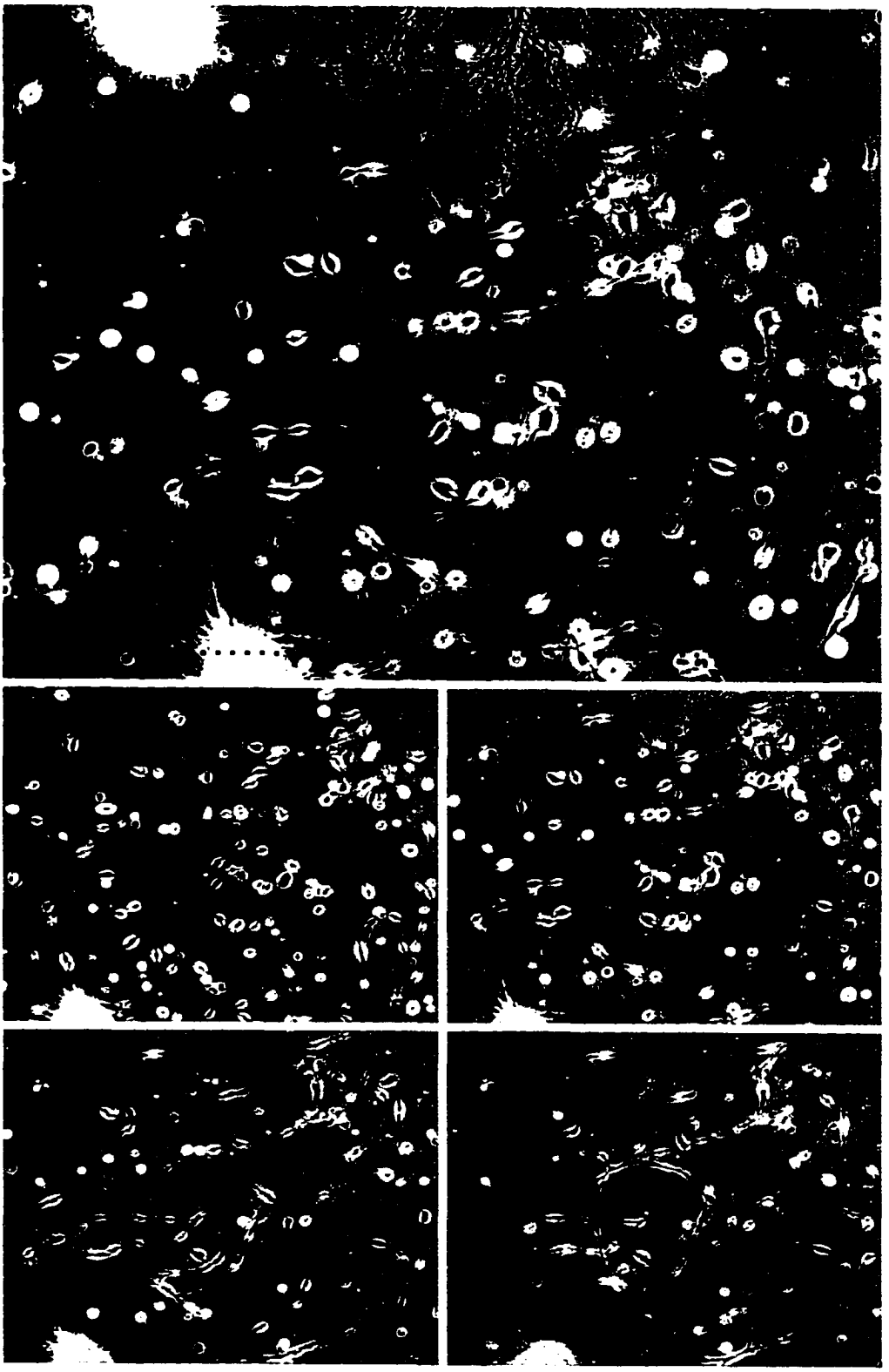

Figure 3.8 AN glial arrays label with antibodies against the GPI-linked isoform of *Manduca* Fasciclin II (GPI-MFas II). **A.** Phase-contrast image of an array at 96 hrs, prior to fixation. **B.** AN glial cells in the array are GPI-MFas II-positive (red). Nuclei are counterstained (green). **C-E.** High magnification view of boxed region in B. **C.** Glial nuclei are aligned. **D.** GPI-MFas II-staining shows web-like appearance of arrays. **E.** Merged image clearly shows that arrays consist of many glial cells. Scale bars: A, B, 100 μm; E, 50 μm.

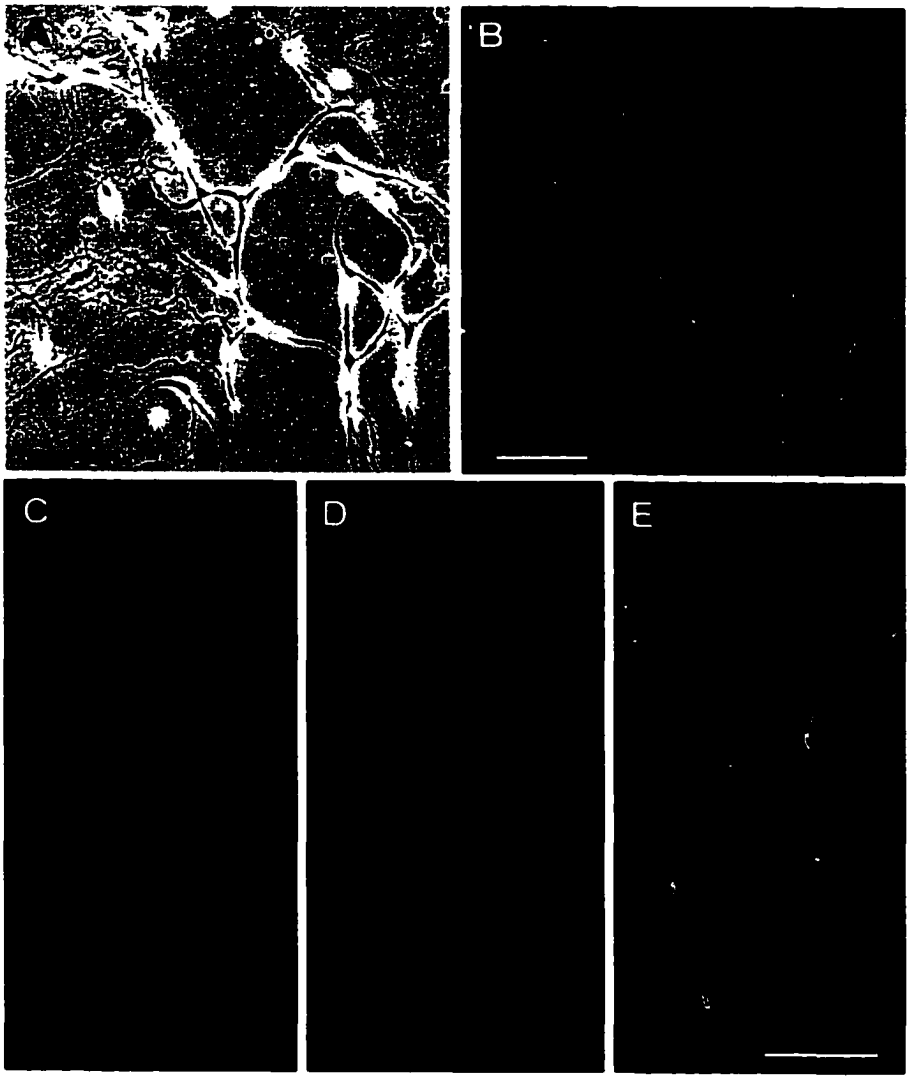
B
C
D
E

Figure 3.9 AN glial cells are mitotically active *in vitro*. Three fields of view containing neuropil-associated (**A-D**), sorting zone (**E-H**), and AN (**I-L**) glia, after bromodeoxyuridine (BrdU) incubation and anti-BrdU immunocytochemistry. **A,E,I.** Phase contrast images. **B,F,J.** DAPI counterstained nuclei. **C,G,K.** BrdU-positive nuclei. **D,H,L.** Merged images; Dapi (green), BrdU (red). **M.** The percentage of glial cells synthesizing DNA is highest in explant-glia co-cultures containing AN glial cells. Arrows correspond to BrdU-positive glia; open arrows correspond to a BrdU-positive explant cell. Scale bars: A, 50 μm, applies to E,I; D, 50 μm, applies to B-L.

Figure 3.10 Explant-conditioned medium does not stimulate array formation. **A.** Diagram illustrating the arrangement of explants and glial cells within double-well dishes in each of three experimental conditions (see Methods). **B.** Phase contrast images of AN glial cells at 24 hrs (left) and 48 hrs (right) after flooding. Glial cells did not form arrays when the opposite well was left blank. **C.** Phase-contrast images of AN glial cells plated opposite to wells containing explants. Glial cells did not form arrays after 24 or 48 hrs in chemical communication with explants. **D.** Phase-contrast images of AN glial cells plated opposite to an explant-glia co-culture. Explant-glia co-cultures failed to induce physically separated AN glial cells to form arrays. **E.** Glial cells formed arrays when plated in the same wells as explants. Arrows point to two glial cells linking to form an array. Scale Bars: B, 100 μm, applies to C,D; E, 100 μm.

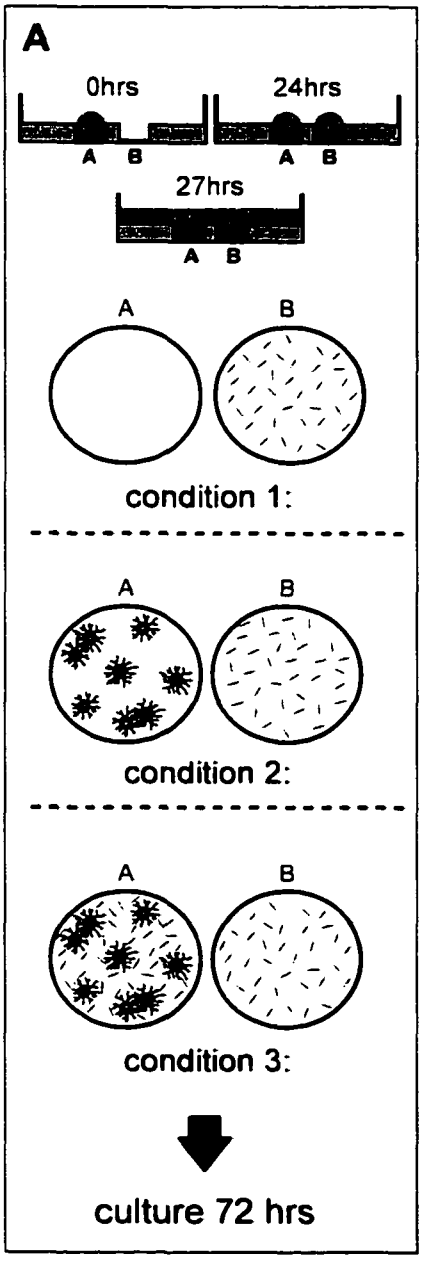
A
0hrs
24hrs
A B
A B
27hrs
A B
A
B
condition 1:
A
B
condition 2:
A
B
condition 3:
culture 72 hrs

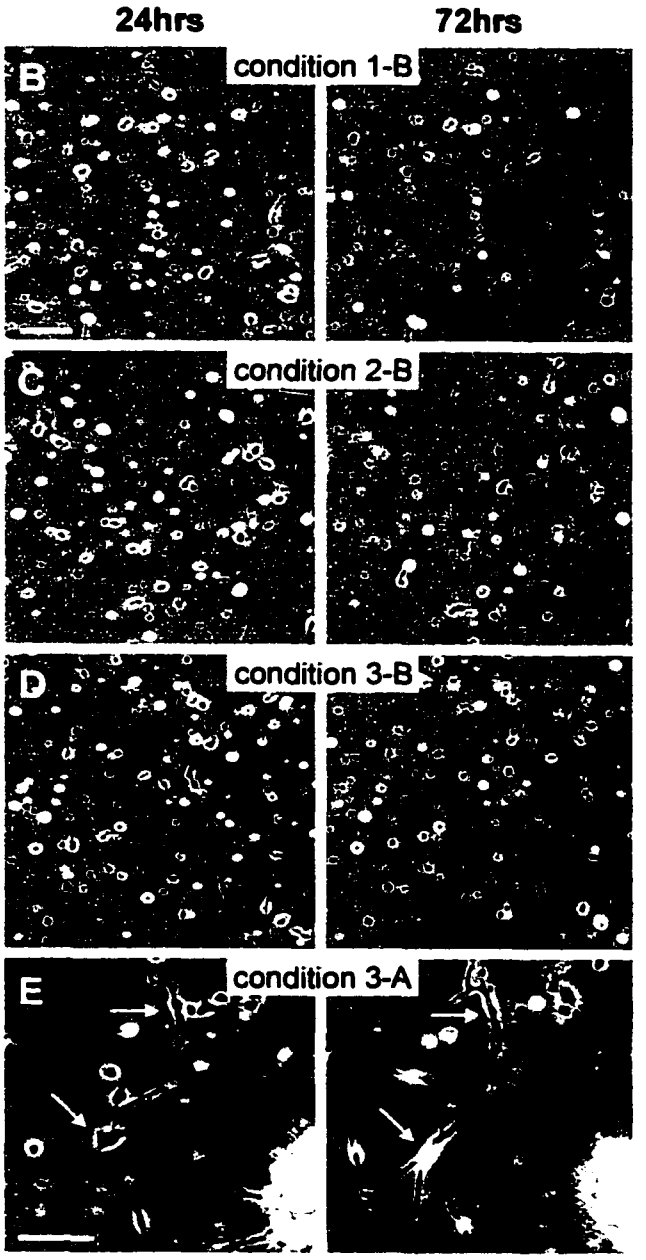
24hrs
72hrs
B
condition 1-B
C
condition 2-B
D
condition 3-B
E
condition 3-A

CHAPTER 4: DISCUSSION

Intercellular interactions between neurons and glia shape multiple aspects of neural development. In vertebrate and invertebrate olfactory systems, neuron-glia interactions are thought to underlie critical events including axon guidance during pathway formation, axon sorting, axon targeting, and glomerulus formation. The olfactory system of the moth *Manduca sexta* has many anatomical and physiological similarities to vertebrate olfactory systems (Boeckh and Tolbert, 1993; Hildebrand and Shepherd, 1997), and has been used extensively to explore intercellular interactions involved in the formation of the olfactory pathway (Oland and Tolbert, 1996; Hildebrand et al., 1997). Glia reduction experiments in *Manduca* have demonstrated that glial cells are required for sorting the axons of olfactory receptor neurons (ORNs) into bundles destined to terminate in particular glomeruli (Rössler et al., 1999), and for stabilizing the borders of protoglomeruli during the process of glomerulus formation (Oland and Tolbert, 1988; Oland et al., 1988; Baumann et al., 1996). The present body of work uses a defined co-culture system to characterize interactions between ORN axons growing from explants of olfactory receptor epithelium and glial cells isolated from the primary olfactory system of *Manduca*. By taking a reductionistic approach, we have monitored how particular types of glial cells, known to influence the behavior of ORN axons *in vivo*, directly affect the behavior and morphology of individual ORN growth cones *in vitro*. These findings have led to the formation of hypotheses concerning the nature of neuron-glia interactions *in vivo*, and provide a means to investigate the molecules and signaling systems that regulate communication between ORN axons and olfactory glia.

occurs within minutes of filopodial contact, and depends on the calcium-dependent cell adhesion molecule N-cadherin (Polinsky et al., 2000). Similar mechanisms may underlie ORN growth cone responses to SZ and NP glial cells from *Manduca*.

The specificity of growth cone responses to contact with SZ and NP glial cells was confirmed by analyzing ORN growth cone interactions with glial cells from the antennal nerve. Growth cone contact with antennal nerve (AN) glial cells resulted in an entirely different set of behaviors than observed following contact with SZ and NP glial cells, with the most striking difference being the continuation of axon elongation after contact. 93% of ORN axons continued to advance following contact with AN glial cells, whereas only 12-13% of ORN axons continued to advance following contact with SZ and NP glial cells. Moreover, ORN axons continued to elongate at an average of 59% of their pre-contact elongation rates after contacting AN glial cells; a rate dramatically higher than the average rates of axon elongation after growth cones contacted SZ (~3%) and NP (~9%) glial cells. Not only did ORN axons continue to elongate after contact with AN glial cells, but ORN growth cones advanced predominantly in direct contact with glial processes. This behavior indicates that AN glial cells are a permissive substrate for ORN axons, and further demonstrates the specificity of growth cone-glial cell interactions since ORN axons never elongated along the surfaces of SZ or NP glial cells. Differential labeling of axons and glial cells in fixed co-cultures revealed that the processes of AN glial cells and ORN axons were often closely apposed, reinforcing live-cell findings that ORN growth cones advanced along the surfaces of AN glial processes. Unlike with SZ and NP glial cells, contact with AN glial cells failed to elicit statistically significant changes in the morphological complexity of ORN growth cones, again highlighting important differences in interactions with AN glial cells compared to SZ and

surrounded by a perineurial sheath (Oland et al., 1998). At stage 3, growing ORN axons first encounter glial cells when they enter the antennal lobe and grow through a continuous border of glia surrounding the antennal lobe neuropil. The entry of ORN axons triggers neuropil-associated glia to extend processes and migrate toward the center of the antennal lobe (Oland and Tolbert, 1987), and additionally, triggers the localized proliferation and migration of central olfactory glia to populate the sorting zone at the base of the antennal nerve (Rössler et al., 1999). Entry of the first ORN axons therefore sets the stage for all subsequent ORN axon ingrowth by causing a redistribution of glial cells that leads to the formation of the glia-rich sorting zone. Since the number of ORN axons in the antennal nerve increases from 3,000 to 300,000 between stages 3-9 (Sanes and Hildebrand, 1976; Oland and Tolbert, 1988), the vast majority of axons growing into the brain encounter the sorting zone glia *en route* to their antennal lobe targets.

Axon behavior changes dramatically in the sorting zone, where ORN axons abruptly change trajectories, shed neighboring axon relationships, and sort into bundles that share common targets in the antennal lobe (Oland et al., 1998). Reduction of glial number prevents the sorting of ORN axons in the sorting zone, and indicates that sorting zone glia influence the behavior of ORN axons by causing them to sort into fascicles that terminate in particular glomeruli (Rössler et al., 1999; Higgins et al., 2002). Glial cells located in the antennal lobe also influence the behavior of ORN axons. ORN axons branch after passing through the shell of glia surrounding the antennal lobe neuropil, and their terminals coalesce into protoglomeruli by the end of stage 5 (Oland and Tolbert, 1990; Oland et al., 1998). In response to axon ingrowth, glial cells associated with the antennal lobe neuropil migrate to the borders of protoglomeruli by stage 6, and act to

stabilize newly forming glomeruli in the antennal lobe (Oland and Tolbert, 1988; Oland et al., 1988; Baumann et al., 1996). Therefore, both populations of central olfactory glia critically regulate the behavior of ORN axons during antennal lobe development, first in the sorting zone and later in the antennal lobe.

Findings from the current *in vitro* studies strongly suggest that SZ and NP glial cells induce contact-dependent alterations in the behavior and morphology of individual ORN growth cones. We proposed that these alterations could result from combined changes to growth cone adhesive properties and the growth cone cytoskeleton (Fig. 10, Chapter 2). Glial contact-mediated changes in growth cone adhesive properties might be essential for the sorting of ORN axons in the sorting zone, where growth cones first find and then adhere to like axons that are destined for the same targets in the antennal lobe. Similarly, glia-induced changes in growth cone adhesive properties could enable like-ORN terminals to segregate into protoglomeruli and prevent the overlap between adjacent, less adherent, ORN terminals. Morphological changes in ORN growth cones could facilitate environmental sampling by growth cones, both in the sorting zone and antennal lobe, and cytoskeletal rearrangements could result in growth cone turning, branching, and the termination of axon growth.

ORN growth cones do not normally encounter peripheral glia in the olfactory pathway until late in development. Peripheral glia in the antenna enter nerve rootlets from the olfactory receptor epithelium at stage 3, migrate to occupy the interior of the antennal nerve nearest the rootlets by stage 4, and not until stage 7 do they invest the entire width and length of the nerve from the antenna to the sorting zone (Rössler et al., 1999). Antennal nerve glia populate the intracranial portion of the antennal nerve after most ORN axons have reached the antennal lobe, and are thus unlikely to influence the

pathfinding decisions made by ORN growth cones. Only axons traveling toward the brain between stages 7-9 would encounter peripherally derived antennal nerve glia in their pathway. Peripheral glia could provide a permissive substrate for axon growth *in vivo*, and permit the extension of late arriving axons into the sorting zone and antennal lobe. Late arriving ORN axons likely project from the most distal antennal segments, and the longer distances traveled by these axons might necessitate additional support form glial cells. *In vitro* findings indicate that AN glia serve as a permissive substrate for the elongation of ORN axons, as growth cones readily advance along glial surfaces. In stark contrast to the morphological and behavioral alterations in ORN growth cones seen following contact with central olfactory glial cells *in vitro*, ORN growth cones seemingly ignore AN glial cells by continuing to advance after contact without displaying long lasting changes in their shapes. The lack of contact-dependent modification of growth cone behaviors following encounters with AN glial cells suggests that peripheral glia, unlike central glia, do not normally instruct growing ORN axons to alter their behaviors *in vivo*.

Instead of playing critical roles during development, antennal nerve glia likely play important roles in the mature nerve where glial processes envelope small fascicles containing 10-70 ORN axons (Sanes and Hildebrand, 1976). Glial ensheathment of non-myelinated axons may allow ephaptic coupling to occur between axons contained within the same nerve bundle, a possibility raised for the mammalian olfactory nerve by Bokil and colleagues (2001).

Axon-mediated effects on glial cell behavior

ORN axons act reciprocally to induce radical change in the behavior of AN glial cells. In explant-glia co-cultures, the behavior of AN glial cells was markedly influenced by the presence of ORN axons. First, time-lapse imaging revealed that AN glial cells often extended processes to meet growing ORN axons. Glial processes often grew along ORN axons, and maintained associations with axons for many hours after contact. Second, AN glial cells linked to form multicellular arrays over several days in co-culture with explants of olfactory epithelium. AN glial arrays formed on and next to ORN axons that extended from cultured explants. Glial arrays were large, and often spanned the distance between multiple explants. Without explants of olfactory receptor epithelium, AN glial cells occasionally formed small aggregations but never formed large arrays, and they usually died between 48-72 hrs *in vitro*. With explants of olfactory receptor epithelium, AN glial arrays developed progressively over successive days in co-culture, and glia within arrays survived at least 96 hrs *in vitro*. AN glial cells failed to form arrays in explant conditioned medium, suggesting that long-range soluble factors did not mediate the response. Since arrays could form without ORN axon contact, we suggest that array formation is dependent on a close-range soluble factor or factors released by ORN axons. Interestingly, ORN axons did not induce behavioral changes in either SZ or NP glial cells. Central olfactory glial cells never extend processes to engage ORN axons or link to form multicellular arrays. In explant-glia co-cultures, AN glia also have a substantially higher frequency of mitotic activity than SZ and NP glial cells. These key differences in glial cell behavior *in vitro* are likely due to the different roles central and peripheral olfactory glia play *in vivo*.

The functional significance of array formation

AN glia and central olfactory glia have different relationships with ORN axons, both *in vivo* and *in vitro*. First, AN glia migrate long distances along ORN axons to populate the intracranial portion of the antennal nerve. AN glia form a continuous web-like investment of the antennal nerve, where glial processes enwrap small bundles of ORN axons. In contrast, SZ and NP glia migrate relatively short distances to reach their final destinations in the sorting zone and antennal lobe. AN glia and central olfactory glia may therefore have different capacities to migrate along and/or associate with ORN axons *in vivo*. Second, AN glia are oriented parallel to axon bundles in the intracranial portion of the antennal nerve, whereas SZ glia have non-uniform distributions in the sorting zone. Although change in glial orientation could be due to a corresponding change in axonal trajectories in the sorting zone, there might be differences between glial types in their propensities to align along bundles of ORN axons. *In vitro*, ORN axons trigger AN glial cells to form multicellular arrays. Under the same conditions, SZ and NP glial cells never form arrays. In order for AN glia to migrate along and infiltrate the antennal nerve *in vivo*, they must make intimate associations with ORN axons. *In vitro*, AN glial cells and ORN axons act mutually to form intimate associations with one another. SZ and NP glial cells, however, fail to extend processes and associate with ORN axons.

The formation of multicellular AN glial arrays *in vitro* was not anticipated, yet this axon-induced glial behavior might well have functional consequences *in vivo*. Perhaps array formation is a two-dimensional reflection of specific AN glial behaviors that normally occurs in three-dimensional space *in vivo*. As AN glia associate with ORN axons and link to form large multicellular arrays *in vitro*, perhaps they are receiving an

axonal signal that normally promotes glial migration, alignment with axons, association with other AN glia, or enwrapment of axon bundles *in vivo*. To date, glia-glia relationships in the antennal nerve have not been fully characterized. The present *in vitro* findings suggest that AN glia form intercellular linkages, and it remains possible that similar glial arrangements exist *in vivo*. 3-D reconstructions of serial electron micrographs or light-level analyses of dye-injected AN glia could be used to further our understanding of glial relationships in the antennal nerve, and determine whether similar glial arrays exist *in vivo*.

Parallels between *Manduca* olfactory glia and glia in the mammalian olfactory system

Like glia in the moth, mammalian olfactory neuroglia populate both the peripheral and central portions of the primary olfactory pathway, and have been implicated in key events during olfactory development. Specialized glia, called olfactory ensheathing cells (Raisman, 1985), migrate from the olfactory placode and enwrap bundles of ORN axons in the olfactory nerve and in the nerve layer of the olfactory bulb (Marin-Padilla and Amieva, 1989; Doucette, 1989, 1991). Olfactory ensheathing cells have a blend of Schwann cell and astrocyte properties (Barber and Lindsay, 1982; Ramon-Cueto and Avila, 1998; Bartolomei and Greer, 2000), and promote the growth of ORN axons through contact-dependent and contact-independent mechanisms (Chauh and Au, 1991; Kafitz and Greer, 1998, 1999; Tisay and Key, 1999). Since olfactory ensheathing cells accompany the first ORN axons to the brain, and express growth-promoting molecules in the olfactory nerve and nerve layer of the bulb (Doucette, 1990; Gong and Shipley, 1996; Treloar et al., 1996), they have been implicated as modulators of olfactory neurite

growth during development. Moreover, the ability of olfactory ensheathing cells to cross into the CNS and support the continued ingrowth of ORN axons during normal adult turnover has led to investigations of their therapeutic potentials in the repair of spinal cord injuries (Bartolomei and Greer, 2000; Wewetzer et al., 2002). AN glia from *Manduca* share some features with mammalian olfactory ensheathing cells. For instance, both have peripheral origins in olfactory epithelia (Chauh and Au, 1991; Rössler et al., 1999), and both enwrap bundles of ORN axons in their respective olfactory nerves (De Lorenzo 1957; Sanes and Hildebrand, 1976). *In vitro* studies additionally suggest that AN glia, like olfactory ensheathing cells, provide permissive substrates for the elongation of olfactory axons (Tisay and Key, 1999; Chapter 3).

Olfactory ensheathing cells have also been implicated in axon guidance and axon sorting in the nerve layer of the olfactory bulb. Several studies have suggested that ensheathing cells express molecules that influence the growth, sorting, and targeting of ORN axons (Puche et al., 1996; St. John and Key, 1999; Tisay et al., 2000; Schwarting et al., 2000). In *Manduca*, SZ glia mediate axon sorting (Rössler et al., 1999), and despite their distinctly different origins, SZ glia may play functionally equivalent roles to mammalian olfactory ensheathing cells (Valverde, 1999). Therefore, in *Manduca*, two types of olfactory glia, the AN and SZ glia, could each play separate roles in facilitating axon ingrowth and mediating axon sorting that are together played by olfactory ensheathing cells in mammals.

In *Manduca*, glia are the first cellular elements to undergo morphogenic changes in response to the ingrowth of ORN axons, and as such, have been hypothesized to participate with neural elements in the construction of olfactory glomeruli (Oland and Tolbert, 1987). Support for this hypothesis comes from experimental findings that glial

In vitro studies

In vitro studies demonstrate that contact with SZ and NP glial cells results in the elaboration of growth cone morphology. This finding can be analyzed statistically by using the fixed-cell cytoskeletal staining approach taken in Chapter 2 to evaluate growth cone complexity. Fixed co-cultures can therefore be used to analyze growth cone complexity in both normal and experimental conditions. We have begun using this assay to examine whether the receptor-ligand pair of axon guidance molecules, Eph and ephrin, participate in growth cone-glial cell interactions. In collaboration with Megumi Kaneko and Alan Nighorn, we have shown that treatment of SZ co-cultures with a polyclonal antibody raised against the ligand binding domain of MsEph blocks glia-induced changes in growth cone complexity, while recombinant receptor (Eph-Fc) and ligand (ephrin-Fc) fusion proteins do not (data not shown). Future experiments could continue to investigate the involvement of Eph-ephrin signaling in growth cone-glial cell interactions. Alternatively, other antibodies, peptides, and/or pharmacological agents could be used in a similar function-blocking capacity to test whether particular molecules or signaling systems operate to produce glia-mediated alterations in growth cone behavior or morphology.

The ease with which explant-glia co-cultures can be experimentally manipulated can also be exploited to characterize axon-induced array formation by AN glial cells. In Chapter 3, we proposed that nitric oxide (NO), released from NO-synthase-positive ORN axons, could act as a short-range chemical signal to induce AN glial cells to form arrays. Future experiments can probe the involvement of NO signaling in array formation. NO

donors can be applied to cultures of AN glial cells grown without explants to determine whether NO can substitute for the presence of ORN axons and promote the formation of glial arrays. Conversely, inhibitors of NO signaling can be applied to explant-glia co-cultures to determine whether the elimination of NO results in the loss of AN glial arrays.

In vivo studies

A logical extension of the current *in vitro* studies is to individually label living ORN axons *in situ*, and monitor their behavior as they travel through the olfactory pathway and encounter various populations of glia. Analyzing the morphology and behavior of growing ORN axons *in vivo* is critical to understanding the nature of the navigational decisions that ORN growth cones face along their trajectories. Previous studies have shown that growth cones of navigating axons usually have simple morphologies unless they are navigating in decision regions, where local environmental cues lead to increased frequency and greater duration of growth cone elaborations (Tosney and Landmesser, 1985; Caudy and Bently, 1986; Bovolenta and Mason, 1987; Godement et al., 1990, 1994; Whitesides and Lamantia, 1996). In fixed *Manduca* preparations, ORN growth cones are only slightly more complex in the sorting zone than in the antennal nerve and the nerve layer of the antennal lobe (Oland et al., 1998), yet contact with SZ and NP glial cells *in vitro* leads to significant elaborations in growth cone morphologies. Since growth cones can display similar shapes and behaviors throughout axon pathways, but change the frequency of those behaviors depending on their location (Mason and Wang, 1997), only *in situ* time-lapse imaging of living axons can determine whether growth cone properties are dynamically altered by glial cells as would be predicted from the current *in vitro* studies. For instance, time-lapse observations of

growth cone behavior *in situ* could determine whether ORN growth cones pause or elaborate when they encounter SZ glia while *en route* to the antennal lobe, or whether ORN growth cones engage in interactions with NP glia before terminally branching. *In situ* imaging, unlike tissue culture experiments, would faithfully preserve endogenous cues from the native tissue. These intrinsic cues may augment or alter the basic growth cone responses observed *in vitro*, and produce a more complex array of growth cone guidance behaviors *in vivo*. Insights gained from *in vitro* analyses will undoubtedly facilitate the interpretation of *in vivo* axon-glia interactions.

REFERENCES

Anton ES, Weskamp G, Reichardt LF, Matthew WD (1994) Nerve growth factor and its low-affinity receptor promote Schwann cell migration. Proc Natl Acad Sci U S A 91:2795-9.

Au WW, Treloar HB, Greer CA (2002) Sublaminar organization of the mouse olfactory bulb nerve layer. J Comp Neurol 446:68-80.

Auld V (1999) Glia as mediators of growth cone guidance: studies from insect nervous systems. Cell Mol Life Sci 55:1377-85.

Bailey MS, Puche AC, Shipley MT (1999) Development of the olfactory bulb: evidence for glia-neuron interactions in glomerular formation. J Comp Neurol 415:423-48.

Barber PC, Lindsay RM (1982) Schwann cells of the olfactory nerves contain glial fibrillary acidic protein and resemble astrocytes. Neuroscience 7:3077-90.

Bartolomei JC, Greer CA (2000) Olfactory ensheathing cells: bridging the gap in spinal cord injury. Neurosurgery 47:1057-69.

Bastiani MJ, Goodman CS (1986) Guidance of neuronal growth cones in the grasshopper embryo. III. Recognition of specific glial pathways. J Neurosci 6:3542-51.

Bastiani MJ, Harrelson AL, Snow PM, Goodman CS (1987) Expression of fasciclin I and II glycoproteins on subsets of axon pathways during neuronal development in the grasshopper. Cell 48:745-55.

Baumann PM, Oland LA, Tolbert LP (1996) Glial cells stabilize axonal protoglomeruli in the developing olfactory lobe of the moth Manduca sexta. J Comp Neurol 373:118-28.

Bentley CA, Lee KF (2000) p75 is important for axon growth and schwann cell migration during development. J Neurosci 20:7706-15.

Bentley D, Caudy M (1983) Pioneer axons lose directed growth after selective killing of guidepost cells. Nature 304:62-5.

Bentley D, Keshishian H (1982) Pioneer neurons and pathways in insect appendages. Trends in Neurosciences 5:364-367.

Bergemann AD, Zhang L, Chiang MK, Brambilla R, Klein R, Flanagan JG (1998) Ephrin-B3, a ligand for the receptor EphB3, expressed at the midline of the developing neural tube. Oncogene 16:471-80.

Bixby JL, Lilien J, Reichardt LF (1988) Identification of the major proteins that promote neuronal process outgrowth on Schwann cells in vitro. J Cell Biol 107:353-61.

Bodian D (1966) Development of fine structure structure of spinal cord in monkey fetuses. I. The moto-neuron neuropil at the time of onset of reflex activity. Bull. Johns Hopkins Hosp. 119:129-149.

Boeckh J, Tolbert LP (1993) Synaptic organization and development of the antennal lobe in insects. Microsc Res Tech 24:260-80.

Bokil H, Laaris N, Blinder K, Ennis M, Keller A (2001) Ephaptic interactions in the mammalian olfactory system. J Neurosci 21:RC173.

Bovolenta P, Dodd J (1991) Perturbation of neuronal differentiation and axon guidance in the spinal cord of mouse embryos lacking a floor plate: analysis of Danforth's short-tail mutation. Development 113:625-39.

Bovolenta P, Mason C (1987) Growth cone morphology varies with position in the developing mouse visual pathway from retina to first targets. J Neurosci 7:1447-60.

Bozza T, Feinstein P, Zheng C, Mombaerts P (2002) Odorant receptor expression defines functional units in the mouse olfactory system. J Neurosci 22:3033-43.

Bray D (1970) Surface movements during the growth of single explanted neurons. Proc Natl Acad Sci U S A 65:905-10.

Bray D (1979) Mechanical tension produced by nerve cells in tissue culture. J Cell Sci 37:391-410.

Brose K, Bland KS, Wang KH, Arnott D, Henzel W, Goodman CS, Tessier-Lavigne M, Kidd T (1999) Slit proteins bind Robo receptors and have an evolutionarily conserved role in repulsive axon guidance. Cell 96:795-806.

Brunjes PC (1994) Unilateral naris closure and olfactory system development. Brain Res Brain Res Rev 19:146-60.

Buck L, Axel R (1991) A novel multigene family may encode odorant receptors: a molecular basis for odor recognition. Cell 65:175-87.

Bulfone A, Wang F, Hevner R, Anderson S, Cutforth T, Chen S, Meneses J, Pedersen R, Axel R, Rubenstein JL (1998) An olfactory sensory map develops in the absence of normal projection neurons or GABAergic interneurons. Neuron 21:1273-82.

Bunge MB (1973) Fine structure of nerve fibers and growth cones of isolated sympathetic neurons in culture. J Cell Biol 56:713-35.

(2000) In: Development of the olfactory system (Burd GDaTLP, ed), pp 233-255. The neurobiology of taste and smell: Wiley-Liss, Inc.

Caudy M, Bentley D (1986) Pioneer growth cone morphologies reveal proximal increases in substrate affinity within leg segments of grasshopper embryos. J Neurosci 6:364-79.

Chuah MI, Au C (1991) Olfactory Schwann cells are derived from precursor cells in the olfactory epithelium. J Neurosci Res 29:172-80.

Chuah MI, Au C (1994) Olfactory cell cultures on ensheathing cell monolayers. Chem Senses 19:25-34.

Chuah MI, West AK (2002) Cellular and molecular biology of ensheathing cells. Microsc Res Tech 58:216-27.

Clyne PJ, Warr CG, Freeman MR, Lessing D, Kim J, Carlson JR (1999) A novel family of divergent seven-transmembrane proteins: candidate odorant receptors in Drosophila. Neuron 22:327-38.

Condron B (1999) Spatially discrete FGF-mediated signalling directs glial morphogenesis. Development 126:4635-41.

Crandall JE, Dibble C, Butler D, Pays L, Ahmad N, Kostek C, Puschel AW, Schwarting GA (2000) Patterning of olfactory sensory connections is mediated by extracellular matrix proteins in the nerve layer of the olfactory bulb. J Neurobiol 45:195-206.

Cuschieri A, Bannister LH (1975) The development of the olfactory mucosa in the mouse: light microscopy. J Anat 119:277-86.

Dai J, Sheetz MP (1995) Axon membrane flows from the growth cone to the cell body. Cell 83:693-701.

De Lorenzo AJ (1957) Electron-microscopic observations of the olfactory mucosa and the olfactory nerve. J Biophys Biochem Cytol 3:839-863.

Dent EW, Callaway JL, Szebenyi G, Baas PW, Kalil K (1999) Reorganization and movement of microtubules in axonal growth cones and developing interstitial branches. J Neurosci 19:8894-908.

Dent EW, Kalil K (2001) Axon branching requires interactions between dynamic microtubules and actin filaments. J Neurosci 21:9757-69.

Dickson BJ (2001) Rho GTPases in growth cone guidance. Curr Opin Neurobiol 11:103-10.

Doucette R (1989) Development of the nerve fiber layer in the olfactory bulb of mouse embryos. J Comp Neurol 285:514-27.

Doucette R (1990) Glial influences on axonal growth in the primary olfactory system. Glia 3:433-49.

Doucette R (1991) PNS-CNS transitional zone of the first cranial nerve. J Comp Neurol 312:451-66.

Drazba J, Lemmon V (1990) The role of cell adhesion molecules in neurite outgrowth on Muller cells. Dev Biol 138:82-93.

Drazba J, Liljelund P, Smith C, Payne R, Lemmon V (1997) Growth cone interactions with purified cell and substrate adhesion molecules visualized by interference reflection microscopy. Brain Res Dev Brain Res 100:183-97.

Drescher U, Kremoser C, Handwerker C, Loschinger J, Noda M, Bonhoeffer F (1995) In vitro guidance of retinal ganglion cell axons by RAGS, a 25 kDa tectal protein related to ligands for Eph receptor tyrosine kinases. Cell 82:359-70.

Dubuque SH, Schachtner J, Nighorn AJ, Menon KP, Zinn K, Tolbert LP (2001) Immunolocalization of synaptotagmin for the study of synapses in the developing antennal lobe of Manduca sexta. J Comp Neurol 441:277-87.

Farbman AI (1990) Olfactory neurogenesis: genetic or environmental controls? Trends Neurosci 13:362-5.

(2000) In: Cell biology of olfactory epithelium (Farbman AI, ed), pp 131-158. The neurobiology of taste and smell: Wiley-Liss, Inc.

Fischer RA (1925) Statistical methods for research workers. Edinburgh: Oliver and Boyd.

Forscher P, Smith SJ (1988) Actions of cytochalasins on the organization of actin filaments and microtubules in a neuronal growth cone. J Cell Biol 107:1505-16.

Futerman AH, Banker GA (1996) The economics of neurite outgrowth--the addition of new membrane to growing axons. Trends Neurosci 19:144-9.

Gao Q, Chess A (1999) Identification of candidate Drosophila olfactory receptors from genomic DNA sequence. Genomics 60:31-9.

Gao Q, Yuan B, Chess A (2000) Convergent projections of Drosophila olfactory neurons to specific glomeruli in the antennal lobe. Nat Neurosci 3:780-5.

Gibson NJ, Nighorn A (2000) Expression of nitric oxide synthase and soluble guanylyl cyclase in the developing olfactory system of Manduca sexta. J Comp Neurol 422:191-205.

Gibson NJ, Rossler W, Nighorn AJ, Oland LA, Hildebrand JG, Tolbert LP (2001) Neuron-glia communication via nitric oxide is essential in establishing antennal-lobe structure in Manduca sexta. Dev Biol 240:326-39.

Gilbert M, Smith J, Roskams AJ, Auld VJ (2001) Neuroligin 3 is a vertebrate gliotactin expressed in the olfactory ensheathing glia, a growth-promoting class of macroglia. Glia 34:151-64.

Gilmour DT, Maischein HM, Nusslein-Volhard C (2002) Migration and function of a glial subtype in the vertebrate peripheral nervous system. Neuron 34:577-88.

Godement P, Salaun J, Mason CA (1990) Retinal axon pathfinding in the optic chiasm: divergence of crossed and uncrossed fibers. Neuron 5:173-86.

Godement P, Wang LC, Mason CA (1994) Retinal axon divergence in the optic chiasm: dynamics of growth cone behavior at the midline. J Neurosci 14:7024-39.

Goldberg DJ, Burmeister DW (1986) Stages in axon formation: observations of growth of Aplysia axons in culture using video-enhanced contrast-differential interference contrast microscopy. J Cell Biol 103:1921-31.

Gong Q, Shipley MT (1996) Expression of extracellular matrix molecules and cell surface molecules in the olfactory nerve pathway during early development. J Comp Neurol 366:1-14.

Gonzalez ML, Silver J (1994) Axon-glia interactions regulate ECM patterning in the postnatal rat olfactory bulb. J Neurosci 14:6121-31.

Goodman CS (1996) Mechanisms and molecules that control growth cone guidance. Annu Rev Neurosci 19:341-77.

Graziadei PPCaMGGA (1978) Continuos nerve cell renewal in the olfactory system. pp 55-82. Handbook of sensory physiology, vol. IX: Springer-Verlag.

Grenningloh G, Rehm EJ, Goodman CS (1991) Genetic analysis of growth cone guidance in Drosophila: fasciclin II functions as a neuronal recognition molecule. Cell 67:45-57.

Hirokawa N (1998) Kinesin and dynein superfamily proteins and the mechanism of organelle transport. Science 279:519-26.

Ho RK, Goodman CS (1982) Peripheral pathways are pioneered by an array of central and peripheral neurones in grasshopper embryos. Nature 297:404-6.

Hosoya T, Takizawa K, Nitta K, Hotta Y (1995) glial cells missing: a binary switch between neuronal and glial determination in Drosophila. Cell 82:1025-36.

Hu H, Marton TF, Goodman CS (2001) Plexin B mediates axon guidance in Drosophila by simultaneously inhibiting active Rac and enhancing RhoA signaling. Neuron 32:39-51.

Jacobs JR (2000) The midline glia of Drosophila: a molecular genetic model for the developmental functions of glia. Prog Neurobiol 62:475-508.

Jacobs JR, Goodman CS (1989) Embryonic development of axon pathways in the Drosophila CNS. I. A glial scaffold appears before the first growth cones. J Neurosci 9:2402-11.

Jan LY, Jan YN (1982) Antibodies to horseradish peroxidase as specific neuronal markers in Drosophila and in grasshopper embryos. Proc Natl Acad Sci U S A 79:2700-4.

Jay DG (2000) The clutch hypothesis revisited: ascribing the roles of actin- associated proteins in filopodial protrusion in the nerve growth cone. J Neurobiol 44:114-25.

Jefferis GS, Marin EC, Stocker RF, Luo L (2001) Target neuron prespecification in the olfactory map of Drosophila. Nature 414:204-8.

Jones BW, Fetter RD, Tear G, Goodman CS (1995) glial cells missing: a genetic switch that controls glial versus neuronal fate. Cell 82:1013-23.

Kafitz KW, Greer CA (1997) Role of laminin in axonal extension from olfactory receptor cells. J Neurobiol 32:298-310.

Kafitz KW, Greer CA (1998) The influence of ensheathing cells on olfactory receptor cell neurite outgrowth in vitro. Ann N Y Acad Sci 855:266-9.

Kafitz KW, Greer CA (1999) Olfactory ensheathing cells promote neurite extension from embryonic olfactory receptor cells in vitro. Glia 25:99-110.

Kawakami A, Kitsukawa T, Takagi S, Fujisawa H (1996) Developmentally regulated expression of a cell surface protein, neuropilin, in the mouse nervous system. J Neurobiol 29:1-17.

Kawana E, Sandri C, Akert K (1971) Ultrastructure of growth cones in the cerebellar cortex of the neonatal rat and cat. Z Zellforsch Mikrosk Anat 115:284-98.

Kennedy TE, Serafini T, de la Torre JR, Tessier-Lavigne M (1994) Netrins are diffusible chemotropic factors for commissural axons in the embryonic spinal cord. Cell 78:425-35.

Kent, K. Metamorphosis of the antennal center and the influence of sensory innervation on the formation of glomeruli in the hawkmoth Manduca sexta. 85. Ph.D. Dissertation, Harvard University.

Kent KS, Harrow ID, Quartararo P, Hildebrand JG (1986) An accessory olfactory pathway in Lepidoptera: the labial pit organ and its central projections in Manduca sexta and certain other sphinx moths and silk moths. Cell Tissue Res 245:237-45.

Kent KS, Oland LA, Hildebrand JG (1999) Development of the labial pit organ glomerulus in the antennal lobe of the moth Manduca sexta: the role of afferent projections in the formation of identifiable olfactory glomeruli. J Neurobiol 40:28-44.

Key B, Akeson RA (1993) Distinct subsets of sensory olfactory neurons in mouse: possible role in the formation of the mosaic olfactory projection. J Comp Neurol 335:355-68.

Key B, St John J (2002) Axon navigation in the mammalian primary olfactory pathway: where to next? Chem Senses 27:245-60.

Key B, Treloar HB, Wangerek L, Ford MD, Nurcombe V (1996) Expression and localization of FGF-1 in the developing rat olfactory system. J Comp Neurol 366:197-206.

Kidd T, Bland KS, Goodman CS (1999) Slit is the midline repellent for the robo receptor in Drosophila. Cell 96:785-94.

Kidd T, Brose K, Mitchell KJ, Fetter RD, Tessier-Lavigne M, Goodman CS, Tear G (1998) Roundabout controls axon crossing of the CNS midline and defines a novel subfamily of evolutionarily conserved guidance receptors. Cell 92:205-15.

Kidd T, Russell C, Goodman CS, Tear G (1998) Dosage-sensitive and complementary functions of roundabout and commissureless control axon crossing of the CNS midline. Neuron 20:25-33.

Kirschenbaum SR, Higgins MR, Tveten M, Tolbert LP (1995) 20-Hydroxyecdysone stimulates proliferation of glial cells in the developing brain of the moth Manduca sexta. J Neurobiol 28:234-47.

Klaes A, Menne T, Stollewerk A, Scholz H, Klambt C (1994) The Ets transcription factors encoded by the Drosophila gene pointed direct glial cell differentiation in the embryonic CNS. Cell 78:149-60.

Kleitman N, Simon DK, Schachner M, Bunge RP (1988) Growth of embryonic retinal neurites elicited by contact with Schwann cell surfaces is blocked by antibodies to L1. Exp Neurol 102:298-306.

Kolodziej PA, Timpe LC, Mitchell KJ, Fried SR, Goodman CS, Jan LY, Jan YN (1996) frazzled encodes a Drosophila member of the DCC immunoglobulin subfamily and is required for CNS and motor axon guidance. Cell 87:197-204.

Korey CA, Van Vactor D (2000) From the growth cone surface to the cytoskeleton: one journey, many paths. J Neurobiol 44:184-93.

Kuhn TB, Meberg PJ, Brown MD, Bernstein BW, Minamide LS, Jensen JR, Okada K, Soda EA, Bamburg JR (2000) Regulating actin dynamics in neuronal growth cones by ADF/cofilin and rho family GTPases. J Neurobiol 44:126-44.

Lamoureux P, Buxbaum RE, Heidemann SR (1989) Direct evidence that growth cones pull. Nature 340:159-62.

Lankford KL, Klein WL (1990) Ultrastructure of individual neurons isolated from avian retina: occurrence of microtubule loops in dendrites. Brain Res Dev Brain Res 51:217-24.

Lemke G (2001) Glial control of neuronal development. Annu Rev Neurosci 24:87-105.

Lemmon V, Burden SM, Payne HR, Elmslie GJ, Hlavin ML (1992) Neurite growth on different substrates: permissive versus instructive influences and the role of adhesive strength. J Neurosci 12:818-26.

Letourneau PC (1975) Cell-to-substratum adhesion and guidance of axonal elongation. Dev Biol 44:92-101.

Letourneau PC (1975) Possible roles for cell-to-substratum adhesion in neuronal morphogenesis. Dev Biol 44:77-91.

Letourneau PC (1983) Differences in the organization of actin in the growth cones compared with the neurites of cultured neurons from chick embryos. J Cell Biol 97:963-73.

Letourneau PC, Roche FK, Shattuck TA, Lemmon V, Takeichi M (1991) Interactions of Schwann cells with neurites and with other Schwann cells involve the calcium-dependent adhesion molecule, N-cadherin. J Neurobiol 22:707-20.

Letourneau PC, Shattuck TA, Roche FK, Takeichi M, Lemmon V (1990) Nerve growth cone migration onto Schwann cells involves the calcium- dependent adhesion molecule, N-cadherin. Dev Biol 138:430-42.

Lim SS, Edson KJ, Letourneau PC, Borisy GG (1990) A test of microtubule translocation during neurite elongation. J Cell Biol 111:123-30.

Lim SS, Sammak PJ, Borisy GG (1989) Progressive and spatially differentiated stability of microtubules in developing neuronal cells. J Cell Biol 109:253-63.

Lin CH, Espreafico EM, Mooseker MS, Forscher P (1996) Myosin drives retrograde F-actin flow in neuronal growth cones. Neuron 16:769-82.

Lin CH, Forscher P (1993) Cytoskeletal remodeling during growth cone-target interactions. J Cell Biol 121:1369-83.

Lin DM, Fetter RD, Kopczynski C, Grenningloh G, Goodman CS (1994) Genetic analysis of Fasciclin II in Drosophila: defasciculation, refasciculation, and altered fasciculation. Neuron 13:1055-69.

Marin-Padilla M, Amieva MR (1989) Early neurogenesis of the mouse olfactory nerve: Golgi and electron microscopic studies. J Comp Neurol 288:339-52.

Martin LV, Weston S, West AK, Chuah MI (2002) Nerve growth factor promotes olfactory axonal elongation. Neuroreport 13:621-5.

Mason C, Erskine L (2000) Growth cone form, behavior, and interactions in vivo: retinal axon pathfinding as a model. J Neurobiol 44:260-70.

Mason CA, Wang LC (1997) Growth cone form is behavior-specific and, consequently, position- specific along the retinal axon pathway. J Neurosci 17:1086-100.

Matheson SF, Levine RB (1999) Steroid hormone enhancement of neurite outgrowth in identified insect motor neurons involves specific effects on growth cone form and function. J Neurobiol 38:27-45.

Matise MP, Epstein DJ, Park HL, Platt KA, Joyner AL (1998) Gli2 is required for induction of floor plate and adjacent cells, but not most ventral neurons in the mouse central nervous system. Development 125:2759-70.

Matise MP, Lustig M, Sakurai T, Grumet M, Joyner AL (1999) Ventral midline cells are required for the local control of commissural axon guidance in the mouse spinal cord. Development 126:3649-59.

McKerracher L, Chamoux M, Arregui CO (1996) Role of laminin and integrin interactions in growth cone guidance. Mol Neurobiol 12:95-116.

Meyer D, Birchmeier C (1995) Multiple essential functions of neuregulin in development. Nature 378:386-90.

Meyer D, Yamaai T, Garratt A, Riethmacher-Sonnenberg E, Kane D, Theill LE, Birchmeier C (1997) Isoform-specific expression and function of neuregulin. Development 124:3575-86.

Ming GL, Song HJ, Berninger B, Holt CE, Tessier-Lavigne M, Poo MM (1997) cAMP-dependent growth cone guidance by netrin-1. Neuron 19:1225-35.

Oland LA, Oberlander H (1994) Factors that influence the development of cultured neurons from the brain of the moth Manduca sexta. In Vitro Cell Dev Biol Anim 30A:709-16.

Oland LA, Orr G, Tolbert LP (1990) Construction of a protoglomerular template by olfactory axons initiates the formation of olfactory glomeruli in the insect brain. J Neurosci 10:2096-112.

Oland LA, Pott WM, Bukhman G, Sun XJ, Tolbert LP (1996) Activity blockade does not prevent the construction of olfactory glomeruli in the moth Manduca sexta. Int J Dev Neurosci 14:983-96.

Oland LA, Pott WM, Higgins MR, Tolbert LP (1998) Targeted ingrowth and glial relationships of olfactory receptor axons in the primary olfactory pathway of an insect. J Comp Neurol 398:119-38.

Oland LA, Tolbert LP (1987) Glial patterns during early development of antennal lobes of Manduca sexta: a comparison between normal lobes and lobes deprived of antennal axons. J Comp Neurol 255:196-207.

Oland LA, Tolbert LP (1988) Effects of hydroxyurea parallel the effects of radiation in developing olfactory glomeruli in insects. J Comp Neurol 278:377-87.

Oland LA, Tolbert LP (1989) Patterns of glial proliferation during formation of olfactory glomeruli in an insect. Glia 2:10-24.

Oland LA, Tolbert LP (1996) Multiple factors shape development of olfactory glomeruli: insights from an insect model system. J Neurobiol 30:92-109.

Oland LA, Tolbert LP (1998) Glomerulus development in the absence of a set of mitral-like neurons in the insect olfactory lobe. J Neurobiol 36:41-52.

Oland LA, Tolbert LP (2002) Key Interactions Between Neurons and Glial Cells During Neural Development in Insects. Annu Rev Entomol.

Oland LA, Tolbert LP, Mossman KL (1988) Radiation-induced reduction of the glial population during development disrupts the formation of olfactory glomeruli in an insect. J Neurosci 8:353-67.

Ramon y Cajal S (1890) A quelle epoque aparaissent les expansions des cellule nerveuses de la moelle epinere du poulet. Anat. Anz. 5:609-613.

Ramon y Cajal S (1937) Recollections of my life. Cambridge, MA.: MIT Press.

Ressler KJ, Sullivan SL, Buck LB (1993) A zonal organization of odorant receptor gene expression in the olfactory epithelium. Cell 73:597-609.

Ressler KJ, Sullivan SL, Buck LB (1994) Information coding in the olfactory system: evidence for a stereotyped and highly organized epitope map in the olfactory bulb. Cell 79:1245-55.

Riethmacher D, Sonnenberg-Riethmacher E, Brinkmann V, Yamaai T, Lewin GR, Birchmeier C (1997) Severe neuropathies in mice with targeted mutations in the ErbB3 receptor. Nature 389:725-30.

Rochlin MW, Wickline KM, Bridgman PC (1996) Microtubule stability decreases axon elongation but not axoplasm production. J Neurosci 16:3236-46.

Roos J, Hummel T, Ng N, Klambt C, Davis GW (2000) Drosophila Futsch regulates synaptic microtubule organization and is necessary for synaptic growth. Neuron 26:371-82.

Rössler WR, Oland LA, Higgins MR, Hildebrand JG, Tolbert LP (1999) Development of a glia-rich axon-sorting zone in the olfactory pathway of the moth *Manduca sexta*. J Neurosci 19:9865-9877.

Rothberg JM, Hartley DA, Walther Z, Artavanis-Tsakonas S (1988) slit: an EGF-homologous locus of D. melanogaster involved in the development of the embryonic central nervous system. Cell 55:1047-59.

Rothberg JM, Jacobs JR, Goodman CS, Artavanis-Tsakonas S (1990) slit: an extracellular protein necessary for development of midline glia and commissural axon pathways contains both EGF and LRR domains. Genes Dev 4:2169-87.

Sabry JH, O'Connor TP, Evans L, Toroian-Raymond A, Kirschner M, Bentley D (1991) Microtubule behavior during guidance of pioneer neuron growth cones in situ. J Cell Biol 115:381-95.

Sepp KJ, Schulte J, Auld VJ (2000) Developmental dynamics of peripheral glia in Drosophila melanogaster. Glia 30:122-33.

Sepp KJ, Schulte J, Auld VJ (2001) Peripheral glia direct axon guidance across the CNS/PNS transition zone. Dev Biol 238:47-63.

Serafini T, Kennedy TE, Galko MJ, Mirzayan C, Jessell TM, Tessier-Lavigne M (1994) The netrins define a family of axon outgrowth-promoting proteins homologous to C. elegans UNC-6. Cell 78:409-24.

Shamah SM, Lin MZ, Goldberg JL, Estrach S, Sahin M, Hu L, Bazalakova M, Neve RL, Corfas G, Debant A, Greenberg ME (2001) EphA receptors regulate growth cone dynamics through the novel guanine nucleotide exchange factor ephexin. Cell 105:233-44.

Shepherd GM (1987) A molecular vocabulary for olfaction. Ann N Y Acad Sci 510:98-103.

Shishido E, Ono N, Kojima T, Saigo K (1997) Requirements of DFR1/Heartless, a mesoderm-specific Drosophila FGF- receptor, for the formation of heart, visceral and somatic muscles, and ensheathing of longitudinal axon tracts in CNS. Development 124:2119-28.

Silver J, Lorenz SE, Wahlsten D, Coughlin J (1982) Axonal guidance during development of the great cerebral commissures: descriptive and experimental studies, in vivo, on the role of preformed glial pathways. J Comp Neurol 210:10-29.

Silver J, Poston M, Rutishauser U (1987) Axon pathway boundaries in the developing brain. I. Cellular and molecular determinants that separate the optic and olfactory projections. J Neurosci 7:2264-72.

Silver J, Sapiro J (1981) Axonal guidance during development of the optic nerve: the role of pigmented epithelia and other extrinsic factors. J Comp Neurol 202:521-38.

Singer MS, Shepherd GM, Greer CA (1995) Olfactory receptors guide axons. Nature 377:19-20.

Snow DM, Steindler DA, Silver J (1990) Molecular and cellular characterization of the glial roof plate of the spinal cord and optic tectum: a possible role for a proteoglycan in the development of an axon barrier. Dev Biol 138:359-76.

Song H, Ming G, He Z, Lehmann M, McKerracher L, Tessier-Lavigne M, Poo M (1998) Conversion of neuronal growth cone responses from repulsion to attraction by cyclic nucleotides. Science 281:1515-8.

Song HJ, Ming GL, Poo MM (1997) cAMP-induced switching in turning direction of nerve growth cones. Nature 388:275-9.

Song HJ, Poo MM (1999) Signal transduction underlying growth cone guidance by diffusible factors. Curr Opin Neurobiol 9:355-63.

Sretavan DW, Reichardt LF (1993) Time-lapse video analysis of retinal ganglion cell axon pathfinding at the mammalian optic chiasm: growth cone guidance using intrinsic chiasm cues. Neuron 10:761-77.

St John JA, Key B (1999) Expression of galectin-1 in the olfactory nerve pathway of rat. Brain Res Dev Brain Res 117:171-8.

St John JA, Key B (2001) EphB2 and two of its ligands have dynamic protein expression patterns in the developing olfactory system. Brain Res Dev Brain Res 126:43-56.

Stahl B, Distel H, Hudson R (1990) Effects of reversible nare occlusion on the development of the olfactory epithelium in the rabbit nasal septum. Cell Tissue Res 259:275-81.

Stoeckli ET, Landmesser LT (1995) Axonin-1, Nr-CAM, and Ng-CAM play different roles in the in vivo guidance of chick commissural neurons. Neuron 14:1165-79.

Stoeckli ET, Sonderegger P, Pollerberg GE, Landmesser LT (1997) Interference with axonin-1 and NrCAM interactions unmasks a floor-plate activity inhibitory for commissural axons. Neuron 18:209-21.

Strotmann J, Wanner I, Krieger J, Raming K, Breer H (1992) Expression of odorant receptors in spatially restricted subsets of chemosensory neurones. Neuroreport 3:1053-6.

Sullivan SL, Adamson MC, Ressler KJ, Kozak CA, Buck LB (1996) The chromosomal distribution of mouse odorant receptor genes. Proc Natl Acad Sci U S A 93:884-8.

Sullivan SL, Bohm S, Ressler KJ, Horowitz LF, Buck LB (1995) Target-independent pattern specification in the olfactory epithelium. Neuron 15:779-89.

Sun B, Salvaterra PM (1995) Characterization of nervana, a Drosophila melanogaster neuron-specific glycoprotein antigen recognized by anti-horseradish peroxidase antibodies. J Neurochem 65:434-43.

Suter DM, Forscher P (2000) Substrate-cytoskeletal coupling as a mechanism for the regulation of growth cone motility and guidance. J Neurobiol 44:97-113.

Suter DM, Pollerberg GE, Buchstaller A, Giger RJ, Dreyer WJ, Sonderegger P (1995) Binding between the neural cell adhesion molecules axonin-1 and Nr- CAM/Bravo is involved in neuron-glia interaction. J Cell Biol 131:1067-81.

Szebenyi G, Callaway JL, Dent EW, Kalil K (1998) Interstitial branches develop from active regions of the axon demarcated by the primary growth cone during pausing behaviors. J Neurosci 18:7930-40.

Szebenyi G, Dent EW, Callaway JL, Seys C, Lueth H, Kalil K (2001) Fibroblast growth factor-2 promotes axon branching of cortical neurons by influencing morphology and behavior of the primary growth cone. J Neurosci 21:3932-41.

Taghert PH, Bastiani MJ, Ho RK, Goodman CS (1982) Guidance of pioneer growth cones: filopodial contacts and coupling revealed with an antibody to Lucifer Yellow. Dev Biol 94:391-9.

Takahashi T, Fournier A, Nakamura F, Wang LH, Murakami Y, Kalb RG, Fujisawa H, Strittmatter SM (1999) Plexin-neuropilin-1 complexes form functional semaphorin-3A receptors. Cell 99:59-69.

Tanaka E, Ho T, Kirschner MW (1995) The role of microtubule dynamics in growth cone motility and axonal growth. J Cell Biol 128:139-55.

Tanaka E, Kirschner MW (1995) The role of microtubules in growth cone turning at substrate boundaries. J Cell Biol 128:127-37.

Tanaka EM, Kirschner MW (1991) Microtubule behavior in the growth cones of living neurons during axon elongation. J Cell Biol 115:345-63.

Tear G, Harris R, Sutaria S, Kilomanski K, Goodman CS, Seeger MA (1996) commissureless controls growth cone guidance across the CNS midline in Drosophila and encodes a novel membrane protein. Neuron 16:501-14.

Tennent R, Chuah MI (1996) Ultrastructural study of ensheathing cells in early development of olfactory axons. Brain Res Dev Brain Res 95:135-9.

Tennyson VM (1970) The fine structure of the axon and growth cone of the dorsal root neuroblast of the rabbit embryo. J Cell Biol 44:62-79.

Tessier-Lavigne M, Goodman CS (1996) The molecular biology of axon guidance. Science 274:1123-33.

Tisay KT, Bartlett PF, Key B (2000) Primary olfactory axons form ectopic glomeruli in mice lacking p75NTR. J Comp Neurol 428:656-70.

Tisay KT, Key B (1999) The extracellular matrix modulates olfactory neurite outgrowth on ensheathing cells. J Neurosci 19:9890-9.

Tolbert LP, Matsumoto SG, Hildebrand JG (1983) Development of synapses in the antennal lobes of the moth Manduca sexta during metamorphosis. J Neurosci 3:1158-75.

Tomaselli KJ, Neugebauer KM, Bixby JL, Lilien J, Reichardt LF (1988) N-cadherin and integrins: two receptor systems that mediate neuronal process outgrowth on astrocyte surfaces. Neuron 1:33-43.

Tosney KW, Landmesser LT (1985) Growth cone morphology and trajectory in the lumbosacral region of the chick embryo. J Neurosci 5:2345-58.

Tosney KW, Wessells NK (1983) Neuronal motility: the ultrastructure of veils and microspikes correlates with their motile activities. J Cell Sci 61:389-411.

Treloar H, Tomasiewicz H, Magnuson T, Key B (1997) The central pathway of primary olfactory axons is abnormal in mice lacking the N-CAM-180 isoform. J Neurobiol 32:643-58.

Treloar HB, Nurcombe V, Key B (1996) Expression of extracellular matrix molecules in the embryonic rat olfactory pathway. J Neurobiol 31:41-55.

Treloar HB, Purcell AL, Greer CA (1999) Glomerular formation in the developing rat olfactory bulb. J Comp Neurol 413:289-304.

Tsui HT, Lankford KL, Ris H, Klein WL (1984) Novel organization of microtubules in cultured central nervous system neurons: formation of hairpin loops at ends of maturing neurites. J Neurosci 4:3002-13.

Tucker, E. S., Oland, L. A., and Tolbert, L. P. In vitro study of interactions between olfactory receptor growth cones and glial cells of the axonal sorting zone. Society for Neuroscience Abstracts 26, 1611. 2000.

Tucker, E. S., Oland, L. A., and Tolbert, L. P. In vitro analysis of interactions between olfactory receptor growth cones and centrally derived glia. Association for Chemoreception Sciences, Abstracts XXIII, 72. 2001.

Tucker, E. S., Oland, L. A., and Tolbert, L. P. Growing olfactory receptor axons from *Manduca sexta* display different interactions with central and peripheral glia *in vitro*. Association for Chemoreception Sciences, Abstracts XXIV, 7. 2002.

Valverde F (1999) Building an olfactory glomerulus. J Comp Neurol 415:419-22.

Valverde F, Santacana M, Heredia M (1992) Formation of an olfactory glomerulus: morphological aspects of development and organization. Neuroscience 49:255-75.

Vassalli A, Rothman A, Feinstein P, Zapotocky M, Mombaerts P (2002) Minigenes impart odorant receptor-specific axon guidance in the olfactory bulb. Neuron 35:681-96.

Vassar R, Chao SK, Sitcheran R, Nunez JM, Vosshall JB, Axel R (1994) Topographic organization of sensory projections to the olfactory bulb. Cell 79:981-991.

Vassar R, Ngai J, Axel R (1993) Spatial segregation of odorant receptor expression in the mammalian olfactory epithelium. Cell 74:309-18.

Vincent S, Reed J, Giangrande A (1995) [Specification of glial lineage in invertebrates]. C R Seances Soc Biol Fil 189:245-52.

Vosshall LB, Amrein H, Morozov PS, Rzhetsky A, Axel R (1999) A spatial map of olfactory receptor expression in the Drosophila antenna. Cell 96:725-36.

Vosshall LB, Wong AM, Axel R (2000) An olfactory sensory map in the fly brain. Cell 102:147-59.

Walsh FS, Doherty P (1997) Neural cell adhesion molecules of the immunoglobulin superfamily: role in axon growth and guidance. Annu Rev Cell Dev Biol 13:425-56.

Walz A, Rodriguez I, Mombaerts P (2002) Aberrant sensory innervation of the olfactory bulb in neuropilin-2 mutant mice. J Neurosci 22:4025-35.

Wang F, Nemes A, Mendelsohn M, Axel R (1998) Odorant receptors govern the formation of a precise topographic map. Cell 93:47-60.

Wang LC, Dani J, Godement P, Marcus RC, Mason CA (1995) Crossed and uncrossed retinal axons respond differently to cells of the optic chiasm midline in vitro. Neuron 15:1349-64.

Wanner IB, Wood PM (2002) N-cadherin mediates axon-aligned process growth and cell-cell interaction in rat Schwann cells. J Neurosci 22:4066-79.

Wewetzer K, Verdu E, Angelov DN, Navarro X (2002) Olfactory ensheathing glia and Schwann cells: two of a kind? Cell Tissue Res 309:337-45.

Whitesides JG 3rd, LaMantia AS (1996) Differential adhesion and the initial assembly of the mammalian olfactory nerve. J Comp Neurol 373:240-54.

Wilkinson DG (2001) Multiple roles of EPH receptors and ephrins in neural development. Nat Rev Neurosci 2:155-64.

Woldeyesus MT, Britsch S, Riethmacher D, Xu L, Sonnenberg-Riethmacher E, Abou-Rebyeh F, Harvey R, Caroni P, Birchmeier C (1999) Peripheral nervous system defects in erbB2 mutants following genetic rescue of heart development. Genes Dev 13:2538-48.

Wood PM, Schachner M, Bunge RP (1990) Inhibition of Schwann cell myelination in vitro by antibody to the L1 adhesion molecule. J Neurosci 10:3635-45.

Woodhall E, West AK, Chuah MI (2001) Cultured olfactory ensheathing cells express nerve growth factor, brain- derived neurotrophic factor, glia cell line-derived neurotrophic factor and their receptors. Brain Res Mol Brain Res 88:203-13.

Wright JW, Copenhaver PF (2000) Different isoforms of fasciclin II play distinct roles in the guidance of neuronal migration during insect embryogenesis. Dev Biol 225:59-78.

Xu XM, Fisher DA, Zhou L, White FA, Ng S, Snider WD, Luo Y (2000) The transmembrane protein semaphorin 6A repels embryonic sympathetic axons. J Neurosci 20:2638-48.

Yamada KM, Spooner BS, Wessells NK (1970) Axon growth: roles of microfilaments and microtubules. Proc Natl Acad Sci U S A 66:1206-12.

Yamada KM, Spooner BS, Wessells NK (1971) Ultrastructure and function of growth cones and axons of cultured nerve cells. J Cell Biol 49:614-35.

Yazaki T, Martuza RL, Rabkin SD (1996) Expression of L1 in primary astrocytes via a defective herpes simplex virus vector promotes neurite outgrowth and neural cell migration. Brain Res Mol Brain Res 43:311-20.

Yoshihara Y, Kawasaki M, Tamada A, Fujita H, Hayashi H, Kagamiyama H, Mori K (1997) OCAM: A new member of the neural cell adhesion molecule family related to zone-to-zone projection of olfactory and vomeronasal axons. J Neurosci 17:5830-42.

Yoshihara Y, Mori K (1997) Basic principles and molecular mechanisms of olfactory axon pathfinding. Cell Tissue Res 290:457-63.

Yu TW, Bargmann CI (2001) Dynamic regulation of axon guidance. Nat Neurosci 4 Suppl:1169-76.

Zakharenko S, Popov S (1998) Dynamics of axonal microtubules regulate the topology of new membrane insertion into the growing neurites. J Cell Biol 143:1077-86.

Zhao H, Reed RR (2001) X inactivation of the OCNC1 channel gene reveals a role for activity- dependent competition in the olfactory system. Cell 104:651-60.

Zheng C, Feinstein P, Bozza T, Rodriguez I, Mombaerts P (2000) Peripheral olfactory projections are differentially affected in mice deficient in a cyclic nucleotide-gated channel subunit. Neuron 26:81-91.